esac

European Space Astronomy Centre
P.O. Box 78
28691
Villanueva de la Cañada
Madrid
Spain

Tel. (34) 91 813 1100
Fax (34) 91 813 1139

www.esa.int

DOCUMENT

NOMAD Experiment to Archive Interface Control Document

EXM-NO-ICD-AER-00001-iss3rev0-EAICD_NOMAD_221221.docx

Prepared by	**Ian Thomas**
Reference	**EXM-NO-ICD-AER-00001**
Issue	**3**
Revision	**0**
Date of Issue	**21/12/22**
Status	**Updates following version 3 data delivery**
Document Type	**EAICD**

European Space Agency
Agence spatiale européenne

APPROVAL

Title NOMAD Experiment to Archive Interface Control Document	
Issue 3	**Revision** 0
Date 21/12/22	
Prepared by	**Signature**
Ian Thomas (NOMAD Project Manager at BIRA-IASB)	
Approved by	**Signature**
Ann Carine Vandaele (NOMAD Principal Investigator, BIRA-IASB)	
Eddy Neefs (Head of Engineering, BIRA-IASB)	
Authorised by	**Signature**
Leo Metcalfe (ExoMars 2016 SOC Development Manager)	

CHANGE LOG

Reason for change	Issue	Revision	Date
Creation of document	0	0	05/08/15
Various updates	0	1	10/08/15
Various updates	0	2	17/09/15
Various updates	0	3	18/09/15
Various updates	0	4	21/09/15
Added extra PDS document structure figures; various corrections	0	5	22/09/15
NOMAD text added by IRT	1	0	19/01/16
Various updates by IRT	1	0	19/01/16
Various updates by IRT before/after DHAWG#7	1	2	24/11/16

Updates to calibration types by IRT	1	5	20/03/17
Various updates by IRT following NOMAD SWT10	1	6,7	14/06/17
Various updates by IRT following NOMAD SWT11	1	8	05/12/17
Various updates by IRT in response to RIDs	1	9	06/03/18
Various updates by IRT and UVIS inputs	1	10	25/10/18
New sections on pipeline, browse products, etc.	1	11	26/10/18
Modifications by UVIS team, quality flag changes	1	12	11/12/18
Modifications following SO/LNO product validation	1	13	30/08/19
Transmittance calculation details updated, UVIS binning options expanded	1	15	03/03/20
Updates to address the RIDs from the document and data review	2	0	12/05/20
Implementation of the RID action items	2	1	05/06/20
Implementation of the RID action items: new solar occultation parameters, slant path distance and pointing deviation	2	2	18/12/20
New observation types added e.g. limb, fullscan, LNO nadir, calibrations etc.	2	3	09/03/22
Updated SO and LNO calibration; browse products of new observation types added e.g. limb, fullscan, LNO nadir, calibrations	3	0	21/12/22

DISTRIBUTION LIST

Recipient	Organisation	Recipient	Organisation

Table of contents:

List of Figures

List of Tables

1 INTRODUCTION

1.1 Purpose and Scope

This Experiment-to-Archive Interface Control Document (EAICD) describes the format and content of the NOMAD (Nadir and Occultation for Mars' Discovery) archived data. It includes descriptions of the data products and associated metadata, including the data format, content, and generation pipeline.

The specifications described in this EAICD apply to all NOMAD products submitted for archive to ESA's ExoMars 2016 Science Ground Segment (SGS), for all phases of the ExoMars 2016 mission. This document includes descriptions of archive products that are produced by both the NOMAD team and by the SGS.

1.2 Applicable Documents

The following documents, of the issue given hereunder, are pertinent to the extent specified herein and impose requirements to the SGS or the SGS schedule. They are referenced in the form [AD XX]:

[AD.01] EM16-SGS-PL-002, ExoMars 2016 Science Data Generation, Validation and Archiving Plan
[AD.02] EM16-SGS-TN-001, ExoMars 2016 Archiving Guide
[AD.03] PDS4 Standards Reference (SR)
[AD.04] PDS4 Data Dictionary (DDDB)
[AD.05] PDS4 Information Model Specification (IM)

1.3 Reference Documents

The following documents, of the issue given hereunder, although not part of this document, amplify or clarify its contents. If no issue given, the most recent issue should be used. They are referenced in the form [RD.XX]:

[RD.01] PDS4 Data Providers Handbook (DPH)
[RD.02] PDS4 Concepts
[RD.03] PSA User Guide
[RD.04] Neefs E., et al. (2015), NOMAD spectrometers on the ExoMars Trace Gas Orbiter Mission: part 1 - design, manufacturing and testing of the infrared channels.

[RD.05] Patel, M. R., et al., NOMAD spectrometers on the ExoMars Trace Gas Orbiter Mission: part 2 – the UVIS channel. (2017)

[RD.06] Vandaele, A. C., (2015), Science objectives and performances of NOMAD, a spectrometer suite for the ExoMars TGO mission.

[RD.07] Vandaele, A. C., (2015), Optical and radiometric models of the NOMAD instrument part I: the UVIS channel.

[RD.08] Thomas, I. R., et al., (2016), Optical and Radiometric Models of the NOMAD Instrument Part II: The Infrared Channels – SO and LNO

[RD.09] NOMAD User Manual: EXM-NO-UMA-OIP-00001-iss2-rev2 NOMAD User Manual_FMMmodif .docx

[RD.10] EXM-NO-TNO-AER-00048-iss2rev5-DataOperationsHandbook-150505.xlsx

[RD.11] Trompet, L., et al., (2016), Improved algorithm for the transmittance estimation of spectra obtained with SOIR/Venus Express. Applied Optics (2016) Vol. 55, Issue 32, pp. 9275 - 9281 https://doi.org/10.1364/AO.55.009275

[RD.12] Vandaele, A. C., et al., (2018), NOMAD, an Integrated Suite of Three Spectrometers for the ExoMars Trace Gas Mission: Technical Description, Science Objectives and Expected Performance, Space Science Reviews, Vol. 214, Issue 5, A80, DOI: 10.1007/s11214-018-0517-2

[RD.13] Liuzzi, G., et al., (2019), Methane on Mars: new insights into the sensitivity of CH4 with the NOMAD/ExoMars spectrometer through its first in-flight calibration, Icarus doi: 10.1016/j.icarus.2018.09.021

[RD.14] Thomas, I. R., et al., (2021), Calibration of NOMAD on ESA's ExoMars Trace Gas Orbiter: Part 1 – The Solar Occultation channel, PSS https://doi.org/10.1016/j.pss.2021.105411

[RD.15] Thomas, I. R., et al., (2021), Calibration of NOMAD on ESA's ExoMars Trace Gas Orbiter: Part 2 – The Limb, Nadir and Occultation (LNO) channel, PSS https://doi.org/10.1016/j.pss.2021.105410

[RD.16] Cruz-Mermy, G., et al., (2021), Calibration of NOMAD on ExoMars Trace Gas Orbiter: Part 3 - LNO validation and instrument stability, PSS https://doi.org/10.1016/j.pss.2021.105399

[RD.17] Mason, J. P., et al., (2022), Removal of straylight from ExoMars NOMAD-UVIS observations, PSS https://doi.org/10.1016/j.pss.2022.105432

[RD.18] Willame, Y., et al., (2022), Calibration of the NOMAD-UVIS data, submitted to PSS

2 NOMAD INSTRUMENT DESCRIPTION

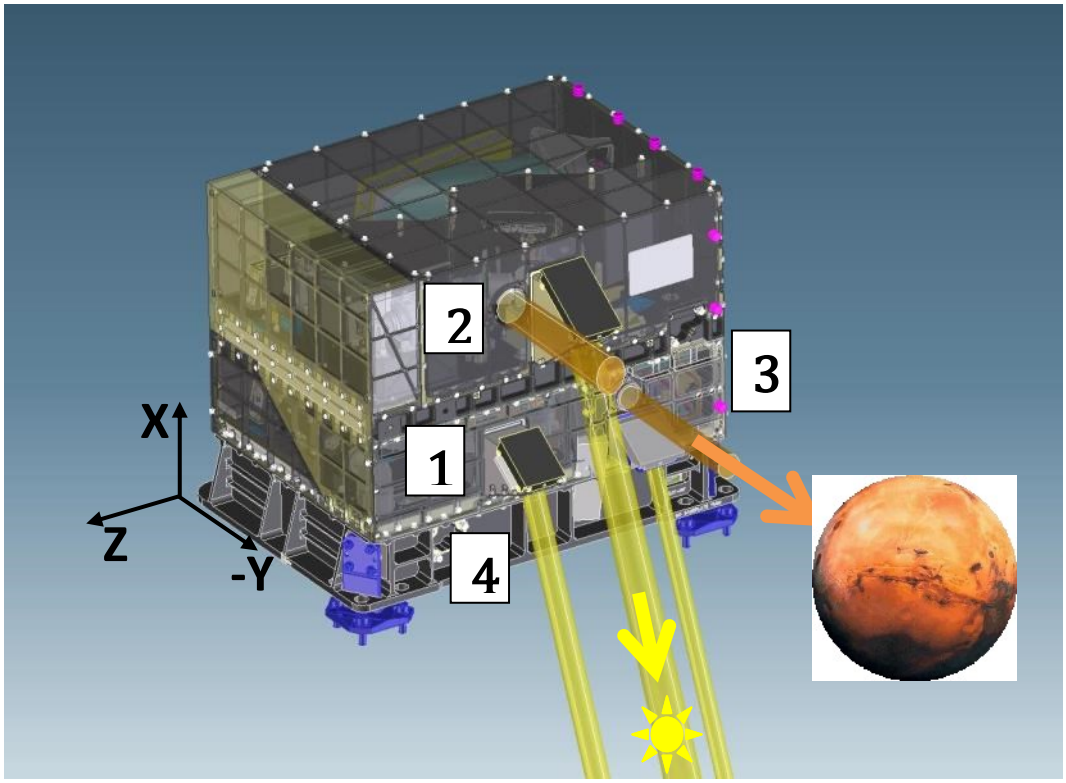

Figure 1: The NOMAD instrument, with the SO (1), LNO (2) and UVIS (3) channels, and the electronics (4). Lines of sight towards the Sun (yellow cylinders) and the nadir direction (orange cylinders) are also indicated. Image from Vandaele et al. (2015) [RD06]

The Nadir and Occultation for MArs Discovery instrument (NOMAD) is a spectrometer suite led by the Belgian Institute for Space Aeronomy (BIRA-IASB), being flown on the ESA/Roscosmos ExoMars Trace Gas Orbiter mission. NOMAD is predominantly based upon the SOIR-channel (Solar Occultations in the Infrared) in the SPectroscopy for the Investigation of the Composition of the Atmosphere of Venus instrument (SPICAV) from the highly successful Venus Express mission, a compact high-resolution echelle grating spectrometer with acousto-optical tunable filter for the infrared domain between 2.3 and 4.3 µm.

NOMAD consists of three separate channels, Solar Occultation (SO), Limb Nadir and Occultation (LNO) and Ultraviolet and VIsible Spectrometer (UVIS), all controlled via a single main electronics unit (SINBAD)

	SO Channel	LNO Channel	UVIS Channel
Detector	2D HgCdTe 320x256 pixel FPA	2D HgCdTe 320x256 pixel FPA	2D 1024x256 pixel CCD
Detector temperature	88 K	88 K	N/A
Line of Sight	periscope lining up with Sun direction	Periscope for lining up with Sun direction – Nadir viewing entrance	2 telescopes lining up with Sun and nadir directions
Spectral range	2.3 – 4.3 µm	2.3 – 3.8 µm	200-650 nm
Resolving power / spectral resolution	~20000 0.15-0.22 cm^{-1}	~10000 0.3-0.5 cm^{-1}	1-2 nm
Full instantaneous field of view IFOV (spectral x spatial)	2 arcmin x 30 arcmin	4 arcmin x 150 arcmin	2 arcmin (solar occ) 43 arcmin (nadir)
Nominal science observation IFOV	2 arcmin x 16 arcmin (solar occultation)	4 arcmin x 16 arcmin (solar occultation) 4 arcmin x 144 arcmin (nadir, limb, etc.)	2 arcmin (solar occ) 43 arcmin (nadir)
Spatial resolution Instantaneous footprint	1 km (Δz at limb)	1 km (Δz at limb) 0.5 km x 17 km	1 km (Δz at limb) 5 km x 5 km (Nadir)
Vertical sampling	180 m to 1 km	180 m to 1 km	< 300 m

Table 1: NOMAD characteristics and performances

2.1 The SO channel

The design of the SO channel has been inspired by the existing SOIR instrument (Nevejans et al., 2006b), which is part of the SPICAV/SOIR spectrometers' suite (Bertaux et al., 2007) on board Venus Express (Svedhem et al., 2007). The SO channel has been optimized for solar occultation observations, i.e. looking at the Sun during sunset and sunrise. It operates at wavelengths between 2.3 and 4.3 µm (2320 to 4550 cm-1), using an echelle grating with a

groove density of 4 lines/mm in a near Littrow configuration in combination with an Acousto-Optical Tunable Filter (AOTF) for spectral window selection. Figure 2 illustrates the schematics of the SO channel. The width of the selected spectral windows varies from 20 to 35 cm-1 depending on the selected diffraction order. The detector is an actively cooled HgCdTe Focal Plane Array and is made up of 320 pixels along the spectral axis and 256 rows. During the ten minutes before an occultation starts, the detector is cooled down to a temperature of ~85K. SO achieves an instrument line profile resolution of 0.15 cm-1, corresponding to a resolving power $\lambda/\Delta\lambda$ of approximately 20000. The slit of the spectrometer is a 2' (spectral direction) by 30' (spatial direction) rectangle. The spectral range is divided into several diffraction orders, one of which can be selected by the AOTF. To do this, a radio-frequency signal is applied to the AOTF crystal so that the central wavelength of the AOTF bandpass corresponds to the centre of the desired diffraction order.

The instrument entrance slit is projected on 30 detector rows, from row 113 to 143 when the top line is designated as row 0. Different binning options can be selected depending directly on the number of different AOTF settings that will be used, knowing that at maximum the equivalent of 24 spectra can be downloaded per second. This will be further discussed in the next section. In most of the observations 6 different values of the AOTF frequency are chosen to record spectra in different spectral intervals per second, hence increasing the number of species potentially detectable quasi-simultaneously. The duration of 1s has been chosen as the default cycle of observation performed by SO. It can be changed by telecommand if needed. All 320 pixels in the spectral direction are measured.

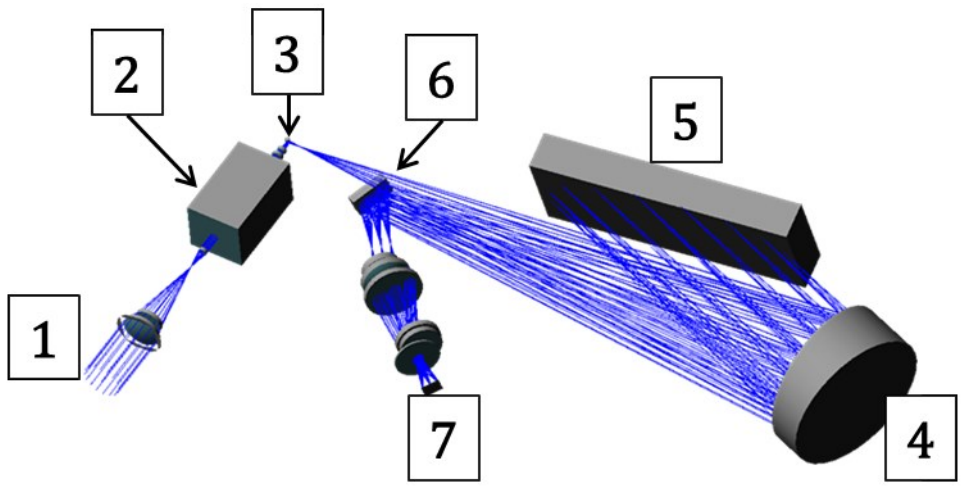

Figure 2: Schematics of the SO and LNO channels: (1) the entrance optics, (2) the AOTF filter, (3) the spectrometer entrance slit, (4 & 6) folding mirrors, (5) the echelle grating, (7) the detector. Image from Vandaele et al. (2015) [RD06]

2.2 The LNO channel

The optical layout of LNO is identical to that of SO (AOTF - echelle spectrometer- cooled detector, see Figure 2). LNO will be measuring in the wavelength range between 2.3 and 3.8 µm (2630-4550 cm-1). To fulfil the Signal to Noise Ratio (SNR) requirement, a number of low risk and easy-to-implement measures were considered to increase the signal throughput as well as to reduce the thermal background of the instrument, e.g. decreasing the highest wavelength limit of the sensitivity of the detector to reduce the impact of thermal noise (from 4.3 µm for SO to 3.8 µm for LNO); increasing the length of the slit from 30' to 150'; using a larger AOTF crystal, and using longer integration times, appropriate pixel binning, and accumulating repeat spectra. For the LNO channel, the width of the slit has been increased to 4', leading to a higher throughput and therefore SNR, but a reduction in resolution to 0.3-0.5 cm-1 and a resolving power of $\lambda/\Delta\lambda \sim 10000$.

The detector of LNO is similar to the one chosen for the SO channel (320 x 256 pixels). Since the slit is larger, more rows will be illuminated, from row 77 to row 227. and like in SO, the equivalent of 24 lines x 320 pixels can be acquired per measurement cycle. To return data from 144 detector rows in only 24 lines, binning is essential for the LNO channel; the different possible combinations for LNO observations will be further discussed in further details in this document. As for SO, up to 6 different AOTF frequencies can be selected per measurement cycle; however since the light level will be far more reduced when using LNO in nadir mode compared to solar occultation viewing, the integration time is increased. The measurement cycle/ sampling rhythm of LNO is typically 15 seconds for nadir observations, although any other value is possible. As for SO, the duration of this cycle can be changed by telecommand.

The LNO channel is equipped with a movable mirror that can be flipped in and out of the optical path. When the mirror is in the optical path, the field of view is pointed towards nadir (i.e. the TGO –Y axis). When the mirror is out of the optical path, it is pointed towards the limb and can perform measurements during solar occultations. The flip mirror is driven by a motor, but has a fail-safe system that puts it permanently in nadir mode should the motor fail.

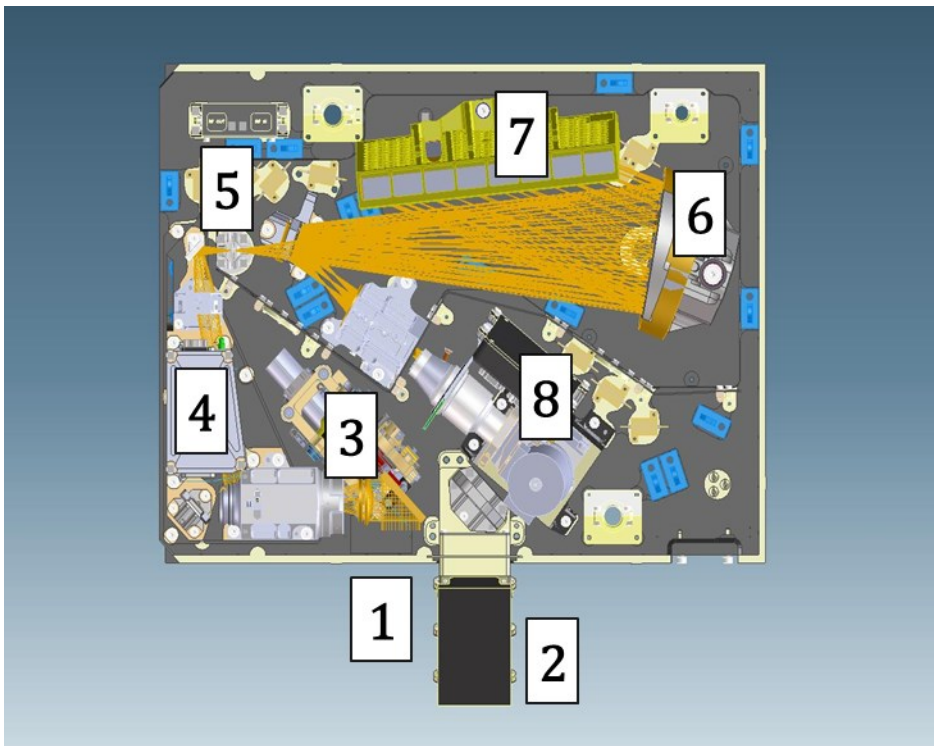

Figure 3: View of the LNO channel and its components: (1) the entrance optics, (2) the solar occultation periscope, (3) the flip-mirror mechanism, (4) the AOTF filter, (5) the spectrometer entrance slit, (6) the folding mirror, (7) the echelle grating, (8) the detector. The SO channel has a very similar layout. Image from Vandaele et al. (2015) [RD06]

2.3 The UVIS channel

The UVIS channel operates in the wavelength domain between 200 and 650 nm. It is a full copy of the instrument designed for the ExoMars lander, with additional telescopic entrance optics for application in orbit. The spectrometer is based on the conventional Czerny-Turner configuration. The main components of the UVIS channel (see Figure 4), are the entrance slit, the aperture (A), the collimating mirror (M1), the diffraction grating (G), the focusing mirror (M2), the 2nd order filter (F) and the detector (CCD). The light is delivered by an optical fibre. The spectrometer is an imaging system with a magnification equal to 1. More details on the instrument can be found in Patel et al. (2015). The spectrometer configuration combines simplicity and high-performance. In particular, the spectral range is very broad (200-650nm) with optimized performance in the UV range. Blaze angle and incidence angle achieve the highest reflectance of the first diffraction order at 220 nm. The 2nd order filter solves the issue of the overlap between the 1st diffraction order and the 2nd diffraction order of the grating. Indeed, due to the wide spectral range of the observed signal (200-650nm),

first diffraction order rays and second diffraction order rays overlap on the detector. Hence a high-pass filter has been placed in front of the detector to block the second order rays. The slit width is 65 µm which corresponds to a spectral resolution better than 1.5 nm. This width results from an optimisation of the resolution and the SNR.

UVIS has one periscope for the solar (narrow field) telescope and a cut out hole in the NOMAD cover for the nadir viewing telescope, see Figure 5. UVIS switches between nadir and solar viewing angles by alternating which optic fibre cable is placed at the input of the spectrometer – the one coming from the solar telescope (narrow field) or from the nadir telescope (wider angle). The selector mechanism is a rotating motor mechanism qualified on several space missions that drives to two hard stops and a central position: one hard stop is the solar fibre and the other the nadir fibre; whilst in the central position is used for acquiring dark frames, where neither fibre is in position.

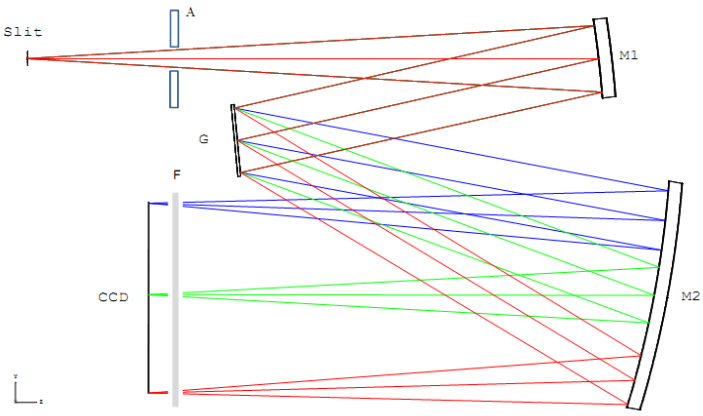

Figure 4: Schematics of the UVIS instrument: the entrance slit (Slit), the aperture (A), the collimating mirror (M1), the diffraction grating (G), the focusing mirror (M2), the 2nd order filter (F) and the detector (CCD).

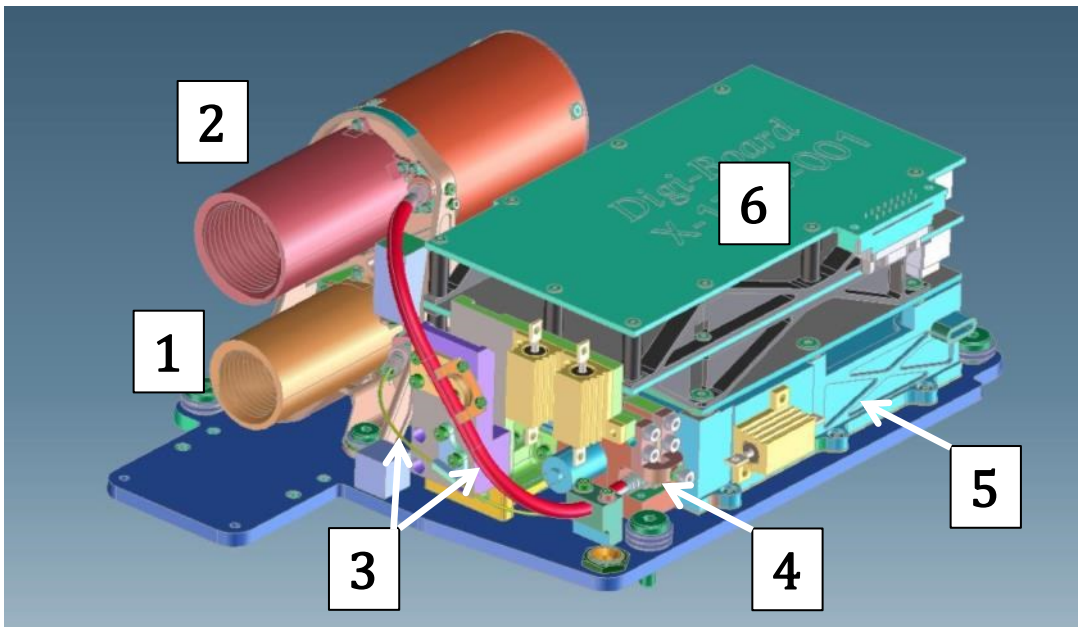

Figure 5: UVIS channel with the 2 entrance telescopes (1: Solar occultation ; 2: nadir), the fibers (3), the selector mechanism (4), the main spectrometer (5), and the proximity electronics (6). Image from Vandaele et al. (2015) [RD06]

Therefore in total there are 5 fields of view. In the spacecraft reference frame, nadir is defined as the –Y direction, and the occultation channels point at ~67 degrees from this, so that they always point towards the limb of Mars when in a 400km circular orbit. The spacecraft directions are shown in Figure 1. In summary:

- SO, which points towards the sun/limb of Mars only (~67° from –Y; ~33° from –X);
- LNO, which nominally points nadir towards the centre of Mars (-Y), but can also point towards the Sun/planet limb (~67° from –Y; ~33° from –X) by moving the flip mirror;
- UVIS, which points towards both nadir (-Y) and the sun/limb (also ~67° from –Y; ~33° from –X).

More information can be found in "The NOMAD Spectrometer on the ExoMars Trace Gas Orbiter Mission: Part 1 - Design, Manufacturing and Testing of the Infrared Channels" by Neefs et al. (2015) and "The NOMAD Spectrometer on the ExoMars Trace Gas Orbiter Mission: Part 2 – The UVIS Channel" by Patel et al. (2016).

2.4 Observation Types

NOMAD operates primarily in dayside nadir and solar occultation modes, which are shown in Figure 6 and Figure 7 with some of the geometric parameters required to analyse the data. Typically, SO and UVIS operate in solar occultation mode, and LNO and UVIS operate in nadir mode. Limb and nightside nadir observations can be made, though these are not in the baseline plan.

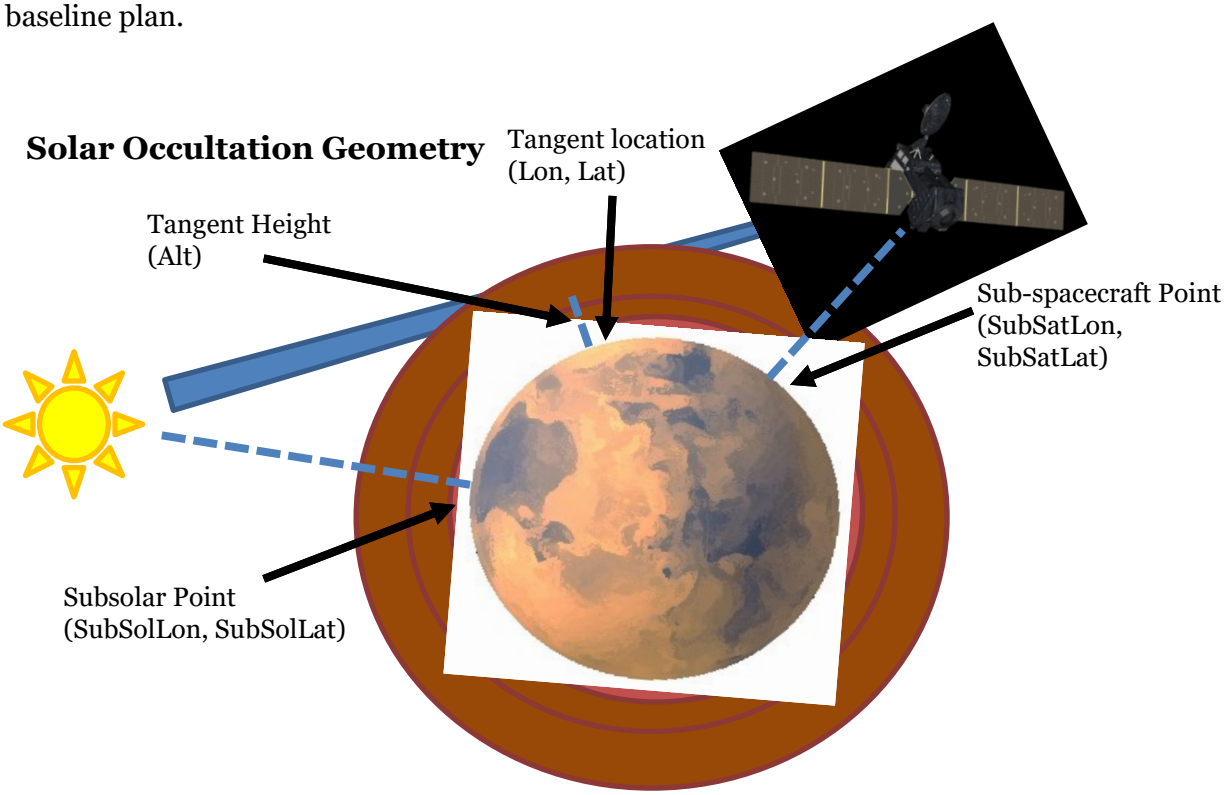

Figure 6: Solar occultation geometry parameters.

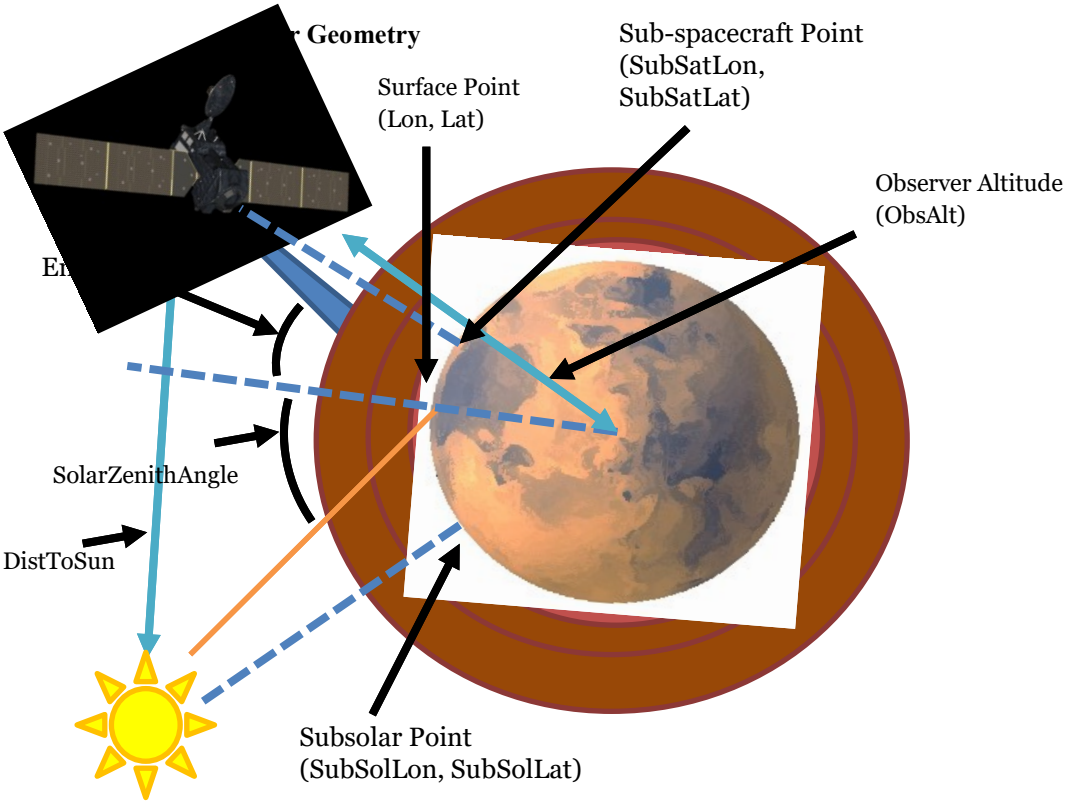

Figure 7: Definitions of the nadir geometry parameters.

2.5 Science Objectives

NOMAD science objectives are summarized in Table 2. Simulations of expected solar occultation spectra are given in Figure 8.

Science Objective	Description
Chemical Composition	Analyse the present-day chemical composition of the Martian atmosphere through detection of a broad suite of trace gases and key isotopes. Extend the detection to the upper atmosphere in order to constrain atmospheric escape processes relating the present-day atmosphere to its past and future evolution. Understand the chemistry in order to constrain the methane origin (i.e. geophysical, exogenous or biological) and destruction processes, and study gases related to possible ongoing geophysical and volcanic activity on Mars.
Climatology and Seasonal Cycles	Characterize the spatial (3D) and temporal variability of trace gases and dust/clouds. Provide an extension and refinement of current climatologies for CO2, H2O, CO, CH4 and other species including dust/clouds, O3, and UV radiation levels at the surface in 3D+time. Contribute to the understanding of fine-scale processes and annual variability, and to the constraint of atmospheric dynamics.
Sources and Sinks	Characterize the production and loss mechanisms of trace gases, including the localization of trace gas sources related to outgassing as well as atmospheric production. Refine processes in the water, carbon, ozone and dust cycles. Relate this to surface mineralogy/ ices and characterize sites of interest.

Table 2: Science objectives of the NOMAD experiment.

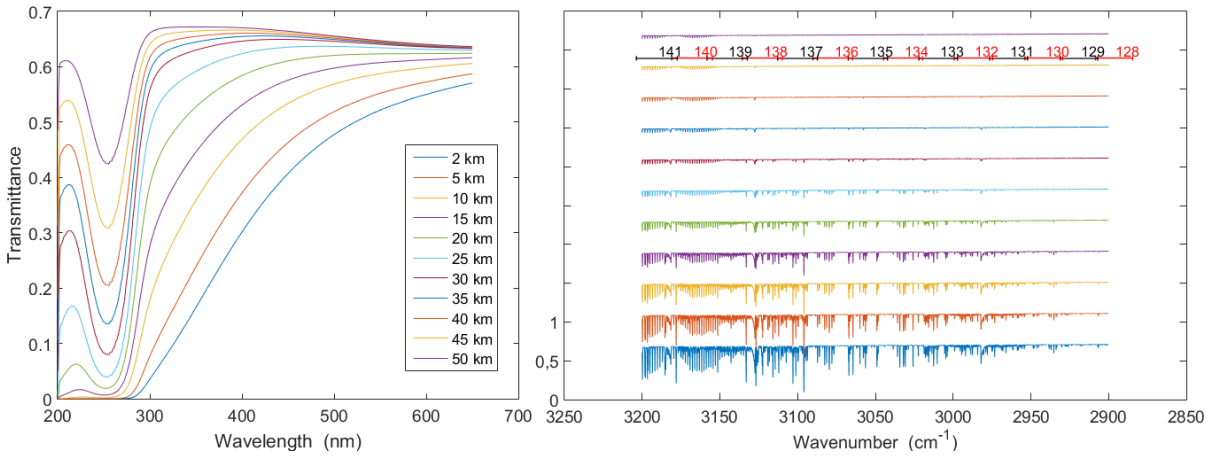

Figure 8: Examples of simulated transmittances obtained during a typical solar occultation in the UV-visible (Left Panel) and the IR (Right Panel) recorded by the UVIS and SO channels respectively. These spectra contain the absorption of CO_2, H_2O, O_3 and CH_4 for a typical clear Mars atmosphere, considering the Rayleigh scattering and a dust loading of tau=0.2. The color code indicates the altitudes to which they correspond. For the IR spectra: The limits of the different diffraction orders covered are shown at the top of the figure and spectra have been artificially shifted by 0.45 for clarity.

More information can be found in "NOMAD, a spectrometer suite for the ExoMars mission" by Vandaele et al. (2015) [RD06].

2.6 Operational Modes

During flight NOMAD is always in one of three modes: two operational modes (safe mode and observing mode) and one non-operational mode (power off mode)

The three modes are:

- **Safe Mode**. This is the default mode at NOMAD power on. SO, LNO and UVIS are powered off. In this mode only the central electronics unit (SINBAD) is powered on. The power consumption is constant. It is suggested to keep SINBAD (and hence NOMAD) on permanently during the science phase of the mission, but switching it on/off as a function of science activity is possible.
- **Observing Mode**. In this mode one or several of the three NOMAD channels (SO, LNO, UVIS) can be powered on, depending on the selected observation sequence. Possible combinations are SO only, LNO only, UVIS only, SO+UVIS and LNO+UVIS. The power consumption depends on the specific configuration.
- **Power Off:** all channels and the SINBAD are in a powered off state. No power is consumed.

In this EAICD, the following nomenclature is used:

- An "observation" is one complete observing run taken by one NOMAD channel e.g. a dayside nadir pass, or a complete solar occultation.
- A "measurement" is a single detector frame/acquisition of Mars as transmitted to Earth.

It should be noted that NOMAD observation sequences are highly programmable and therefore any specific cases described here are subject to change depending on instrument priorities and performance. Figure 9 and Figure 10 show two possible sequences for the infrared channels – the former has on-board background subtraction enabled, and in the latter it is background subtraction is done manually.

Generally, science operations during one orbit around Mars can be split into four distinct observations:

1. On the day side, NOMAD will perform nadir observations with the LNO (in nadir mode) and UVIS (in nadir mode) channels, or limb observations with LNO in occultation mode.
2. At the sunset terminator a solar occultation measurement will be performed with the SO and UVIS (in occultation mode) channels.

3. On the night side, atmospheric emission measurements can be performed, if desired, with LNO and/or UVIS in nadir mode).
4. At the sunrise terminator a solar occultation measurement will be performed with SO and UVIS (in occultation mode).

It is also possible to use LNO instead of SO during solar occultations by moving the flip mirror into the occultation position. Using SO and LNO simultaneously is forbidden due to spacecraft power limitations, including in precooling mode.

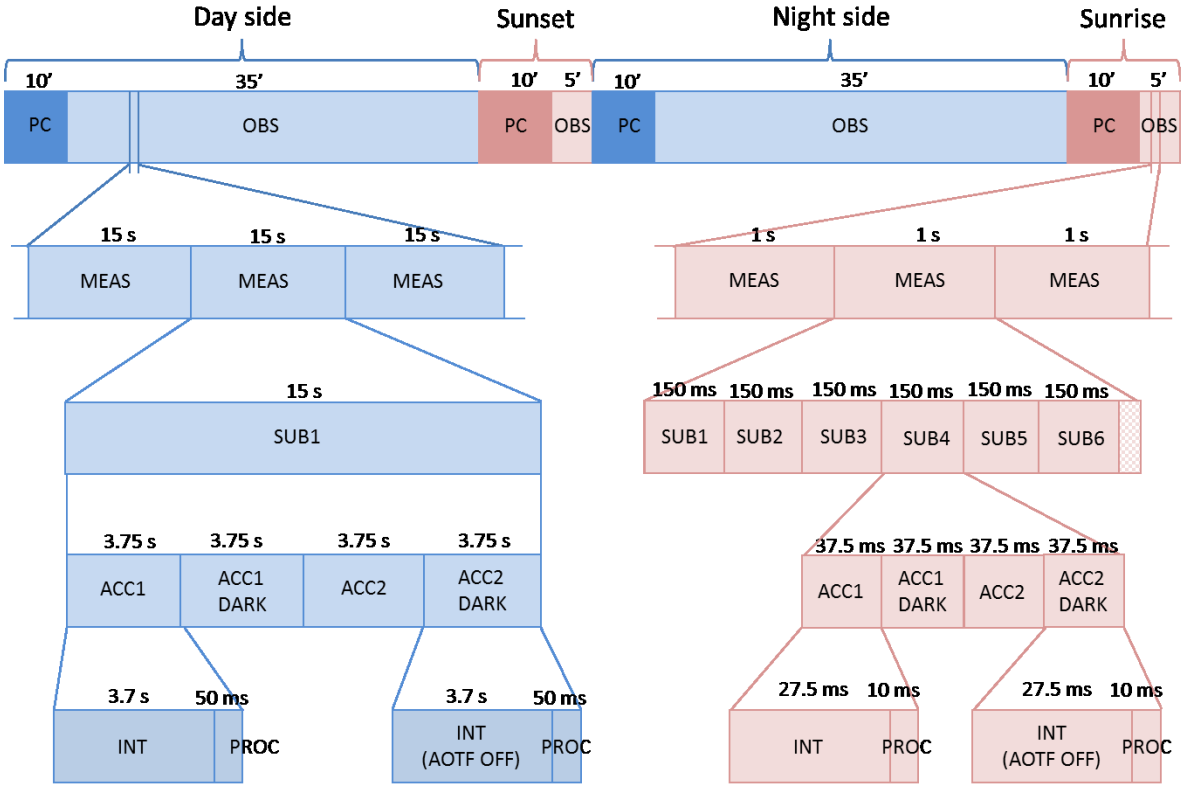

Figure 9: A NOMAD observation sequence with onboard background subtraction. PC = precooling; OBS = observation (nadir or solar occultation); MEAS = measurement; SUB = subdomain; ACC = accumulation; INT = integration time; PROC = process time (including detector read-out, AOTF settling, etc.). Left (blue): nadir observation with 1 subdomain, two accumulations, spectra with 3.7 s integration time. Right (red): solar occultation observation with 6 subdomains, 2 accumulations in subdomain 4, spectra with 27.5 ms integration time. Dark frames are automatically subtracted; the result of which is transmitted back to Earth.

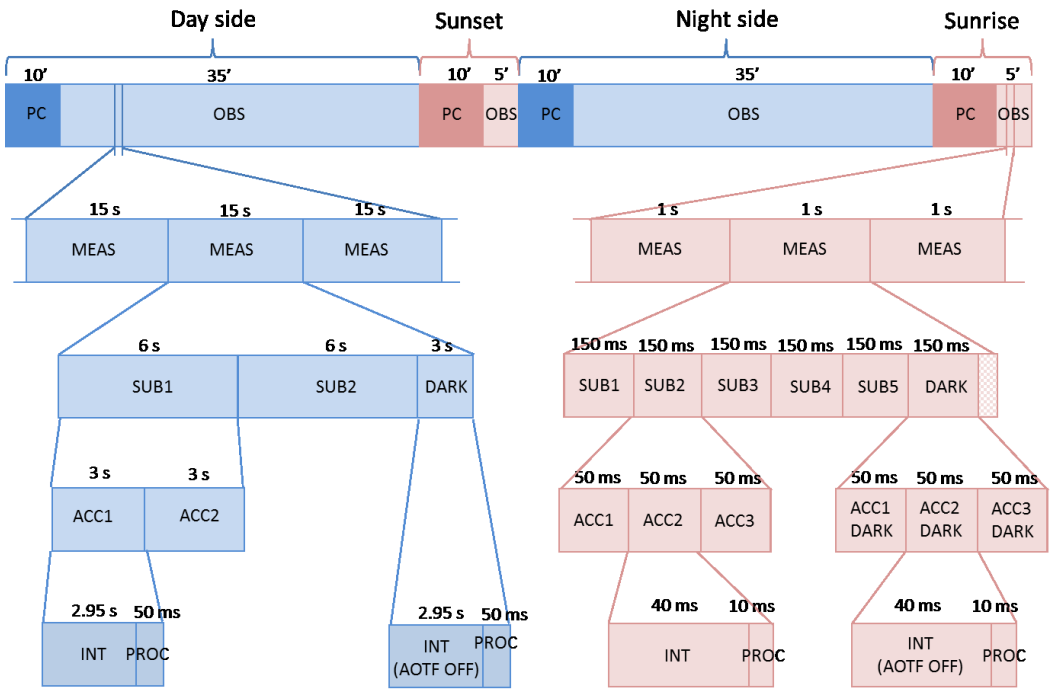

Figure 10: A NOMAD observation sequence with manual background subtraction. PC = precooling; OBS = observation (nadir or solar occultation); MEAS = measurement; SUB = subdomain; ACC = accumulation; INT = integration time; PROC = process time (including detector read-out, AOTF settling, etc.). Left (blue): nadir observation with 2 subdomains, 2 accumulations, spectra with 2.95 s integration time. The dark measurement has only 1 accumulation, so must be multiplied by 2 during processing. Right (red): solar occultation observation with 5 subdomains, 3 accumulations in subdomain 2, spectra with 40 ms integration time. The dark measurement also has 3 accumulations.

2.6.1 Infrared (SO and LNO) Channels

Just before starting a nadir observation or solar occultation measurement with one of the infrared channels it is necessary to cool the detector down to its operating temperature of ~85 K. A command packet is sent from SINBAD to the channel to start this precooling phase. This packet contains parameters such as the cooler temperature set point, an open or closed loop flag and some cooler coefficients allowing smooth regulation. During precooling, which lasts 600 s by default, no spectra are recorded - only housekeeping is sent every second. At

the end of the precooling phase, the channel starts a science observation upon reception of a new command packet. This time the command contains parameters that will permit the channel to do 'real' measurements, such as the AOTF frequency and AOTF power set points[1], the detector integration time, window frame dimensions, the binning factor, and more. For nadir, longer integration times are anticipated and therefore the typical sampling rhythm of 15 s has been chosen. During solar occultations integration times will be much shorter and the sampling rhythm is 1 s.
The command parameters needed to program the precooling phase and the science observation phase, are sent from the S/C to NOMAD by means of a TC20 telecommand packet (over the 1553 bus). One such TC20 defines completely one observation sequence (more details see 2.5.3)

The on-board software of the channels offers a wide range of features to tailor the measurements to the scientific needs. During one measurement rhythm, i.e. in the time frame of 1 second (solar occultation) or 15 seconds (nadir) it is possible to perform up to 6 consecutive measurements, each with different parameter settings. In this hopping mode it is possible to measure in 6 different spectral domains (6 AOTF frequency settings corresponding to 6 grating orders). It is possible to switch from a set of 6 initial subdomains (used during the first half of the observation) to a different set of subdomains in the second half of the occultation. This is especially useful during solar occultation, where the science interest in the upper atmosphere can be quite different from that in the lower atmosphere.

Within one subdomain measurement, a series of consecutively recorded spectra can be co-added, increasing the SNR of a single measurement. These added spectra are called accumulations, which are added together in onboard memory and the sum transmitted to Earth. This is particularly useful to avoid detector saturation, either from the instrument thermal background during nadir measurements or from a combination of solar flux and thermal background during occultation measurements. In these situations, an integration time is chosen so that the detector does not saturate, and the number of accumulations is chosen so that each subdomain is filled with integrations. The combination of integration time and number of accumulations must fit within the duration of one subdomain measurement, and all the subdomains must fit within the time frame of one measurement (determined by the channel's sampling rhythm).

[1] AOTF power settings were calculated in the laboratory prior to assembly of NOMAD. These will not be updated during the mission.

Similarly, consecutive rows of pixels can be binned together to further increase the SNR. The data rate is limited to 24 lines per sampling rhythm (1 or 15 seconds for SO or LNO respectively), meaning that it is not possible to record an entire detector frame pixel-by-pixel during a typical measurement. Spectral binning, where adjacent columns are summed, is not performed, hence binning must be done in the spatial direction to produce 24 lines of superpixels. In occultation mode, approximately 18-22 pixels will be illuminated by the Sun, depending on the Sun-Mars distance. A typical frame measured frame is shown in Figure 11. If 6 subdomains are used, then each subdomain can transmit 4 lines of superpixels only – therefore by binning 5 or 6 rows together, data from all 20 or 24 pixels can be recorded. In nadir mode, 144 pixels will be illuminated, so if 2 subdomains are chosen, a binning factor of 12 will record all illuminated pixels (144 pixels / 12 superpixels per subdomain = 12). The number of illuminated lines in nadir mode will always be >24, therefore vertical binning must always be used to read out all illuminated lines. Typically 144 lines will be illuminated, implying a binning of at least 6. An example of this is given in Table 3.

Sampling Rhythm (seconds)	No. of diffraction orders (subdomains)	Observation time per diffraction order (including dark)	No. of lines per rhythm	No. of lines per diffraction order	No. of lines illuminated by Sun/Mars	Pixel binning required
1 (occ.)	5 + 1 dark	1/6th second	24	4	24	6
1	5+1 dark	1/6th second	24	4	20	5
1	5+1 dark	1/6th second	24	4	16	4
1	6 (on board background subtraction)	1/6th second	24	4	16	4
15 (nadir)	6 (on board background subtraction)	2.5 secs	24	6	144	24
15	4 (back sub.)	3.75 secs	24	6	144	24
15	3 (back sub.)	5 secs	24	8	144	18
15	2 (back sub.)	7.5 secs	24	12	144	12
15	1 (back sub.)	15 secs	24	24	144	6

Table 3: Examples of binning factors required for various observations. Note that the number of lines per rhythm is a data rate limitation imposed by the central processor, and cannot be exceeded. The observation time includes detector readout time, data processing time, and any dark measurements – hence in reality the time spent observing mars can be significantly less than this.

Dark subtraction and the number of diffraction orders are chosen based on a range of factors, as each measurement type has advantages and disadvantages. For SO solar occultations, not subtracting the dark onboard means that the dark frame is transmitted separately. This means that only 5 diffraction orders can be measured, but knowledge of the dark frame means that the transmittance error can be calculated more effectively. Subtracting the dark onboard means that 50% of the available observation time is lost to dark frame measurements, and hence the SNR is reduced, but 6 orders can be measured. For LNO, background subtraction is essential, and the choice of number of diffraction orders is based on the measurement goals for that particular observation. Fewer orders means that more time is spent observing Mars, and hence a higher SNR is achieved, but at the expense of spectral range covered. Typically only 2 or 3 orders should be measured in one observation, if the goal is to measure atmospheric absorption lines. Conversely, measuring 6 diffraction orders gives more spectral coverage, and so can be more useful when absorption lines are not required, for example if the objective is to measure the average reflected radiance in a given order to measure dust or bulk surface properties. The choice can also depend on the solar zenith angle – a smaller angle means the sun is directly overhead and hence the reflected signal is larger.

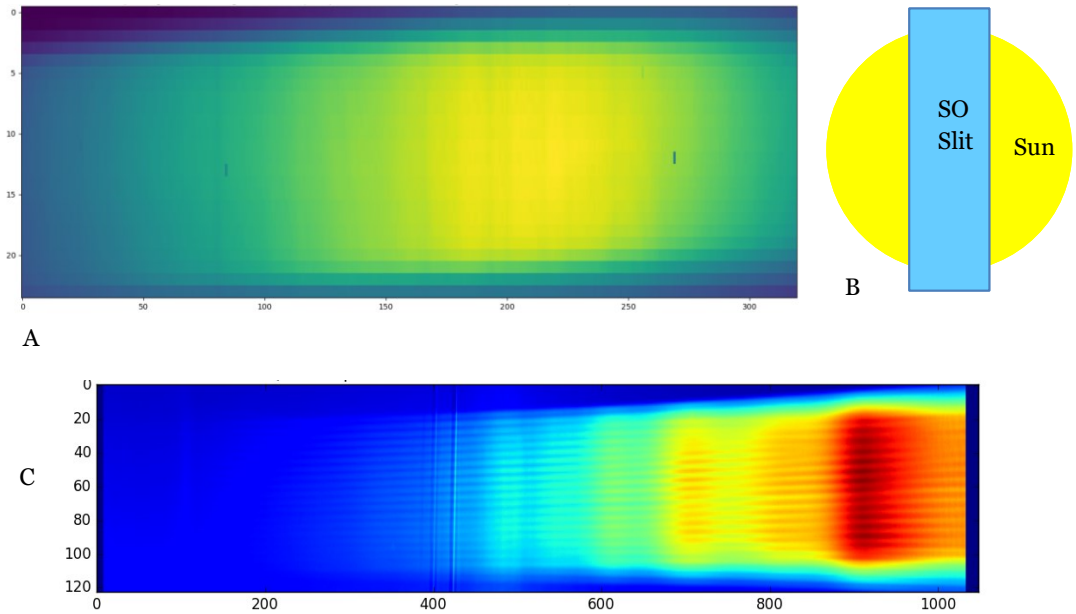

Figure 11: Typical SO occultation (A) and UVIS nadir (C) detector frames. In SO, the horizontal direction is the spectral dimension and the vertical is the spatial dimension corresponding to the long edge of the slit centred on the solar disk (B). In UVIS, the

horizontal direction is the spectral dimension, however no spatial information is retained in the vertical dimension – the illumination pattern follows the layout of the optical fibres.

2.6.2 UVIS Channel

The UVIS channel operates without subdomains, and so an entire spectrum can be recorded each time. There are several options available, the choice of which largely depends on the available data volume:

- Full/reduced spectrum. A full spectrum acquisition consists of 1024 pixels in the spectral dimension, however any subsection of this can be selected, e.g. only the ultraviolet region.
- Unbinned or vertical/horizontal binning. The pixel rows can be binned vertically to produce a frame containing a 1 line x 1024 pixel spectrum (assuming full spectrum), or each pixel value can be transmitted to Earth individually for processing by the data pipeline. Horizontal binning is another option, where every N pixels are binned in the horizontal direction, reducing the spectral resolution (and data volume) but avoiding vertical binning. A final option, square binning, is available where N pixels are binned in the vertical and horizontal directions, but this is not used.

Note that the calibration is severely impaired when vertical binning is used, therefore this mode is avoided (except at the beginning of the science phase, when this was not known). At the time of writing, the data pipeline does not calibrate vertically binned observations and so any observations made using this mode will not appear in the PSA archive. If a calibration pipeline is made in future to treat these observations, they will be delivered to the archive at a later time.

The number of accumulations, number of lines to bin, spectral region, and integration time can all be programmed like the SO and LNO channels, as can the number of frames generated per second. UVIS is also highly programmable, but typically, one occultation or nadir observation consists of:

1. A reverse-clock measurement to measure the bias readout level, consisting of two lines of spectra.
2. Bias frame(s). This contains a frame of spectra measured with a zero integration time, to determine the voltage offset and electronic noise in the CCD and readout electronics.
3. Science frames, with dark frames every N measurements. Science frames are taken of Mars with the required observation parameters (integration time, binning parameters

etc.). Dark frames are taken with the same integration time, binning parameters, but with the selector mechanism in the central position where no light from either solar or nadir fibres can enter the spectrometer. N can be varied from 1 (alternating dark and science frames) to infinity (no dark frames).

4. Final dark and bias frame(s) [optional].

The measurement rate and observation type depends mainly on the available data volume: if large, the value for each detector pixel can be returned individually (or horizontally binned) for processing on ground. When the required data volume is not available, one of the options above can be employed, or the measurement rate can be reduced (by introducing a delay between acquisitions). This applies to both UVIS occultation and nadir; however in occultation mode there are fewer detector rows illuminated and so the vertical range is smaller.

The measurement rate depends on the time taken to acquire the image (integration time), read out the detector, and process/transmit the data. In flight UVIS uses a wide range of integration times, typically 5-15 seconds in nadir and ~100s of milliseconds in occultation mode, and so the measurement rhythm is very variable. Additionally, returning unbinned data requires more time for processing and transmission, and hence a slower rhythm than would be otherwise possible.

2.6.3 Housekeeping and Telemetry

NOMAD is commanded by sending a NOMAD_START_OPERATIONS telecommand [herein referred to as a TC20], which initiates a measurement. Upon reception of the NOMAD_START_OPERATIONS telecommand i.e. a TC20, NOMAD begins an observation. SINBAD will turn on the relevant channels at the correct time. Different types of observations (configurations) can be performed with combinations of the three NOMAD channels: looking at the sun (occultation of the sun by Mars), looking at the limb of Mars, and looking at the surface of Mars beneath TGO (nadir). The TC20 telecommand contains all parameters needed to set up any of these observations.

At all times that NOMAD is switched on, housekeeping (HSK) data is collected by the central processor (SINBAD) and sent to the spacecraft for transmission to Earth. This data contains instrument-wide voltages and temperature data, plus status and error reports, mainly for

engineering purposes and (besides temperature data) are of less importance to this EAICD. One set of HSK data, consisting of three packets, is generated every 30 seconds.

During observations, the channels that are operating generate their own dedicated housekeeping. Science data and supporting data, such as integration time, binning parameters, etc. is also transmitted back to Earth by the channels when they are switched on. The contents of the data returned depends on the channel:

- Each SO/LNO science packet contains a description of the observation parameters provided to the channel by the TC20 telecommand, such as AOTF frequency, number of accumulations, binning type, and whether background subtraction is enabled, etc., to provide context to the science data. Different parameters can be used in different subdomains within one measurement; therefore there is one set of parameters per diffraction order.
- Each UVIS science packet also contains a description of the observation parameters and housekeeping related to each detector frame acquired. In addition to this, UVIS also sends a dedicated packet containing the COP row parameters (TC27) sent to the channel, and an additional housekeeping packet every second whilst operating (TC29). More information can be found in the following section and in the NOMAD User Manual RD09.

2.6.3.1 ***Packet Type Numbers***

Data is uploaded/downloaded from TGO in the form of packets, each type of which has been designated a number. The majority of these are off no interest to PSA users, such as those for patching software or moving the LNO flip mirror, for example. Packet types 122 and 125 are explained in section 3.3.1. The TC20 parameters are explained below.

Packet Type Number	Packet Type	Description
TC20	Telecommand	Instruction to start observation
TM22	SO SpaceWire data	Scientific data from SO channel
TM25	LNO SpaceWire data	Scientific data from LNO channel
TM27	UVIS applied parameters	Observation parameters returned from UVIS channel

TM28	UVIS SpaceWire data	Scientific data from UVIS channel
TM29	UVIS SpaceWire housekeeping	Additional housekeeping data from UVIS channel
TM60	SINBAD (NOMAD central processor) system logs	Engineering system logs from NOMAD central processor (not for PSA users)
TM122	Corrected SO SpaceWire data	Corrected scientific data from SO channel
TM125	Corrected LNO SpaceWire data	Corrected scientific data from LNO channel

Table 4: Packet types and their associated numbers. Packet types 122 and 125 are explained in section 3.3.1.

2.6.4 NOMAD TC20 Parameters

A TC20 telecommand initiates a science measurement, containing the timing and observational parameters. The latter are shown in bold below:

- SO start time
- SO start time science 1
- SO start time science 2
- SO duration reference 1
- SO duration reference 2
- SO duration time
- **SO COP general (FIXED COP Table)**
- SO COP precooling
- **SO COP science 1 (SUBDOMAIN COP Table)**
- **SO COP science 2 (SUBDOMAIN COP Table)**
- LNO start time
- LNO start time science 1
- LNO start time science 2
- LNO duration reference 1
- LNO duration reference 2
- LNO duration time
- **LNO COP general (FIXED COP Table)**

- LNO COP precooling
- **LNO COP science 1 (SUBDOMAIN COP Table)**
- **LNO COP science 2 (SUBDOMAIN COP Table)**
- UVIS start time
- UVIS duration time
- **UVIS COP row (UVIS COP Table)**

Each of the parameters in bold contains a pointer to a line in the SO FIXED, SO SUBDOMAIN, LNO FIXED, LNO SUBDOMAIN and UVIS COP (Command Operation Parameter) tables, which contain values that specify a particular type of measurement. These COP tables are described in Table 5. A description of the timing parameters is shown in Figure 12.

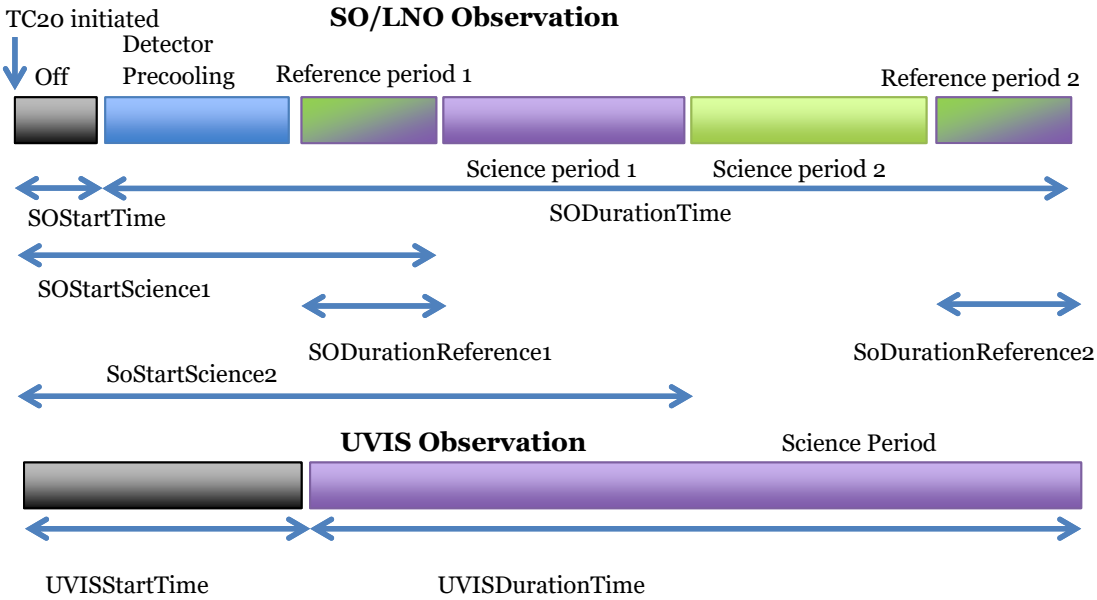

Figure 12: TC20 timing parameters and how they relate to observation start and end times. Note that all references to SO also apply to LNO, however a nadir observation generally uses no reference periods and a single science period only. In these cases, LNOStartTime, the precooling time (10 minutes) and the LNODurationTime parameters are sufficient to calculate the observation timing. The UVIS science period normally begins at the same time as the SO/LNO reference period for solar occultations, or at the beginning of the LNO detector precooling for nadir observations.

COP Table	Brief description of each line in the table

bira_so_precooling_table.csv	Contains SO detector cooling parameters (not applicable here)
bira_so_fixed_table.csv	Contains SO window size, window position and measurement rhythm parameters
bira_so_sub_domain_table.csv	Contains pointers to lines in the so_science_table. Allows up to 6 different science measurements to be made in one measurement rhythm period. For calibration, only one pointer is typically specified
bira_so_science_table.csv	Contains pointers to the so_stepping and so_aotf tables, plus measurement parameters such as binning, integration time, background subtraction etc.
bira_so_stepping_table.csv	Contains SO stepping parameters typically used for calibration measurements e.g. instructions to step integration time, AOTF frequency, window position, diffraction order etc.
bira_so_aotf_table.csv	Contains SO AOTF RF driver power and frequency parameters for each diffraction order and miniscan.
bira_lno_precooling_table.csv	Contains LNO detector cooling parameters (not applicable here)
bira_lno_fixed_table.csv	Contains LNO window size, window position and measurement rhythm parameters
bira_lno_sub_domain_table.csv	Contains pointers to lines in the lno_science_table. Allows up to 6 different science measurements to be made in one measurement rhythm period. For calibration, only one pointer is typically specified
bira_lno_science_table.csv	Contains pointers to the lno_stepping and lno_aotf tables, plus measurement parameters such as binning, integration time, background subtraction etc.
bira_lno_stepping_table.csv	Contains LNO stepping parameters typically used for calibration measurements e.g. instructions to step integration time, AOTF frequency, window position, diffraction order etc.
bira_lno_aotf_table.csv	Contains LNO AOTF RF driver power and frequency parameters for each diffraction order and miniscan.
bira_uvis_table.csv	Contains the observation parameters for UVIS measurements

Table 5: COP tables in NOMAD

These COP tables are programmed into NOMAD, but can be modified by patching the filesystem. Each line in the tables contain a different selection of values, so by selecting a certain combination of FIXED and SUBDOMAIN lines, many different types of measurements can be made.

2.7 Calibration

2.7.1 Expected Performance

For NOMAD's Critical Design Review, a radiometric model was made to calculate the expected performance of NOMAD's channels in all possible observation modes.

With NOMAD having 5 fields of view (see section 2), pointing in two directions, it was not possible to test them all during ground calibration – and therefore the two nadir channels were given priority (the occultation channels can in theory be calibrated in-flight using the solar reference spectrum taken at the beginning or end of the observation period). Spectral calibration of the occultation channels was performed, but radiometric performance was not tested – and hence, importantly, the theoretical radiometric model is described here. Expected performances will be confirmed during calibration and science phases.

In general, calibration can be split into several individual tests to determine specific instrument characteristics. These are:

- Spectral calibration, including AOTF passband shape and spectral location vs. applied driver frequency and diffraction order limits
- Determination of true SNR (Signal-to-Noise Ratio)
- Mapping of bad detector pixels
- Pixel linearity of response w.r.t. incident radiance
- Detector thermal saturation time/dark current
- Straylight calibration

2.7.1.1 Infrared Channels

Table 6 and Table 7 show the theoretical diffraction order wavelengths for the SO and LNO channels, calculated from the optical parameters of the channels, taken from Neefs et al. (2015). Here:

- λ_c is the central wavelength of that order, which lies on the centre of the detector
- ν_c is the central wavenumber of that order
- $\Delta\lambda_o$ is the range of wavelengths within the free spectral range (FSR) of that diffraction order
- $\Delta\lambda_e$ is the range of wavelengths that are incident on the detector in the given order.

Note that LNO has a smaller total spectral range than SO, therefore has less measurable orders.

Order	λ_c (µm)	ν_c (cm^{-1})	FSR $\Delta\lambda_o$ (µm)	Detector $\Delta\lambda_e$ (µm)

100	4.4302	2257	4.4082 - 4.4524	4.4123 - 4.4477
110	4.0275	2483	4.0093 - 4.0459	4.0112 - 4.0434
120	3.6919	2709	3.6765 - 3.7073	3.6770 - 3.7064
130	3.4079	2934	3.3948 - 3.4210	3.3941 - 3.4213
140	3.1661	3158	3.1532 - 3.1758	3.1517 - 3.1769
150	2.9535	3386	2.9437 - 2.9637	2.9416 - 2.9651
160	2.7689	3612	2.7603 - 2.7776	2.7577 - 2.7798
170	2.6060	3837	2.5984 - 2.6137	2.5955 - 2.6163
180	2.4612	4063	2.4544 - 2.4681	2.4513 - 2.4709
190	2.3317	4289	2.3256 - 2.3379	2.3223 - 2.3409
200	2.2151	4514	2.2096 - 2.2207	2.2062 - 2.2239

Table 6: Theoretical values for λ_c, $\Delta\lambda_o$ and $\Delta\lambda_e$ for SO from Neefs et al. (2015) [RD04]

Order	λ_c [µm]	ν_c (cm^{-1})	λ_{o+} [µm]	λ_{e^-} [µm]
120	3.6914	2709	3.6761 - 3.7069	3.6765 - 3.7059
130	3.4076	2935	3.3944 -3.4206	3.3937 -3.4208
140	3.1641	3160	3.1528 -3.1754	3.1513 -3.1765
150	2.9531	3386	2.9433 -2.9630	2.9412 -2.9647
160	2.7686	3612	2.7599 -2.7772	2.7574 -2.7794
170	2.6057	3838	2.5980 -2.6134	2.5952 -2.6159
180	2.4609	4064	2.4541 -2.4678	2.4510 -2.4706
190	2.3314	4289	2.3253 -2.3376	2.3220 -2.3406
200	2.2148	4515	2.2093 -2.2204	2.2059 -2.2235

Table 7: Theoretical values for λ_c, $\Delta\lambda_o$ and $\Delta\lambda_e$ for LNO from Neefs et al. (2015) [RD04]

The SNR of a detector pixel in the NOMAD channels is obtained in the radiometric model by taking into account the signal flux and sources of noise incident on that pixel during the given exposure time.

The model showed that in solar occultation mode, the SNR is expected to be around 3000-5000; whilst in nadir, LNO is expected to have an SNR of around 30-100. A wide variation is expected due to variable dust opacities, illumination angles, instrument temperature, etc. These values represent idealized cases, where the integration time is chosen to maximise the signal without saturating the detector and observation conditions are nominal. In nadir mode, where SNRs are lower, a good signal can only be recovered by binning all illuminated pixels in multiple accumulations. Therefore, here all 144 illuminated pixels have been binned, and the number of accumulations has been set to fill a 15s measurement: in reality, each 15 seconds will be split into multiple diffraction orders, plus time will be used for dark

measurements and detector readout. For SO and LNO in solar occultation mode, the expected signal is very high and therefore spatial information will be retained.

More information on this can be found in Vandaele, A. C. et al. (2015) " Optical and Radiometric Models of the NOMAD Instrument Part I: The UVIS Channel" [RD07] and Thomas et al. (2015) "Optical and Radiometric Models of the NOMAD Instrument Part II: The Infrared Channels - SO and LNO (2016)" [RD08].

2.7.2 On-ground Calibration Measurements

The following tests on the given channels were performed during ground calibration:

- Mapping of bad detector pixels (SO/LNO/UVIS)
- Pixel linearity w.r.t. radiance (SO/LNO/UVIS)
- Detector thermal saturation time/dark current at different temperatures (SO/LNO/UVIS)
- Spectral calibration of channel and/or AOTF at different temperatures (LNO/UVIS nadir)
- Spectral calibration of channel and AOTF (SO)
- Blackbody measurements at various temperatures to correlate observations with SNR model (LNO)
- Straylight calibration (UVIS nadir)

The SO/LNO and UVIS ground calibration papers are currently in preparation. This section will be updated accordingly when complete.

2.7.3 In-flight Calibration Measurements

Three calibrations campaigns were performed prior to the start of the nominal science mission:

- Near-Earth Commissioning (NEC) in April 2016
- Mid-Cruise Checkout (MCC) in June 2016
- Mars Capture Orbit (MCO) in November 2016, after EDM separation and orbit insertion.

In addition to this, if NOMAD has, for any reason, been inactive for a month during the science phase, a calibration campaign will be performed. Otherwise, calibration sessions will be planned within the science phase, as part of normal operations, to assess instrument performance. Some require specific pointing and will be planned with the MOC.

The following operations are planned during Near Earth Checkout:

- Functional check (typical science orbit measurement with pointing)
- Line of sight (LoS) misalignment
- Dark sky (thermal background) calibration
- 'Light sky' calibration
- Spectral calibration
- Straylight calibration
- Earth/Jupiter/Stellar pointing calibration
- UVIS CCD and nadir-to-occultation-mode mechanism calibration

2.7.3.1 LoS Misalignment

The misalignment between the NOMAD solar LoS and the pointing axis of the S/C has to be checked in flight. When a new boresight vector has been calculated, this will be updated in the SPICE kernel for the channel affected. This calibration session will be repeated every 4 to 5 months during the science phase.

2.7.3.2 Dark Sky Calibration

During dark sky calibration sessions, dark current and (thermal) background measurements are performed for different integration times of the detectors. These measurements are used to determine the optimum integration time that does not saturate the detector (nadir), and can also be used to map dead pixels (all channels). For UVIS, a photon transfer curve can be calculated from the data. These differ from the individual dark frames taken during science observations: the latter are simply frames taken with the same integration time as the light frame but with the AOTF off (SO/LNO) or selector mechanism in dark position (UVIS), to allow background subtraction. For dark sky calibrations, the boresights are pointed towards dark space, and many frames are measured consecutively with gradually increasing integration times to produce a curve of signal vs integration time. For LNO nadir measurements, the instrument thermal background dominates the signal from Mars, therefore the saturation integration time can be determined from this curve, in addition to bad pixels (i.e. pixels giving unexpected values) and detector non-linearity (i.e. deviations from a straight line).

2.7.3.3 'Light Sky' Calibration

These are integration time stepping measurements as above, except that the occultation fields of view are pointed towards the sun. These measurements are also used to determine the optimum integration time that does not cause detector saturation for solar occultation measurements, where the sun signal dominates the thermal background.

2.7.3.4 Spectral Calibration

For the SO and LNO channels, a spectral calibration is performed by stepping the AOTF driving frequency through the spectral domain while a source with known emission/absorption lines is being viewed (i.e. the sun). This allows calibration of the AOTF driver and the pixel-wavenumber relation to be derived. UVIS takes a complete spectrum each time, therefore the spectral calibration is derived by comparing the observed solar absorption/emission lines to a reference solar spectrum

2.7.3.5 Straylight Calibration

Straylight calibration sessions serve to check the instrument's immunity to stray light generated inside the instrument by the Sun or solar reflection on the S/C. This involves slewing the spacecraft so that the occultation fields of view (SO/LNO occultation/UVIS occultation) point initially at dark space, then move across the solar disk, and end on dark space again. The amount of solar signal detected when pointing at dark space provides an estimate of the straylight entering the instrument during science measurements. This calibration session has to be done 2 or 3 times during the mission.

2.7.3.6 Earth/Mars/Phobos Pointing Calibration

The boresight of LNO could not be measured on the ground, and therefore this type of measurement is essential to calculate the misalignment between the LNO boresight and the TGO axis + UVIS nadir boresight.

The sun is too bright for calibration of the UVIS nadir channel and TGO is not permitted to point the nadir-facing surface towards the sun – therefore the LoS misalignment calibration of LNO and UVIS nadir requires a fainter source. During Near Earth Commissioning, the Earth was sufficiently close to the spacecraft to be visible by both channels, however the observation was forbidden due to the nadir boresights pointing too close to the Sun.

Other sources, such as Jupiter and stars were attempted during NEC and MCC, but the results were inconclusive, and therefore the misalignment was performed when around Mars by repeatedly scanning the limb of the planet. The nadir boresights were measured successfully during MCO-1 and MCO-2, by scanning the LNO and UVIS nadir fields of view across the limb of Mars to determine the limb crossing time.

2.7.3.7 UVIS CCD and selector mechanism calibration

The UVIS channel records spectra of an illuminated source using either the solar or nadir entrance optics. The selector mechanism, starting from its rest position (dark), travels to the solar occultation hard stop, then to the nadir hard stop, and finally to the solar occultation hard stop again, before returning to the initial rest position. This characterises the fibre-slit

alignment, allowing the exact motor position to be determined when the light can pass from the entrance optics into the spectrometer section.

Measurement Type	Channel	Calibration Type	Implementation
Line of sight	All	Boresight misalignment	Boresight vector (implemented in SPICE kernel)
	SO/LNO	Vertical detector calibration	Detector illumination region (implemented in choice of detector region in all observations)
Light sky (sun integration time stepping)	All	Detector linearity, optimum integration time determination	Detector linearity curve (calibration product)
Dark sky (dark space integration time stepping)	All	Detector linearity	Detector linearity curve (calibration product)
	SO/LNO	Bad pixel map	Bad pixel map (calibration product)
	LNO nadir	Optimum nadir integration time determination	Integration time as implemented in all observations by inst. team
Miniscan	SO/LNO	Spectral calibration of AOTF (order and transfer function) and detector (pixel-wavenumber relation), blaze function.	AOTF frequency coefficients, AOTF transfer function coefficients, blaze function coefficients
Fullscan (sun pointing)	SO/LNO occ.	Optimum integration time per diffraction order	Integration time as implemented in all observations by inst. team
	LNO	Solar spectrum per diffraction order for radiance calibration	Solar spectrum per order product (like occultation product without radiometric calibration)
Geometric straylight (solar raster scan)	LNO nadir	Determination of geometric straylight from outside the field of view	Removal of affected frames
Spectral straylight	UVIS	Determination of spectral straylight from known radiance sources in lab	Straylight correction spectrum

Table 8: Calibration measurement types and how the results are used to calibrate NOMAD.

As described in sections 2.7.2 and 2.7.3, there are a wide range of calibration measurement types, and an equally wide range of calibration parameters derived from these. Table 8 shows how the measurements made relate to the calibration types, and how the calibration is implemented in the pipeline.

The SO/LNO and UVIS in-flight calibration papers are currently in preparation. This section will be updated accordingly when complete.

2.8 Observation types for NOMAD data products

All NOMAD observations are defined using one of the observation types listed below. The observation type letter is included in all calibrated product filenames for ease of use. The raw and partially processed products do not contain this information.

I = Ingress solar occultation.

NOMAD performs an observation during a sunset, where TGO points the boresights to the centre of the Sun. The observation will start some minutes before the line of sight enters the atmosphere (full sun reference spectra) and will continue some minutes after the line of sight has hit the Martian disk (dark spectra). These are standard science measurements where for SO a small selection of diffraction orders are cycled through repeatedly. This is the baseline science observation during an ingress.

E = Egress solar occultation.

NOMAD performs an observation during a sunrise, where TGO points the boresights to the centre of the Sun. The observation will start some minutes before the line of sight leaves the Martian disk (dark spectra) and will continue some minutes after the line of sight has left the atmosphere (full sun reference spectra). These are standard science measurements where for SO a small selection of diffraction orders are cycled through repeatedly. This is the baseline science observation during an egress.

G = Grazing solar occultation (currently only applies to SO data in levels 0.3K and above).

TGO points the boresights to the centre of the Sun, except in this case the line of sight never intersects the planet's surface due to the Sun-Mars-satellite geometry. The observation begins above the atmosphere and ends above the atmosphere. Due to the lack of dark spectra, an error is not calculated and therefore these observations do not pass through the data pipeline. Data will be made available when a calibration routine is ready. **At present these observations are not converted to transmittance by the pipeline, though the other calibrations are applied. Prior to level 0.3K, grazing and merged occultations are given the letter I.**

S = Fullscan (SO/LNO only, during a solar occultation observation).

TGO points the NOMAD boresights to the centre of the Sun during this observation. This has to be done while the FOV passes through the atmosphere, i.e. a normal Ingress or Egress observation has to be sacrificed, or the fullscan has to be combined with the Ingress or Egress observation (only during a long occultation at high beta angle). The SO or LNO channel will perform a sweep over the complete or a subset of the spectral range, one diffraction order at a time. These measurements could be calibrated spectrally and radiometrically, but will not typically pass through the occultation pipeline. If operating simultaneously, UVIS will observe in normal Ingress or Egress mode during this time: a fullscan does not apply to UVIS.

F = Fullscan (SO/LNO only, during a nadir observation).

TGO will point the NOMAD nadir boresights to nadir during this observation, i.e. a normal dayside or nightside nadir observation has to be sacrificed. The LNO channel will perform a sweep over its complete or a subset of the spectral range, one diffraction order at a time. These measurements can be calibrated spectrally and radiometrically, but will not typically pass through the nadir pipeline (they are typically used for testing purposes). If operating simultaneously, UVIS will observe in normal nadir mode during this time: a fullscan does not apply to UVIS.

D = Dayside nadir.

TGO will be in its nominal pointing conditions, i.e. the –Y direction is aimed approximately towards the centre of Mars, perpendicular to the surface directly underneath it. The sun is positioned such that the surface is illuminated. In principle NOMAD can measure with LNO and UVIS at any time that the TGO axis is pointing nadir. These are standard science measurements where for LNO a small selection of diffraction orders are cycled through repeatedly. This is the baseline science observation during a nadir.

N = Nightside nadir.

TGO will be in its nominal nadir pointing condition, i.e. –Y direction approximately towards the centre of Mars. The region of the surface in nadir is in darkness. These are standard science measurements where for LNO a small selection of diffraction orders are cycled through repeatedly. This is the baseline science observation during a nadir.

P = Phobos

TGO will point a nadir boresight (typically either LNO, UVIS or the spacecraft -Y) towards the moon Phobos. LNO performs either a standard science measurement, usually with a reduce field of view, where a small selection of diffraction orders are cycled through repeatedly, or a fullscan over a subset of the spectral range, one diffraction order at a time. UVIS typically observes in full frame mode, as the moon is small and so the signal does not fill the entire field of view.

Q = Deimos

TGO will point a nadir boresight (typically either LNO, UVIS or the spacecraft -Y) towards the moon Deimos. LNO performs either a standard science measurement, usually with a reduce field of view, where a small selection of diffraction orders are cycled through repeatedly, or a fullscan over a subset of the spectral range, one diffraction order at a time. UVIS typically observes in full frame mode, as the moon is small and so the signal does not fill the entire field of view.

L = Limb

One or more NOMAD channel FOVs will be pointed towards the limb of Mars. This can be achieved by rotating the spacecraft, so that the nadir (-Y) face of the spacecraft is pointed to the limb, or for LNO by using the occultation channel whilst not pointed to the sun. These are standard science measurements where a small selection of diffraction orders are cycled through repeatedly, and measurements will be calibrated using the nadir pipeline.

C = Calibration

This type encompasses all calibration measurements, which are given a secondary letter to distinguish the calibration type:

- CL = Pointing calibrations, where TGO performs a line or raster scan around a target (typically the Sun). From these measurements the misalignment can be calculated between the S/C pointing axis and the NOMAD boresights. This misalignment value will be used afterwards to correct the S/C pointing vector.

- CF = Fullscans (SO/LNO only), but when the FOV does not pass through the atmosphere. The S/C will point a boresight to the centre of the Sun during this observation, which can be done at any time when the Sun is visible. The NOMAD SO and/or LNO channels will perform a sweep over their complete spectral range. These measurements can be calibrated spectrally but not radiometrically.

- CM = Miniscans (SO/LNO only), where the channels will perform a sweep over a fraction of their spectral range whilst pointing towards the sun (but when the FOV does not pass through the atmosphere). These are used for spectral calibration, namely to generate a set of coefficients to calibrate all the other observations. These measurements can be calibrated spectrally but not radiometrically.
- CS = Solar/dark sky stare. The channel observes the Sun for an extended period of time; this is occasionally performed by UVIS during an SO/LNO solar fullscan or miniscan observation. The SO and LNO channels can performed an integration time stepping observation, where the integration time is gradually increased so that the saturation time can be determined. Channels may be pointed towards the Sun or dark sky. These measurements can be calibrated spectrally but not radiometrically.

The correct observation type letter will be included in all calibrated PDS4 product filenames that are generated by the PI institute (see section 4.4).

2.9 NOMAD Observation Strategy

2.9.1.1 Possible Observation and Measurement Types

As described above, all three channels of NOMAD are very versatile and able to run many different types of measurements and in many different observation modes. For reference, all possible modes and measurement types are given in Table 9 and Table 10.

Observation Types	Description
Ingress solar occultation	Normal solar occultation starting when the line of sight is above the atmosphere and ending when sun is blocked by the surface.
Egress solar occultation	Normal solar occultation starting when the line of sight to the sun is blocked by the surface and ending when it is above the atmosphere.
Merged solar occultation	Double solar occultation, consisting of an ingress, starting above atmosphere, and an egress, ending above atmosphere. These occur when there is insufficient time between the ingress and egress to cool down the infrared detector for the second measurement, and will be split into normal ingress and egress occultations.
Grazing solar occultation	Solar occultation where, due to orbital geometry, the sun is never blocked by the surface. Starting above the atmosphere, the line of sight passes through the atmosphere to a minimum altitude, then increases to end above the atmosphere.
Dayside Nadir	Nadir measurement on the illuminated side of the planet. Observations can be of variable length, beginning and ending near the nightside terminator to cover the whole dayside, or shorter and centred on the subsolar latitude. Can also be split into 3 separate measurements.
Nightside Nadir	Nadir measurement on the nightside of the planet.
Dayside Limb	Measurement of the illuminated limb of the planet.
Nightside Limb	Measurement of the non-illuminated limb of the planet.
Calibration	Many types e.g. sun pointing, solar line scan, etc.

Table 9: All possible observation types currently envisaged by the NOMAD team

Measurement Types - SO/LNO Channels	Description
Solar occultation (50km switch)	5 diffraction orders + 1 dark per second. When the line of sight reaches 50km , the combination of diffraction orders being measured is changed. No onboard background subtraction.
Solar occultation (0-	5 diffraction orders + 1 dark per second, same order selection

250km)	throughout. No onboard background subtraction.
Solar occultation (50km switch, dark subtraction)	6 diffraction orders per second, diffraction order selection changed at 50km. Dark frames subtracted onboard.
Solar occultation (0-250km, dark subtraction)	6 diffraction orders per second, same order selection throughout. Dark frames subtracted onboard.
Nadir	Nadir measurement of 2 to 6 diffraction orders per 15 seconds, dark subtracted onboard.
Limb	Limb measurement of 2 diffraction orders per 15 seconds, dark subtracted onboard.
ACS Boresight Limb	Special limb measurement of 2+ diffraction orders, measured during an ACS/MIR or ACS/TIRVIM solar occultation where line of sight is pointed close to the sun but not directly at the solar disk. Onboard dark subtraction.
Fullscan (slow)	Nadir, limb or occultation diffraction order stepping over any range/number of orders, dark subtracted onboard.
Fullscan (fast)	Solar occultation order stepping over any range/number of orders at a high cadence rate, dark subtracted onboard.
Calibration	Many types e.g. line of sight, solar fullscan, solar miniscan, integration time stepping, etc.
Measurement Types - UVIS Channel	**Description**
Solar occultation (binned)	Detector pixel values are vertically binned onboard. 3 full or partial spectra are recorded per second. No dark subtraction is made onboard.
Solar occultation (unbinned)	Each pixel value is stored individually. Full or partial spectra can be transmitted to Earth at a variety of cadence rates. No dark subtraction is made onboard.
Solar occultation (horizontally binned)	N pixels are horizontally binned (in the spectral dimension), but not in the vertical direction. Full or partial spectra can be transmitted to Earth at a variety of cadence rates. No dark subtraction is made onboard.
Nadir (binned)	Detector pixel values are vertically binned onboard. Full or partial spectra can be transmitted to Earth at a variety of cadence rates. Occasional dark frames are taken and transmitted to Earth
Nadir (unbinned)	Each pixel value is stored individually. Full or partial spectra can be transmitted to Earth at a variety of cadence rates. Occasional dark frames are taken and transmitted to Earth.
Nadir (horizontally	N pixels are horizontally binned (in the spectral dimension), but

binned)	not in the vertical direction. Full or partial spectra can be transmitted to Earth at a variety of cadence rates. Occasional dark frames are taken and transmitted to Earth.
Calibration	Many types e.g. line of sight, integration time tests, etc.

Table 10: All possible measurement types currently envisaged by the NOMAD team.

2.9.1.2 Nominal Observation Modes and Measurement Types

Given the large number, it is not feasible to describe every possible observation mode and measurement type combination, and hence this EAICD will detail only the nominal science modes, as given in Table 11, for which the data will be converted to PDS4 format and delivered to the PSA. This list will increase as more observation types are calibrated.

Channel	Observation Mode	Measurement Type(s)	Description
SO	Ingress	Solar occultation, 0-250km, or 0-50km and 50-250km	1-6 diffraction orders
	Egress	Solar occultation, 0-250km, or 0-50km and 50-250km	1-6 diffraction orders
	Merged	Solar occultation, 250km-0-250km	1-6 diffraction orders. Occultations will be split into Ingress and Egress
LNO	Dayside Nadir	Nadir, observation centred on surface point with lowest solar incidence angle	1-6 diffraction orders
UVIS Occultation	Ingress	Solar occultation, 0-250km	Detector is horizontally binned or unbinned.
	Egress	Solar occultation, 0-250km	Detector is horizontally binned or unbinned
	Merged	Solar occultation, 250km-0-250km	Detector is horizontally binned or unbinned. Occultations will be split into Ingress and Egress
UVIS Nadir	Dayside Nadir	Nadir, observation centred on surface point with lowest solar incidence angle	Detector is horizontally binned or unbinned

Table 11: Nominal science modes that will be converted to PDS4 format and delivered to the PSA.

3 DATA GENERATION AND ANALYSIS PROCESS

The NOMAD science products are produced by the NOMAD Instrument Team in cooperation with the SGS. The data generation and analysis process is described in this section, and follows the general concept for data generation, validation and archiving described in the Archiving Plan [AD.01].

Science data received by the SGS from the NOMAD team are made available to end users through the ExoMars 2016 archive following the policies described in the Archiving Plan [AD.01].

3.1 Data Flow Overview

Under the full responsibility of the PI institution (IASB-BIRA), the NOMAD team will produce and archive the data of the NOMAD instrument adhering to the recommendations and specifications imposed by ESA/NASA for this mission, with timely delivery of data products in appropriate formats to the ESA PSA.

NOMAD's science and instrument housekeeping data (including copies of all telecommands and relevant S/C housekeeping data), captured via the DSN, collected in the MOC and transferred to the SOC, will be recovered through the ESA PSA as soon as available during the complete mission duration. The PI institute will archive the science and instrument housekeeping data recovered from the PSA.

Documentation on the data acquisition, conversion and processing is crucial to the long-term success of the project. Conversion from raw to calibrated data is documented here in this EAICD (section 3.3) and is updated when modifications are made. The data pipeline code, including software algorithms and code of all stages in the reduction process (recovery, validation, reduction, archiving etc.) is kept under version control at all times.

Data products generated by the PI institute will be delivered via the ESA PSA when successfully validated.

3.1.1 Data levels

The levels to be delivered to the ESA PSA are given in Table 12. The ESA SOC delivers raw binary Level 0.0 instrument data via the EDDS. Upon receipt, NOMAD's In-flight Operations Team perform a consistency check on the data. In case of unexpected behaviour, actions will be undertaken to guarantee the safety of the instrument during further operations.

Raw PDS4 products are generated by the SOC from raw telemetry, and are deposited directly into the PSA archive. Partially processed PDS4 products are also generated by the SOC, and are deposited directly into the PSA archive. In these products, housekeeping data is converted from raw binary to physical units using the following formulae given in the appendix in Table 4645, Table 4746, Table 4847, and Table 4948.

The PI data processing pipeline will convert raw data to calibrated (Level 1.0 and above) data on a regular basis, which will be integrated automatically into the NOMAD archive. Calibrated data will be made available in PDS4 format via the PSA. All NOMAD Co-Is will have access to the calibrated data immediately and without restriction. As the conversion from raw to calibrated data is fully automated, a swift delivery of raw, calibrated and ancillary data products to ESA and NASA's planetary archive systems is achievable once the data processing pipeline is ready and has been reviewed. Production, archiving and delivery of science (Level 2.0, 3.0 and above) data products are under the responsibility of NOMAD's Science Team jointly steered by PI and Co-PIs.

If errors are detected in an observation that cannot be corrected, the data pipeline will reject the measurement and a corresponding calibrated product will not be produced. This is particularly true for solar occultations, where the calibration involves an extrapolation (see section 3.3.19) - a check is performed to ascertain whether the extrapolation is valid or not. If not valid, the data is not processed further.

Primary Data	
Processing Level Description	**Processing Level Description**
Raw	Raw products from science telemetry packets, in the form of ASCII tables
Partially Processed	HSK corrected data Detector corrections (linearity, dark current, etc) fully reprocessed when in-flight calibration available
Calibrated	Calibrated data + supporting geometry (Level 1.0) Full reprocessed when updated in-flight calibration available

	SO, LNO and UVIS (solar occultation mode): pixel-wavenumber/wavelength, transmittance LNO, UVIS (nadir mode): pixel-wavenumber/wavelength + radiance
Derived	Retrieved atmospheric profiles/columns with supporting geometry (Level 2.0) Global atmospheric fields from GCM (Level 3.0)
Supplementary Data	
Type	**Description**
Calibration	Calibration coefficients and products made from calibration observations
Miscellaneous	Additional data products: Telecommands; data conversion history;

Table 12: ESA PSA data levels for NOMAD as defined in the Science Data Generation, Validation and Archiving Plan.

3.2 Data Processing Pipeline Outline

BIRA-IASB's internal data levels are summarised below, to show which calibration and data conversion steps take place at each level. Those in purple will be generated in PDS4 format and made available on the ESA PSA; the remainder will be generated by the PI team for internal science team use only. A flowchart of this process is shown in Figure 13.

Broadly speaking, observations can be sorted into 3 categories - science, test, and calibration observations:

- Science observations. These are the vast majority of observations, denoted by all the observation type letters except those related to calibration (CL, CS, CF, CM etc.). These pass through the normal data pipeline, meaning that the full data processing treatment is applied to them, and are provided to the ESA PSA by default.
- Test observations. These are non-calibration datasets that do not pass through the data pipeline for various reasons (calibration not ready, observation made only for testing, etc.)

- Calibration observations. These datasets are used only to calibrate NOMAD and have no direct scientific value. They cannot be radiometrically calibrated but in some instances can be spectrally calibrated. These are provided to the ESA PSA as calibration products

In addition to the observations listed above, products containing derived calibration coefficients have also been delivered to the ESA PSA.

All the steps taken to process the data are detailed below. At BIRA-IASB, the pipeline consists of multiple levels, with each step modifying the files or applying a specific calibration routine. These steps will not be visible to a PSA user, however to explain how the data is calibrated it is essential to detail all the steps taken.

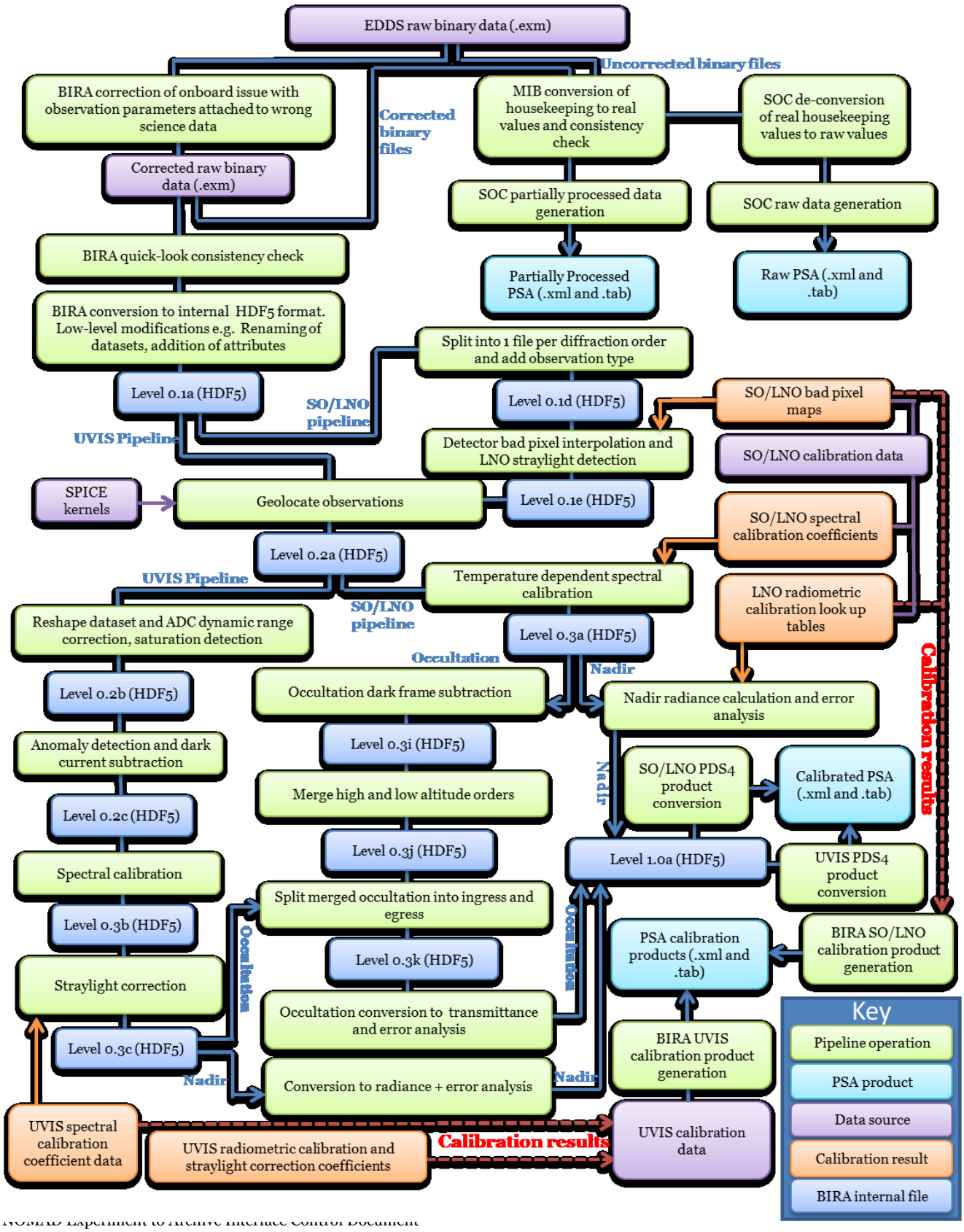
EDDS raw binary data (.exm)
Uncorrected binary files
BIRA correction of onboard issue with observation parameters attached to wrong science data
Corrected binary files
MIB conversion of housekeeping to real values and consistency check
SOC de-conversion of real housekeeping values to raw values
Corrected raw binary data (.exm)
SOC partially processed data generation
SOC raw data generation
BIRA quick-look consistency check
Partially Processed PSA (.xml and .tab)
Raw PSA (.xml and .tab)
BIRA conversion to internal HDF5 format. Low-level modifications e.g. Renaming of datasets, addition of attributes
Split into 1 file per diffraction order and add observation type
Level 0.1a (HDF5)
SO/LNO pipeline
Level 0.1d (HDF5)
SO/LNO bad pixel maps
UVIS Pipeline
Detector bad pixel interpolation and LNO straylight detection
SO/LNO calibration data
SPICE kernels
Geolocate observations
Level 0.1e (HDF5)
SO/LNO spectral calibration coefficients
Level 0.2a (HDF5)
UVIS Pipeline
Temperature dependent spectral calibration
LNO radiometric calibration look up tables
Reshape dataset and ADC dynamic range correction, saturation detection
SO/LNO pipeline
Level 0.3a (HDF5)
Occultation
Nadir
Calibration results
Level 0.2b (HDF5)
Occultation dark frame subtraction
Nadir radiance calculation and error analysis
Anomaly detection and dark current subtraction
Level 0.3i (HDF5)
Nadir
SO/LNO PDS4 product conversion
Calibrated PSA (.xml and .tab)
Merge high and low altitude orders
Level 0.2c (HDF5)
Level 0.3j (HDF5)
Level 1.0a (HDF5)
UVIS PDS4 product conversion
Spectral calibration
Split merged occultation into ingress and egress
Occultation
Level 0.3b (HDF5)
PSA calibration products (.xml and .tab)
BIRA SO/LNO calibration product generation
Occultation
Level 0.3k (HDF5)
Straylight correction
Occultation conversion to transmittance and error analysis
Key
Level 0.3c (HDF5)
BIRA UVIS calibration product generation
Pipeline operation
Nadir
Conversion to radiance + error analysis
Nadir
PSA product
UVIS spectral calibration coefficient data
UVIS radiometric calibration and straylight correction coefficients
Calibration results
UVIS calibration data
Data source
Calibration result
BIRA internal file

Figure 13: Flowchart outlining the expected data pipeline, including internal data levels and calibration inputs/outputs

3.3 Data Processing Pipeline Conversion Steps

3.3.1 Level 0.0b - SO/LNO Binary Data Correction

During analysis of inflight data, an issue was discovered which can cause errors in the SO and LNO channel binary data files transmitted from the spacecraft. NOMAD is made of a central processor (SINBAD) and three channels (SO, LNO and UVIS). SO and LNO operate very similarly, and so only SO will be discussed here, though LNO is effectively the same. UVIS operates differently and is therefore not affected by this issue.

SINBAD contains several timers, which dictate when actions are performed. It directly controls the SO channel, sending observation parameters (such as AOTF frequency, integration time, binning, etc.) to the channel to initiate measurements. Detector data is then returned from the channel, via a buffer, to SINBAD, which reads this buffer when a specific timer is activated. SINBAD then builds a SpaceWire data packet, collating the observation parameters with the data returned from the SO channel and adding a timestamp and housekeeping. This packet is then sent to TGO via SpaceWire as a TM(22) or TM(25) packet.

The issue arises occasionally, when there is a mismatch between the timer that reads the SO channel buffer and the timer that generates the SpaceWire packet. When the mismatch occurs, the detector data is read from the buffer and is added to the correct packet, but there is then a delay in adding the SINBAD data (observation parameters, timestamp, channel housekeeping) to the same packet. Under certain conditions, the timer mismatch increases until the delay is greater than the sampling rhythm (1 second for SO). When this happens, SINBAD has already generated the observation parameters/timestamp/HSK for the next measurement, and so these are erroneously added to the current packet. This results in a mismatch between the detector data and the other (observation parameters/ timestamp/ HSK) data in a SpaceWire packet. When the mismatch occurs, the two timers are effectively resynched and the issue does not then occur in the following packet, meaning that the issue emerges as an intermittent problem affecting a limited number of packets. The issue does not occur in LNO nadir observations, as the LNO sampling rhythm is typically 15 seconds, which is much less than the maximum timer mismatch.

No detector data is lost, because the packet is always generated after the data is received by SINBAD, but occasionally the wrong observation parameters/ timestamp/ HSK data are "glued" onto this packet. The parameters/ timestamp/ HSK actually come from the next observation, and so it is simple to identify the incorrect packets, as the timestamp has the same value in two consecutive packets – which is never possible as the minimum time between two packets is always at least one second in reality.

3.3.1.1 Creation of TM122 and TM125 packets

To correct this, the EDDS binary files are sent to BIRA-IASB and run through a program that checks the measured observation parameters and timestamps against the expected values. When a mismatch is found, it is corrected and a new binary file is generated and will be sent to the SOC for processing into raw and partially processed PSA data products.

Importantly, to avoid issues with users downloading the wrong files, and to prevent reanalysis of already-corrected files, the corrected binary products are assigned new packet type numbers as follows:

- TM(122) = a corrected TM(22) SO SpaceWire Packet
- TM(125) = a corrected TM(25) LNO SpaceWire Packet

The new files are ingested into the SOC data pipeline as if they were new file types, and the old PDS4 products made from packet types 22 or 25 should not be sent to the PSA archive.

The BIRA-IASB and SOC data pipeline start from these corrected packets. Coefficients and conversion formula, to convert raw data values into partially processed values, are provided in the appendix. The steps to convert partially processed data into calibrated data are detailed in the following sections.

3.3.2 Level 0.1E - LNO straylight

Straylight can be observed in the data when the LNO channel is observing in nadir and the spacecraft is in a particular geometry which only occurs when slewing to an ACS solar occultation. This happens only on the nightside of the planet and so no science is lost. However, a signal is observed in the data, and so the affected frames are removed to avoid misinterpretation of the spectra.

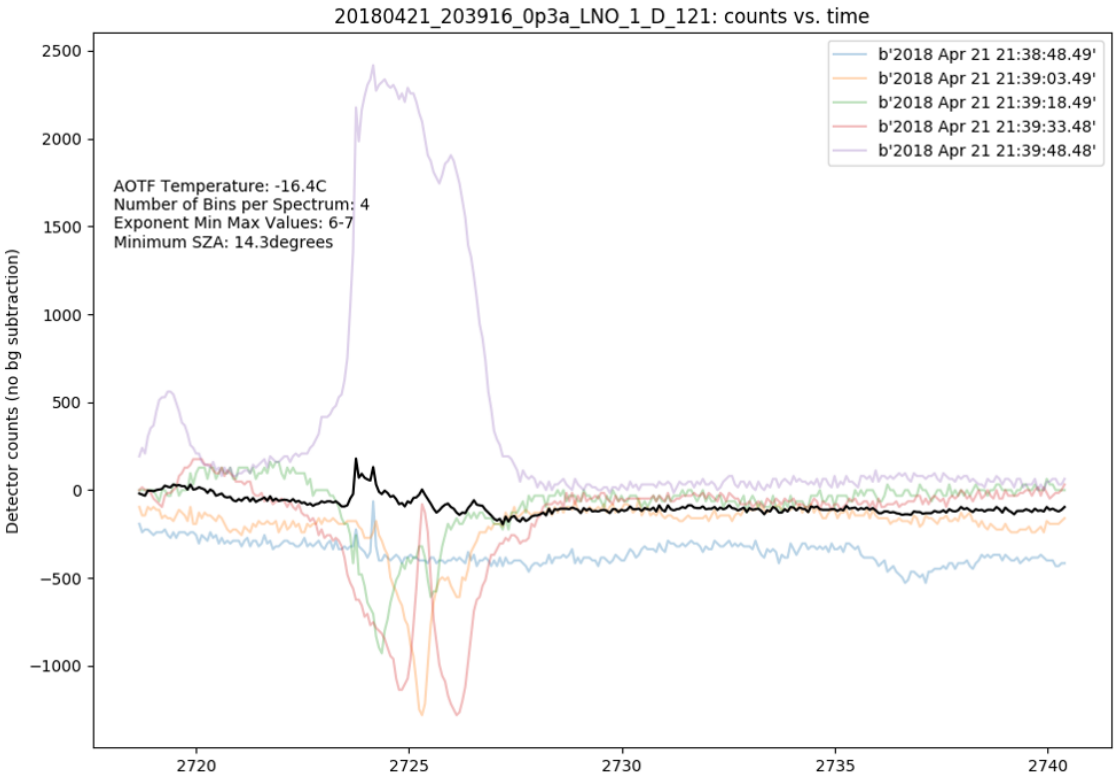

Figure 14: Solar straylight entering LNO has a huge impact on the signal. As LNO is background-subtracted, the straylight manifests itself as positive or negative values depending on whether it hits the detector during the dark or measurement frame.

Frames containing this straylight are removed automatically, based on a set of detection criteria - i.e. spacecraft orientation with respect to the Sun, and anomalous detector values. The frames directly before and after are also removed, to ensure that all incorrect data is removed. The data is not recoverable when straylight is present, and so all spectra are removed from the product. Assuming straylight has been detected in measurement frame 4, the data would be as shown in Table 13.

LNO Radiance			
Measurement 1, Pixel 1 Value	Pixel 2 Value	...	Pixel 320 Value
Measurement 2, Pixel 1 Value	Pixel 2 Value	...	Pixel 320 Value
removed	*removed*	...	*removed*
removed	*removed*	...	*removed*

removed	*removed*	...	*removed*
Measurement 6, Pixel 1 Value	Pixel 2 Value	...	Pixel 320 Value

Table 13: Radiance values in the tab file, showing how the data is modified if straylight is detected in measurement 4.

3.3.3 Level 0.1E - SO/LNO bad pixel

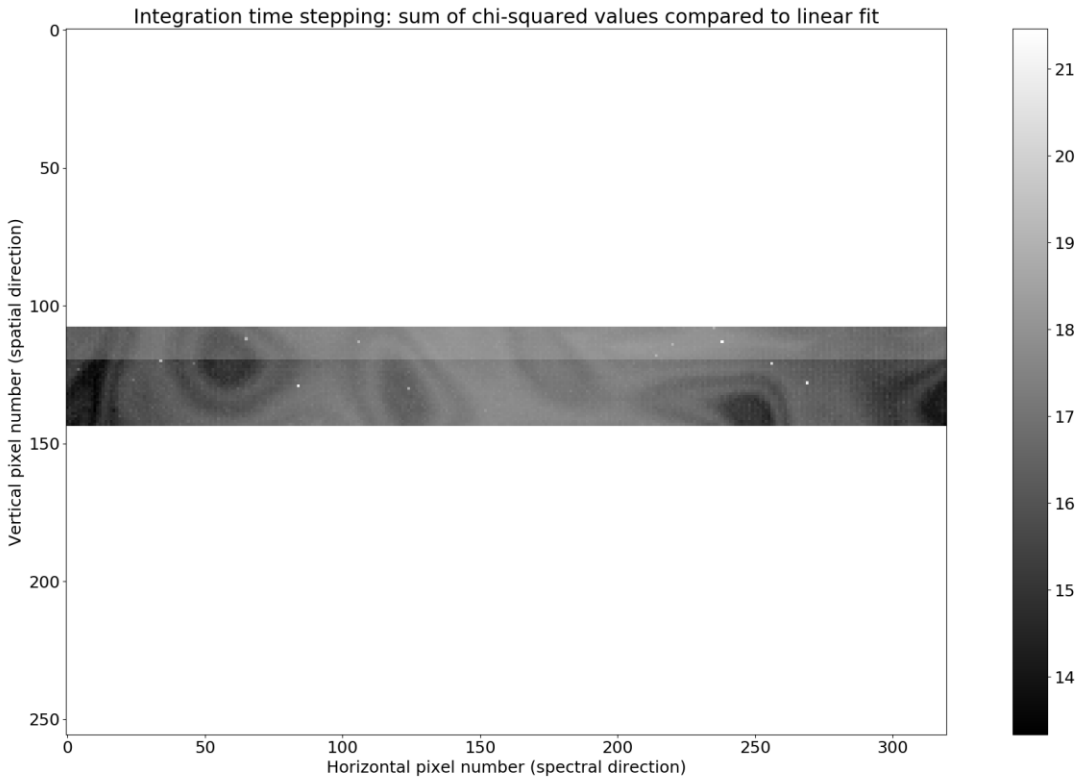

Figure 15: SO bad pixel map. White dots indicate bad pixels. Two observations were required to cover all the pixels required, hence the small difference between the top and bottom rows is likely due to slightly different instrument temperature.

Bad pixels were determined by analysing a subset of spectra and finding the pixels that behave anomalously compared to adjacent pixels throughout a measurement. This method works even for the narrowest absorption lines, as there is always a spectral overlap between consecutive pixels, and so an anomalous value in one pixel only can only be due to the pixel, not a spectral feature in the atmosphere or surface of Mars. A list of SO bad pixels is given in Table 14.

BinStart	Bad pixels (where 0 = 1st pixel)
120	256
122	112
123	101
126	84, 200, 269
127	84, 124, 269
128	84, 269, 124
130	124
134	157
135	152, 157

*Table 14: List of SO bad pixels. The **BinStart** field contains the starting detector row for each bin.*

If a pixel behaves anomalously the value is corrected by linearly interpolating from adjacent pixels. Pixels at the edge of the detector, where the signal is already very small, are given the same value as the adjacent pixel. It should be noted that some bad pixels only give anomalous readings occasionally, and so some spectra can still contain spikes after transmittance/radiance calibration. These will need to be removed by the PSA user.

3.3.4 Level 0.1E - LNO detector offsets

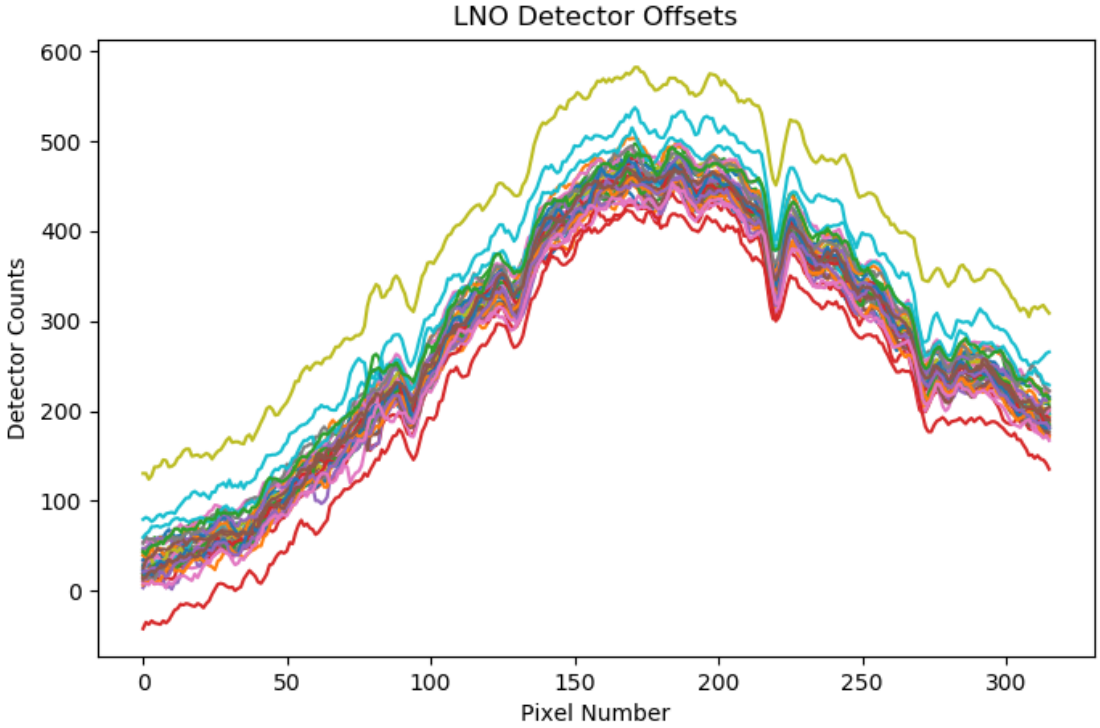

Figure 16: LNO detector spectra before offset correction

The zero offset level can shift up and down due to the detector grounding and the very small values generated by a nadir measurement (Figure 16). To correct this, an offset correction is calculated from the mean of the first 50 pixels. The offsets are subtracted from each spectrum to remove the anomalous offset, as shown in Figure 17.

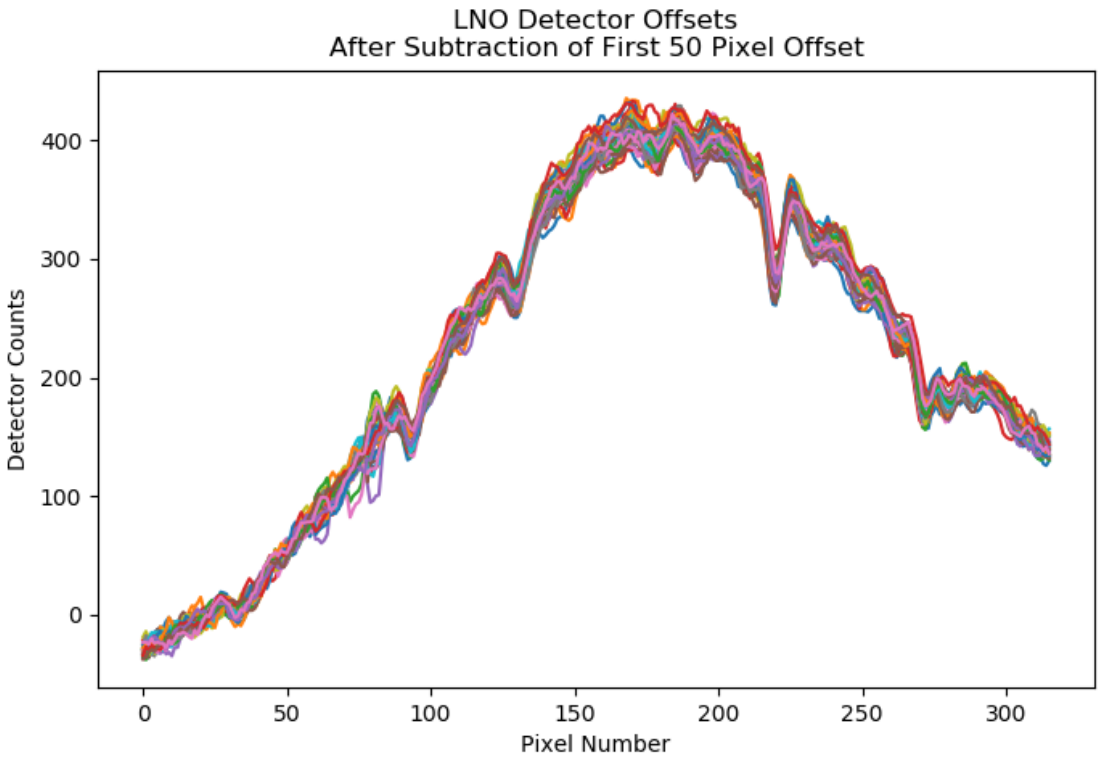

Figure 17: LNO nadir spectra after subtraction of the offset. A second offset is added to shift the curve upwards, removing the negative counts in the first pixels.

Removing the offset means that the first pixels can be less than zero, therefore a second offset is subsequently added to the data. This offset is derived from solar calibration measurements of the same diffraction order, where a ratio is calculated between the mean of the centre pixels [160-240] and the mean of the first 50 pixels when pointing at the sun. An offset is then added to each nadir spectrum so that the same ratio is present in the data.

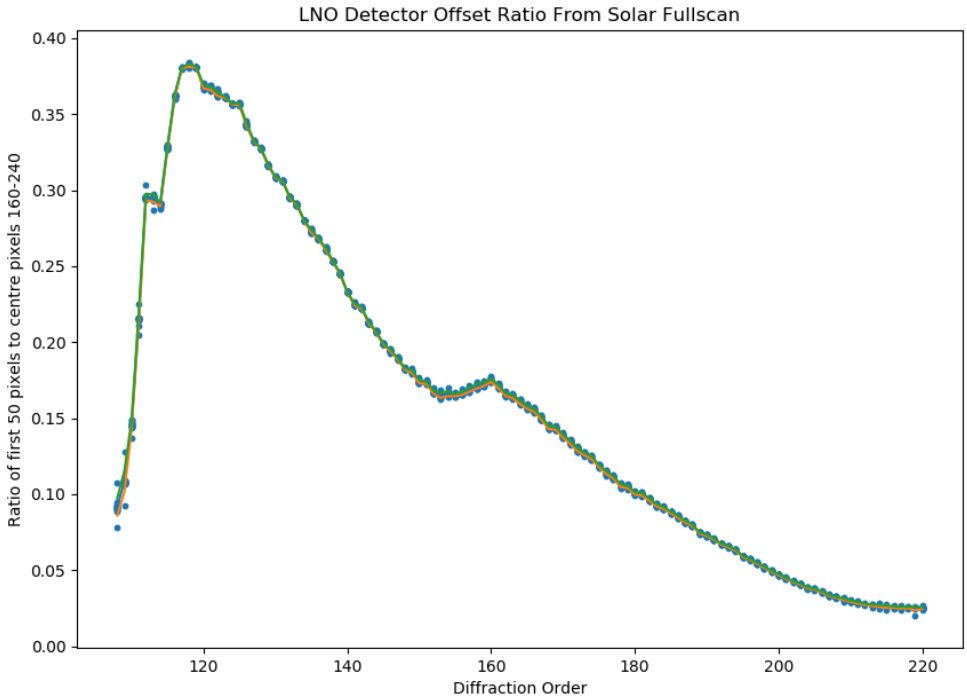

Figure 18: Ratio of mean value of first 50 pixels to mean value of pixels in centre of detector, calculated from viewing the sun for each diffraction order. This ratio is then applied to the data, shifting the nadir curves upwards so that the same ratio is observed in the spectra.

3.3.5 Level 0.1E - LNO nadir data vertically binned

The SNR of the LNO channel is low when observing in nadir, and so the spectra measured for each detector bin (of the same measurement) must be summed together to produce one spectrum.

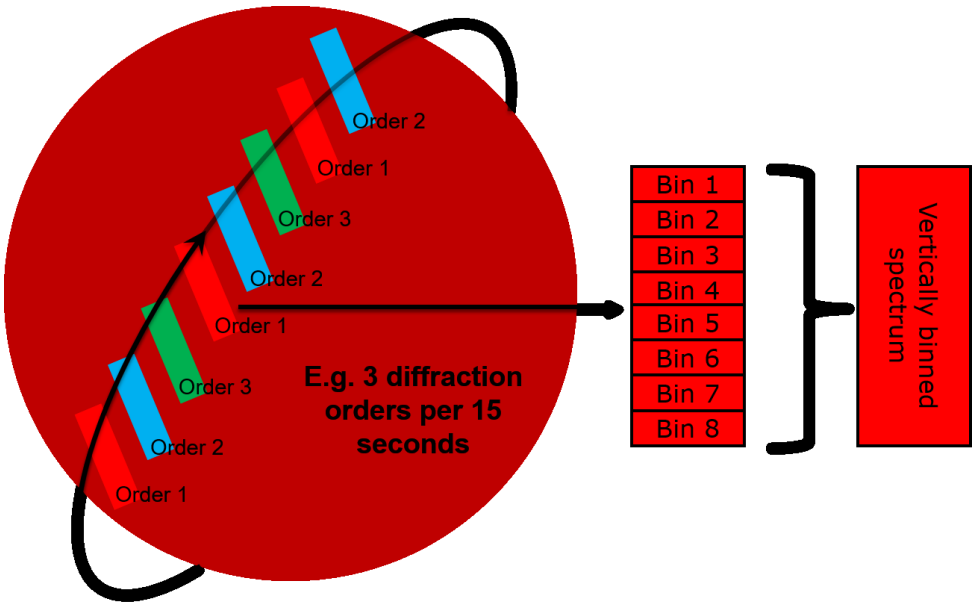

Figure 19: Vertical binning of one LNO nadir detector frame (red). Here 3 diffraction orders are measured, generating 8 individual spectra for a given measurement.

The SO and LNO channel always return 24 lines per sampling rhythm (where the rhythm is typically 1 second for occultation or 15 seconds for nadir observations). Therefore here, 3 orders are measured per rhythm and so 8 spectra are returned per order, each measured for 5 seconds. If 4 orders were measured, 6 spectra would be returned; if 2 orders then 12 spectra would be returned per order, etc.

The 6, 8 or 12 LNO nadir spectra are then vertically binned to give a single spectrum per order per measurement period (Figure 19).

The detector bins observe different locations on the planet, and this spatial information is lost when the detector rows are vertically binned. However the spatial information is also lost as the field of view (FOV) sweeps the planet. Considering an example where 3 orders are measured per 15 second sampling rhythm, this means that each spectrum is acquired for approximately 5 seconds in total (minus some readout time of ~500 milliseconds). TGO travels at ~3.3 km/s, and so in 5 seconds the instantaneous field of view (IFOV) has moved ~17 km. The IFOV on the surface is 0.5 x 17 km, and so the smearing of the FOV due to spacecraft movement is comparable to the longest extent of the IFOV. Most importantly

though, individual bins do not have sufficient SNR to be scientifically useful, and so binning of the detector is essential.

3.3.6 Level 0.1E - SO/LNO detector bins flattened

SO and LNO radiance/transmittance values are converted from a 3D array (size = number of observations x number of bins x 320 pixels) to a 2D array (size = [number of observations x number of bins] x 320 pixels). **BinStart** and **BinEnd** fields contains the start and end detector row for each bin. LNO nadir observations have already been vertically binned into a 2D array, and so the rows remain unchanged.

3.3.7 Level 0.2A – Geometry overview

There are three types of shape models used to calculate geometric parameters:

- **Ellipsoid** - this is the most basic shape model, where Mars is modelled as a tri-axial ellipsoid of radii 3396.19km x 3396.19km x 3376.2km as defined by NASA/NAIF in the SPICE toolkit.
- **Areoid** - this is the equivalent to a "sea level" for Mars, where the gravitational and rotational potential is constant across the entire surface. The zero level is defined by MGS/MOLA using a 4 pixels per degree model
- **Surface** - this is the real surface elevation, calculated from a digital shape kernel (DSK) by MGS/MOLA at a resolution of 4 pixels per degree using the MGM1025 model (Lemoine et al., 2001).

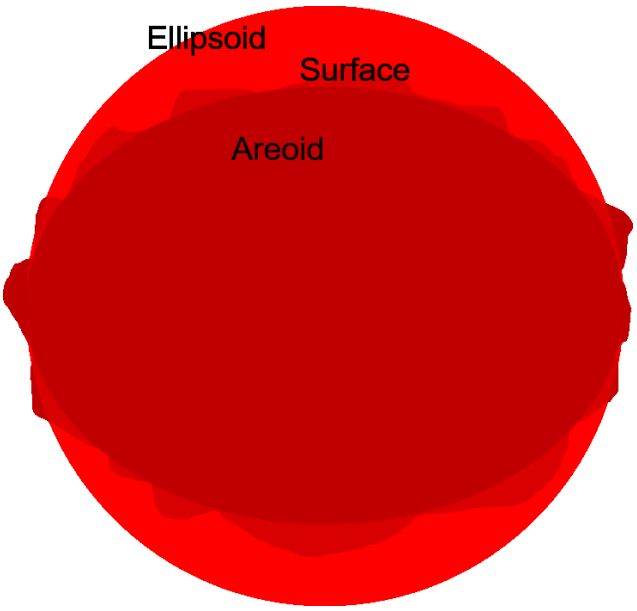

Figure 20: Pictorial representation of the difference between ellipsoid, surface and areoid geometries.

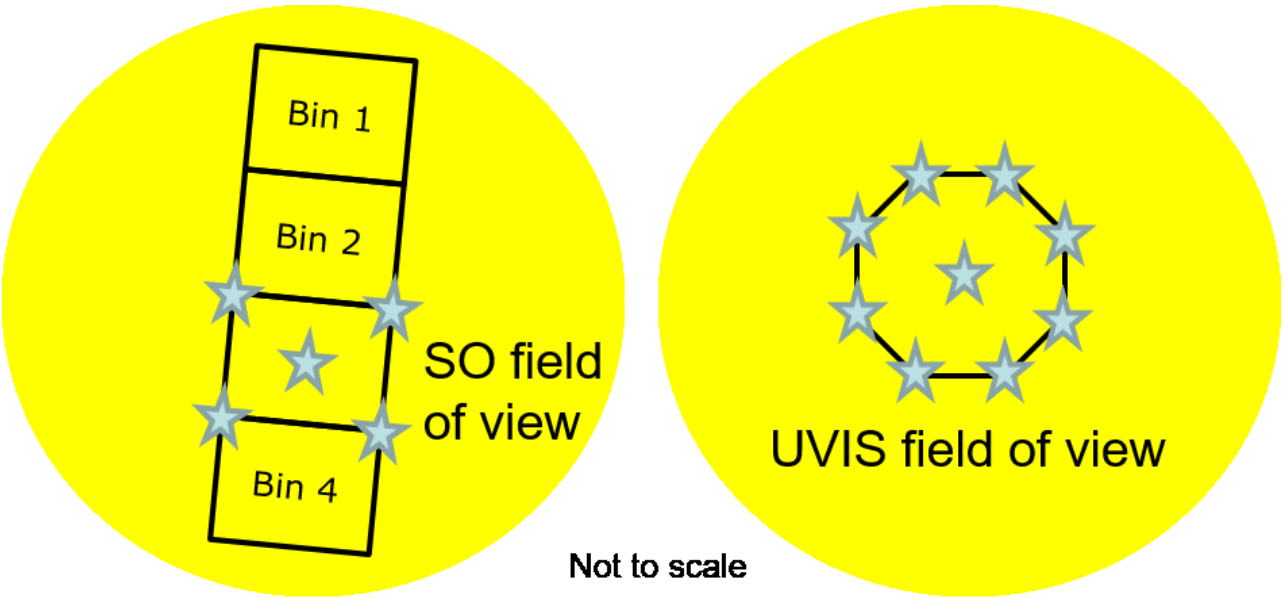

Figure 21: SO and UVIS solar occultation geometry, showing the 5 points per bin for SO and 9 points for UVIS.

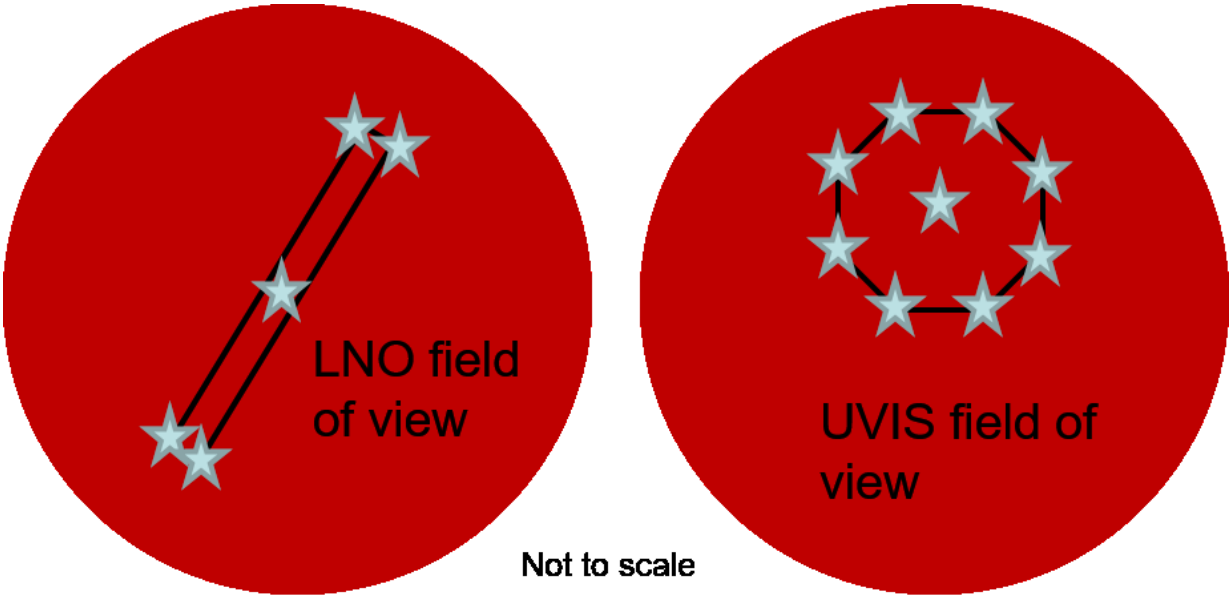

Figure 22: LNO and UVIS nadir geometry, showing the 5 points per bin for SO and 9 points for UVIS

Geometry is stored for each pointing direction (Figure 21 and Figure 22). There are 5 points for SO/LNO solar occultations and nadir observations:

- **Point0** is the centre of the entire field of view of the bin
- **Point1** to **Point4** define the corners of the field of view of the bin

UVIS has a circular aperture, defined by 9 points:

- **Point0** is the centre of the field of view
- **Point1** to **Point8** form an octagon around the field of view edge.

As described above, the LNO nadir frame has been vertically binned, and so there is effectively just one bin per measurement. Therefore points 1-4 define the corners of the entire LNO field of view.

The fields of view of the bins are defined using points as shown in Figure 23. Relevant geometric parameters, such as latitude, longitude and viewing angle information are calculated for each point. The relative x and y positions of each point (the numbers in brackets in Figure 23) are given in the fields PointX0, PointY0, PointX1, PointY1, etc. Their direction is defined by the SPICE instrument kernel reference frame for each channel, where X points along the long edge of the SO/LNO slit and Y the short edge.

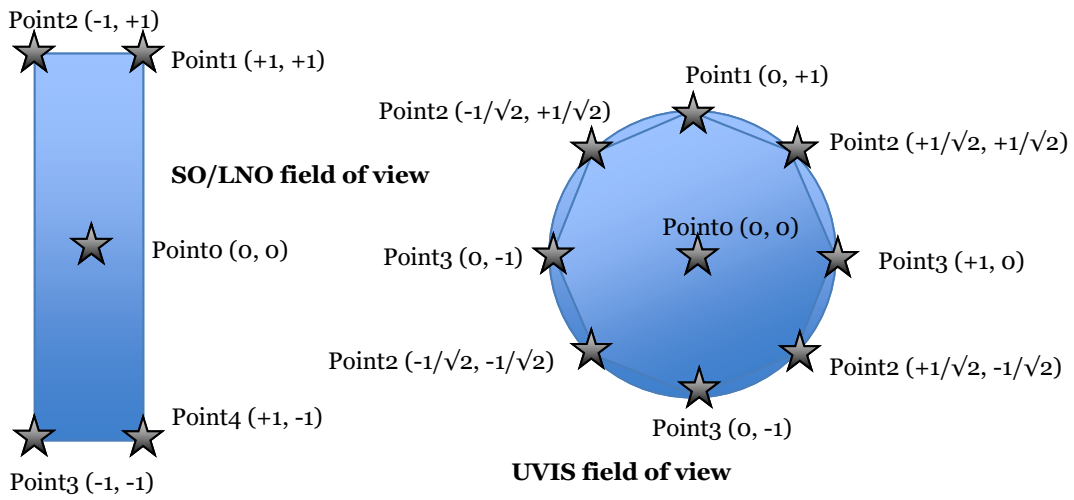

Figure 23: Geometry points as defined in relation to the channels' fields of view.

A complete list of geometric parameters in the metadata and data tables are given in Table 3736, Table 3837, Table 4241 and Table 4342. Some geometric parameters do not depend on pointing direction, for example **SubObsLat** and **SubObsLon**. Start and end values are recorded per spectrum acquired, i.e. **StartSubObsLat** and **EndSubObsLat**. These are calculated using the ellipsoid model.

Some geometric parameters have different values depending on the point – therefore there are two values (start and end times) per point per spectrum acquired. An integer is appended to the field name to indicate the point number, e.g. **LonStart3** and **LonEnd3** are the start and end longitudes for point 3. Latitudes and longitudes are calculated using the ellipsoid model.

Using the surface shape model means that the geometric surface parameters **EmissionAngle** (angle between surface normal and spacecraft), **PhaseAngle** (angle between sun, surface and spacecraft) and **IncidenceAngle** (angle between Sun and surface normal) are based on the real surface contours rather than a reference ellipsoid. All of the fields above are point-dependent, e.g. **EmissionAngle** is defined as **EmissionAngleStart0**, **EmissionAngleEnd0, EmissionAngleStart1**, etc. for the 0 and 1 correspond to field of view (FOV) points 0 and 1. Latitude and longitude are effectively independent of shape model and hence are provided for ellipsoid model only.

LST is the local solar time, in hours, defined using the SPICE kernel definition = 12 + (surface longitude for a point – solar longitude)/15. This is calculated using the ellipsoid model. Values are given separately for the start and end acquisition time of each spectra and for each point on the field of view, e.g. **LSTStart0**, **LSTEnd0**, etc.

In solar occultation mode, the geometry is defined at the tangent point, i.e. the point on the Mars ellipsoid closest to the line of sight vector of each point. The tangent height is different for each shape model, therefore all are provided in the calibrated product. The most important is the height above the areoid; this is given as **TangentAltAreoid** in the products, while the tangent height above the ellipsoid is **TangentAltEllipsoid** and the tangent height above the DSK surface is **TangentAltSurface**. The distance between the satellite and the tangent point is provided by the parameter **SlantPathDistance**. Values are given separately for the start and end acquisition time of each spectra and for each point on the field of view, e.g. **TangentAltStart0**, **TangentAltEnd0**, **SlantPathDistanceStart4**, **SlantPathDistanceEnd4** etc.

Every occultation observation ends 30 seconds after the field of view intersects the planet (calculated using the ellipsoid model), therefore many spectra are acquired when the tangent height is below the surface. We remove these spectra, except those where the ellipsoid

tangent height is less than 8km below the surface. Therefore negative tangent heights can be found in the data.

LSubS, the planetocentric solar longitude, commonly referred to as Ls (pronounced "L sub S", or "L-S"), is the position of Mars relative to the Sun measured in degrees from the vernal equinox (start of northern Spring). This number is used as a measure of Martian seasons: Northern Spring/Southern Autumn start at 0°, Northern Summer/Southern Winter start at 90°, Northern Autumn/Southern Spring start at 180°, and Northern Winter/Southern Summer begin at 270°. Values are given separately for the start and end acquisition time of each spectra, e.g. **StartLSubS** and **EndLSubsS**, but values do not change with field of view point.

Invalid geometry values are set to -999.0. This could occur, for example, if the nadir channel points off-planet during an observation, which can happen if the spacecraft is slewing to/from another measurement. Likewise, if the solar occultation FOV hits the surface, the tangent point latitude and/or longitude is undefined and therefore set to -999.0.

In approximately 1% of all solar occultations, the spacecraft fails to maintain the required solar pointing, typically when a star tracker is unable to be used e.g. if pointing towards the planet. In these cases, the pointing deviates from the centre of the sun – if the deviation is sufficiently large, the FOV points away from the centre of the solar disk and so the signal (and therefore the transmittance) appears to be reduced. This could be interpreted incorrectly as a cloud or other absorption feature; therefore a parameter called **PointingDeviation**. Has been included, which measures the difference in angle (in arcminutes) between the Sun centre and the nominal pointing Sun centre. Nominal values are typically <0.1 arcminutes; a larger number (e.g. >0.5) indicates that the pointing was not correctly maintained and so interpretation of the corresponding spectra should be done with caution. Two values are given per spectrum for the start and end of the acquisition i.e. **StartPointingDeviation** and **EndPointingDeviation**.

3.3.7.1 SO/LNO Occultation (50km switch)

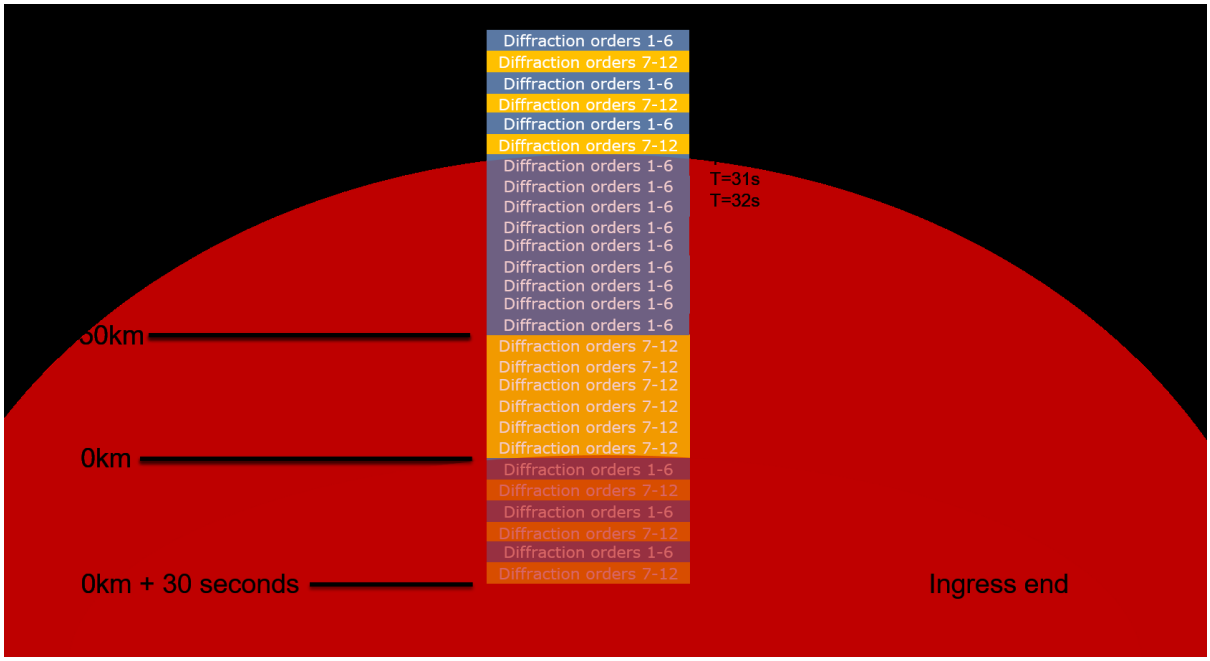

Figure 24: Diagram showing the SO data acquired during a solar occultation where the set of diffraction orders is changed 50km above the surface.

3.3.7.2 SO/LNO Occultation (0-250km)

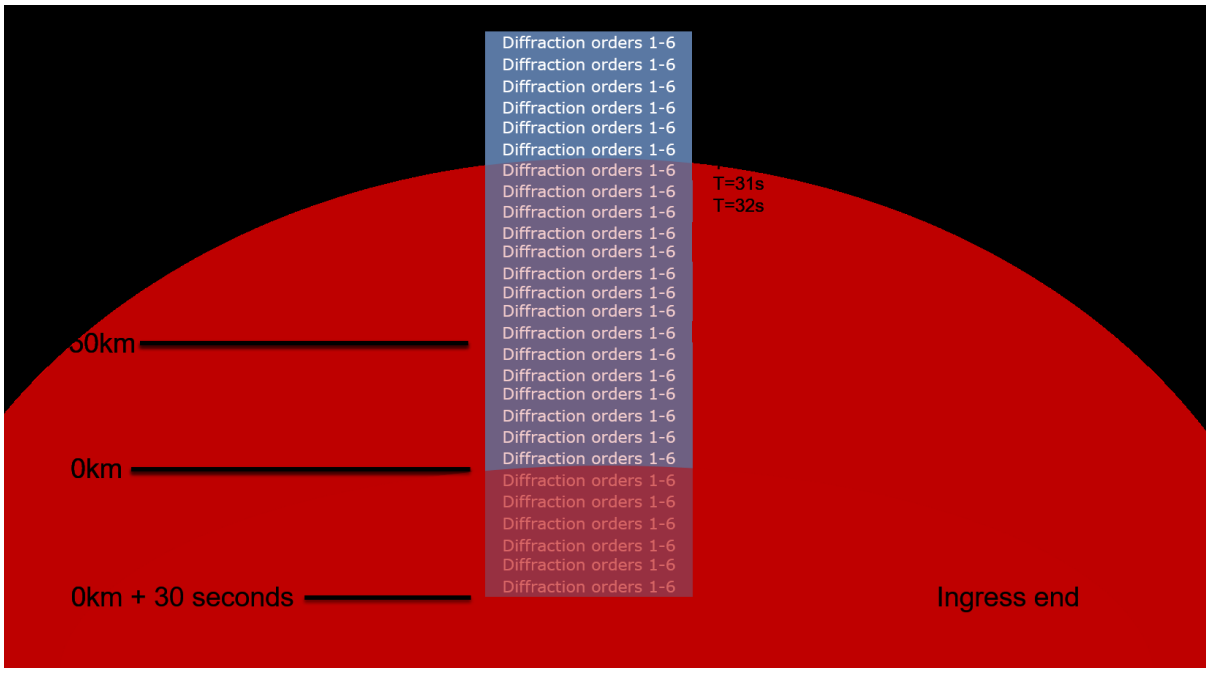

Figure 25: An SO occultation where the same diffraction orders are measured throughout.

Figure 24 and Figure 25 show the principal two types of solar occultations measured by the SO channel. Note that, in cases where onboard dark subtraction is switched off, diffraction orders 6 and 12 are normally dark frames, hence only 5 or 10 diffraction orders are measured.

The SO data has been flattened into a 2D array (section 3.3.6), and so the data is now in the format shown in Table 15, with one spectrum per bin per measurement per row. For each transmittance spectrum there is a **BinStart** and **BinEnd** value to specify the detector rows used to acquire that bin.

SO Transmittance			
Measurement 1, Bin 1, Pixel 1	Pixel 2	…	Pixel 320
Measurement 1, Bin 2, Pixel 1	Pixel 2	…	Pixel 320
Measurement 1, Bin 3, Pixel 1	Pixel 2	…	Pixel 320
Measurement 1, Bin 4, Pixel 1	Pixel 2	…	Pixel 320
Measurement 2, Bin 1, Pixel 1	Pixel 2	…	Pixel 320

Measurement 2, Bin 2, Pixel 1	Pixel 2	...	Pixel 320

BinStart	BinEnd
Bin 1 Detector Row Start	Bin 1 Detector Row End
Bin 2 Detector Row Start	Bin 2 Detector Row End
Bin 3 Detector Row Start	Bin 3 Detector Row End
Bin 4 Detector Row Start	Bin 4 Detector Row End
Bin 1 Detector Row Start	Bin 1 Detector Row End
Bin 2 Detector Row Start	Bin 2 Detector Row End

Table 15: SO transmittance and binning data.

3.3.7.3 LNO nadir

Due to the low SNR in nadir mode, all the LNO bins have been summed into a single spectrum per measurement. Therefore, in the absence of separate bins, the tabulated data contains just one spectrum per measurement. BinStart and BinEnd therefore are the same for all measurements and reflect the start and end row of the detector readout (Table 16).

LNO Radiance			
Measurement 1, Pixel 1	Pixel 2	...	Pixel 320
Measurement 2, Pixel 1	Pixel 2	...	Pixel 320
Measurement 3, Pixel 1	Pixel 2	...	Pixel 320
Measurement 4, Pixel 1	Pixel 2	...	Pixel 320

BinStart	BinEnd
Detector Row Start	Detector Row End
Detector Row Start	Detector Row End
Detector Row Start	Detector Row End
Detector Row Start	Detector Row End

Table 16: LNO radiance and corresponding binning data

3.3.7.4 UVIS Nadir and Occultation

UVIS acquires one spectrum per measurement, with no bins or diffraction orders (Table 17).

UVIS Transmittance/Radiance			
Measurement 1, Pixel 1	Pixel 2	...	Pixel 1048
Measurement 2, Pixel 1	Pixel 2	...	Pixel 1048
Measurement 3, Pixel 1	Pixel 2	...	Pixel 1048
Measurement 4, Pixel 1	Pixel 2	...	Pixel 1048
Measurement 5, Pixel 1	Pixel 2	...	Pixel 1048

Table 17: UVIS transmittance data for a full spectrum (1048 pixels)

3.3.7.5 LNO Limb

At the time of writing, only the LNO channel can observe the limb using its flip mirror while the spacecraft continues in nadir pointing mode. The signal entering the UVIS solar occultation boresight is attenuated, and so the spacecraft must be orientated with the nadir channel pointing towards the limb for both LNO and UVIS to measure it.

LNO observes the limb passively, with no control over pointing, and so the pointing can vary between and within observations. In future it is hoped that the limb can be measured in a controlled way, viewing at a fixed altitude, or with the UVIS nadir boresight.

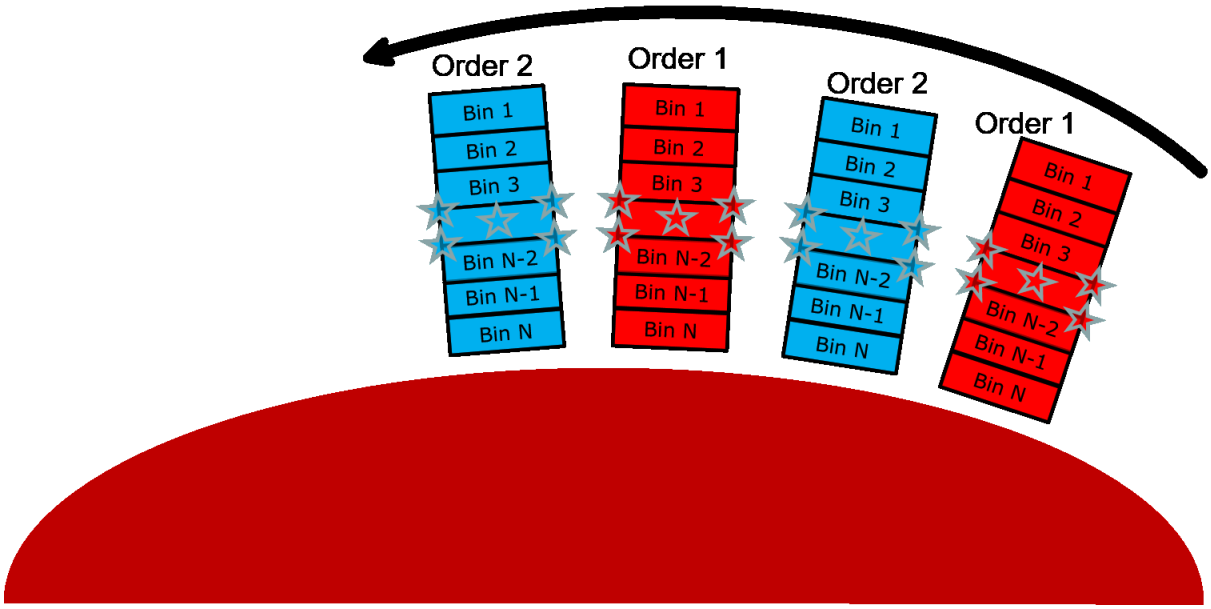

Figure 26: An LNO limb observation using two diffraction orders. The FOV generally sweeps across the limb as the spacecraft moves, in the direction of the short edge of the slit.

The LNO limb data is arranged like SO/LNO solar occultations, split into bins and using the same geometric parameters, even though the SNR is too low per bin to be usable for science. This is because the altitude information is lost if the entire detector is binned, and so the SNR should be increased by summing each bin in time for a given altitude range.

Limb measurements are not yet ready for PDS production, however they will be prepared and made available to the community in future.

3.3.8 Level 0.3A - SO/LNO spectral calibration

Spectral calibration of the SO and LNO channels is complicated by the presence of the AOTF and diffraction grating. Without an AOTF, there would be >100 diffraction orders hitting the detector simultaneously, and so attributing an absorption line to a specific wavelength would be impossible.

The AOTF solves this by permitting only a limited spectral range to pass through it. In an ideal situation, the AOTF transmittance would be a boxcar function, of width exactly equal to the spectral range of the desired diffraction order. However, in reality the AOTF has a more complicated shape, akin to a sinc^2 function, with sidelobes that allow radiance to pass through it and hit the detector from adjacent diffraction orders. Accurate calibration is essential, so that all features present in a spectrum can be attributed to the principal or adjacent diffraction orders – and the shape of the AOTF function is correct so that the absorption depths of those features can be correctly used to determine the concentration of gas species in the atmosphere of Mars. Similarly, accurate wavenumber calibration of the diffraction grating is required so that the features observed match those in spectroscopic databases. This is further complicated by the effects of instrument temperature – NOMAD is not kept at a fixed temperature, and the metal diffraction grating is mounted to the instrument structure, and therefore can expand and contract as the temperature changes. This results in a temperature-dependent wavelength shift which must be corrected by the spectral calibration calculation. AOTF shape coefficients and spectral resolution vary by diffraction order.

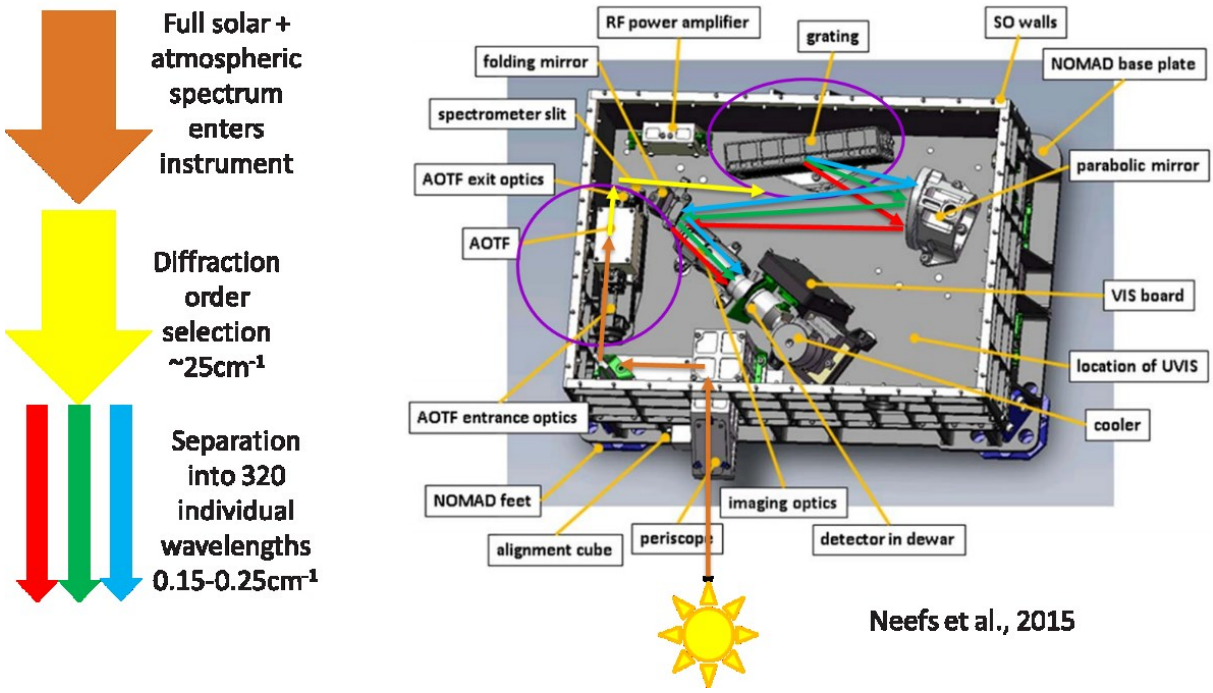

Figure 27: SO/LNO optical layout. A broad spectrum of infrared radiation enters the instrument; the AOTF selects a limited spectral range corresponding to a diffraction order; and the grating splits the radiation within the diffraction order onto the 320 detector pixels

The spectral calibration is, and will be, continually refined during the mission, and so the calibration coefficients and equations are likely the change often. The following published articles contain calibration coefficients and equations:

- Liuzzi et al. 2019 [RD.11] - AOTF-wavenumber relation and diffraction order – AOTF frequency relation - which were derived from solar calibration measurements taken from Mars orbit in 2016, prior to aerobraking
- Thomas et al. 2021 [RD.14] – SO detector bin illumination and pointing - which were derived from solar calibration observations
- Thomas et al. 2021 [RD.15] – LNO spectral calibration temperature dependence and detector bin illumination - which were derived from ground and solar calibration observations
- The supplementary materials section of Villanueva et al. 2022 [RD.19] – the most recent SO ILS parameters, AOTF shape, and FSR - which were derived from solar calibration and occultation measurements taken during the science phase

- Trompet et al. 2022 [RD.20] – SO temperature-dependent spectral calibration - which were derived from solar occultation measurements taken during the science phase
- Willame et al. 2022 [RD.18] for UVIS calibration coefficients

Coefficients are provided in calibration products in the PSA archive (section 5.5).

3.3.8.1 SO/LNO AOTF Calibration

The AOTF function is centred on the desired diffraction order by driving it with a specific radio frequency. Note that the diffraction order m is always an integer, and the AOTF frequency is always chosen so that the peak AOTF function matches the centre of a diffraction order.

The relation between the AOTF centre (in cm^{-1}) and the wavenumber is given as:

$$AOTF(v) = G_0 + G_1 A + G_2 A^2$$

Where AOTF(v) is the central wavenumber in cm^{-1} and *A* the AOTF frequency in kHz. The coefficients are:

Coefficient	AOTF tuning relation
G_0	305.0604
G_1	0.1497089
G_2	1.34082×10^{-7}

The AOTF centre shifts with temperature according the following relationship:

AOTF(v) = AOTF(v) + ([coefficient] * [channel temperature] * AOTF(v))

Where the coefficient here is the AOTF frequency shift due to temperature [relative cm-1 from Celsius] = -6.5278E-05

The channel temperature is taken from the field **InstrumentTemperature**.

Following Villanueva et al. 2022, the AOTF shape is now a combination of a sinc² added to a wide Gaussian. The following coefficients are used:

Coefficient	**0**	**1**	**2**
Sinc width [cm-1 from AOTF frequency cm-1]	2.01730360E+01	7.47648684E-04	-1.66406991E-07
Sidelobe factor [scaler from AOTF frequency cm-1]	4.08845247E+00	-3.30238496E-03	8.10749274E-07
Asymmetry factor [scaler from AOTF frequency cm-1]	-1.24925395E+00	1.29003715E-03	-1.54536176E-07
Gaussian peak intensity [coefficients for AOTF frequency cm-1]	1.60097815E+00	-9.63798656E-04	1.49266526E-07

The following are calculated from the AOTF centre frequency in wavenumbers e.g.

Sinc width(v) = 2.01730360E+01 + 7.47648684E-04 * AOTF(v) - 1.66406991E-07 * AOTF(v)²

The width of the Gaussian is assumed to be 50cm⁻¹ centred at the peak of the AOTF

The AOTF is then defined from the four shape values as follows:

```
def sinc(dx,width,lobe,asym,gauss_peak):
    sinc = (width*np.sin(np.pi*dx/width)/(np.pi*dx))**2.0
    ind = (abs(dx)>width).nonzero()[0]
    if len(ind)>0: sinc[ind] = sinc[ind]*lobe
    ind = (dx<=-width).nonzero()[0]
    if len(ind)>0: sinc[ind] = sinc[ind]*asym
    sigma = 50.0
    sinc += gauss_peak*np.exp(-0.5*(dx/sigma)**2.0)
```

return sinc

Where dx is the relative wavenumber from the AOTF peak

3.3.8.2 SO/LNO Grating Spectral Calibration

The wavenumber-pixel calibration is:

$$\frac{\nu_p}{m} = F_0 + F_1 p + F_2 p^2$$

Where ν_p is the wavenumber in cm^{-1} of detector pixel p in diffraction order m and F_0, F_1 and F_2 the coefficients of a second order polynomial derived from ground and in-flight spectral calibration campaigns. The coefficients are:

SO Coefficient	Pixel spectral calibration coefficient
F_0	22.4701
F_1	5.480E-04
F_2	3.32E-08

Normally here, the values of p would range from 0-319 for the 320 spectral pixels on the detector, but instead the wavelength shift due to temperature is accounted for by modifying the values of p used in the equation above to range from (0+offset) to (319+offset). The value of this offset is determined from the temperature of NOMAD at the start an observation, and varies linearly with instrument temperature T:

$$\text{offset} = Q_0 + Q_1 T$$

Where T is the **InstrumentTemperature** and the coefficients are:

SO Coefficient	Temperature shift coefficient (px/°C)
Q_0	0.0
Q_1	-0.8276

At present, the offset is constant throughout an entire observation, however in future this may be subject to change.

The temperature-dependent calculation of the spectral calibration is hidden from the PSA user, as the wavenumber corresponding to each pixel is given directly in the PSA products in the **Wavenumber** group field

3.3.8.3 SO/LNO Grating Blaze Function Calibration

The SO and LNO gratings are more efficient in diffraction radiation towards the centre of a diffraction order rather than at the edges, according to the blaze function. This is modelled as a sinc² function:

$$F_{blaze}(p, p_0, w_p) = w_p^2 \frac{\left[sin \frac{\pi(p - p_0)}{w_p}\right]^2}{\pi^2 (p - p_0)^2}$$

where w_p is the width of the blaze function (also known as the free spectral range, FSR) and x is the relative wavenumber for each pixel from the blaze peak b_p.

The initial FSR or blaze width, w_{p1}(v) is defined as:

w_{p1}(v) = W_0 + W_1(AOTF(v) – 3700) + W_2(AOTF(v) – 3700)² + W_3(AOTF(v) – 3700)³+

Where the coefficients are:

SO Coefficient	FSR / blaze width coefficient (cm-1)
W_0	2.25863468e+01
W_1	9.79270239e-06
W_2	-7.20616355e-09
W_3	-1.00162255e-11

And the temperature-corrected FSR or blaze width, w_p(v) is calculated as follows:

$w_p(v) = w_{p1}(v) + w_{p1}(v) * [Y_0 + Y_1T + Y_2T^2]$

Where T is the **InstrumentTemperature** and the coefficients are:

SO Coefficient	**FSR / blaze width relative frequency shift coefficients [shift/frequency from Celsius]**
Y_0	-1.90001923e-04
Y_1	-2.30708836e-05
Y_2	-2.44383699e-07

The blaze peak b_p is then simply the diffraction order * width of the FSR i.e. m * $w_p(v)$

3.3.9 Level 0.2B - UVIS reshape dataset

If dataset is unbinned, remove unmeasured detector rows from the datasets (size = number of observations x 256 x 1048) to reflect the detector region used (size = number of observations x [**vstart** - **vend** + 1] x 1048).

Note that there is a mode where the measured pixels on the detector are vertically binned onboard, and a single spectrum transmitted back to Earth. In this case, the calibration is severely impaired and therefore this mode is avoided (except at the beginning of the science phase, when this was not known). At present the data pipeline does not calibrate vertically binned observations, and so any observations made using this mode will not appear in the PSA archive. If a calibration pipeline is made in future to treat these observations, they will be delivered to the archive at a later time.

3.3.10 Level 0.2B - UVIS spectral calibration

The temperature-dependent spectral calibration is applied to all pixels. The wavelength corresponding to each pixel is given directly in the PSA products in the group field **Wavelength**.

3.3.11 Level 0.2C - UVIS detector saturation detection

Check for saturated pixels. If detected, set relevant pixel in the group field **Mask** to 1.

3.3.12 Level 0.2C - UVIS anomaly detection in dark measurements

Check the presence of anomalies at the pixel level in the dark measurement: detection of cosmic rays and hot pixels; update of the **Mask** (mask set to 1 for cosmic ray); a temporary dark measurement dataset, corrected for cosmic rays, is created and used in the next step of the dark current (DC) removal.

The routine uses comparisons between consecutive dark observations: dark measurements are supposed to be relatively constant over all pixels of a full CCD frame. Exceptions occur: 1) with “hot pixels” which behave differently than other pixels and 2) with cosmic ray hits on the CCD. The routine identifies these perturbed pixels and assigns them: as “hot pixels” when the pixel appear perturbed in several dark measurements and as “cosmic ray” when the pixel is perturbed in only one dark measurement.

The temporary dark measurement dataset created to be used in DC removal is obtained by replacing the values of all cosmic ray pixels by the mean on all non-perturbed pixels from the CCD frame of the dark measurement considered.

3.3.13 Level 0.2C - UVIS dark current removal

Removal of the dark current using the dark measurements (corrected for cosmic rays, cf. previous step) taken before and after a set of science frames. Knowing the temperature at which each science frame has been recorded, a dark frame corresponding to this temperature is interpolated between the nearest two measured dark frames and subtracted from the science frame. This is detailed in Willame et al. 2022 [RD.18].

3.3.14 Level 0.2C - UVIS anomaly detection

Check the presence of anomalies at the pixel level in the science measurements: detection of cosmic rays, dummy pixels and update of the **Mask** (mask set to 1 for cosmic ray). The routine uses comparisons between consecutive observations: it takes the ratio at all

wavelengths between consecutive spectra. This ratio must remain smooth all along the wavelengths, due to the smooth wavelength dependencies of the Martian atmosphere/surface properties. Therefore when an abrupt change is detected at one (or some consecutive) wavelength(s), it means that a cosmic ray has hit the detector at these wavelengths which are then flagged.

3.3.15 Level 0.3C - UVIS straylight removal

Vertically bin the data from the detector readout region selected, taking into account the **Mask** and divide it by the number of lines used. If an observation contains a **Mask** with a value of 1, the straylight will not be removed and the flag **YValidFlag** is to 0 to indicate the data is not valid.

Remove the infrared straylight based on an estimation of the quantity of IR entering inside UVIS telescope (between 650 and 1100nm). This estimation rely on a typical IR spectra of Mars given by M. Wolff simulation and rescale to fit the real measurement at 650nm of UVIS. This IR quantity is then converted into Straylight by extrapolating the behaviour of the NOMAD flight spare model corresponding to the injection of IR radiation.

Once the IR straylight is removed, remove the UV-Visible straylight (based on Yuquin NIST method) by multiplying the data by a correction matrix [1048x1048] determined on the NOMAD flight spare model of UVIS.

The UVIS calibrated products contain a Boolean group field named **Mask** where the Nth value is set to 0 if pixel N is ok, and set to 1 if pixel N has been rejected.

3.3.16 Level 0.3I – SO/LNO occultation dark frame subtraction

In nominal occultation science observations, where 5 diffraction orders and one dark frame are measured per second, the dark frames are added to the science files and the darks are discarded. In some measurements, the dark frame is subtracted onboard automatically, in which case the SO file passes this step unmodified.

3.3.17 Level 0.3J – SO/LNO occultation merge high and low altitude orders

In nominal occultations science observations, two different combinations of diffraction orders can be measured during one solar occultation – one set for high altitudes and one set for low altitudes. To prepare for the transmittance conversion, any orders which are measured in both sets are merged together to form a single observation, and the bins within the merged file are sorted by altitude, from low to high.

3.3.18 Level 0.3K – SO/LNO/UVIS split merged occultations into ingress and egress

The SO and LNO detectors require 10 minutes of precooling time to cool down the detector to cryogenic temperatures. If the time between ingress and egress occultations is too small, and there is insufficient time to cool the detector for the egress, the two occultations are merged together and the detector remains on throughout. Such merged occultations are split into separate ingress and egress files.

3.3.19 Level 1.0A – SO/LNO occultation transmittance calibration

The transmittance calculation follows the method of Trompet et al. 2016 and is summarised in Figure 2829 and below:

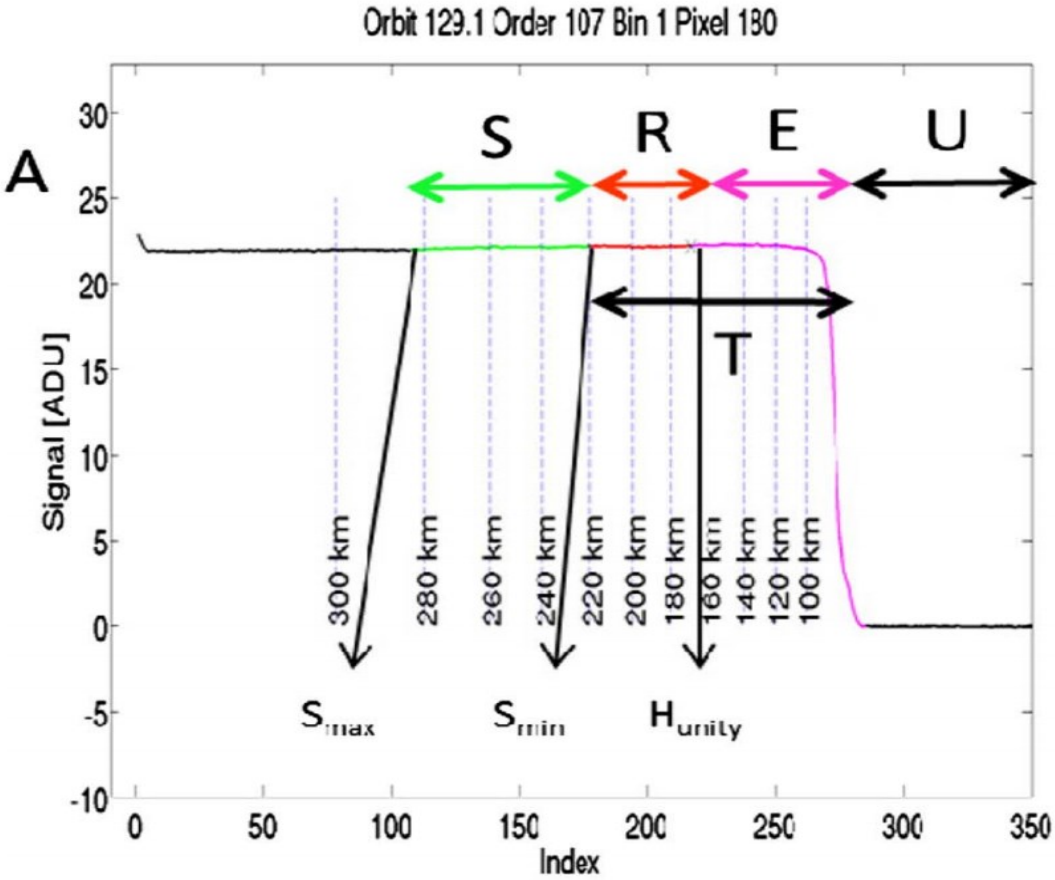

Figure 28: An example SOIR solar occultation of Venus, showing how the signal of a single pixel varies during an ingress occultation, where index = spectrum number. Each solar occultation spectrum is split into 5 regions, S, R, E, U and T, corresponding to a given tangent altitude range.

In the figure:

- S is the region in the Sun region that is used to calculate the linear regression. S_{min} is wavenumber dependent.
- T is the whole subregion on which the transmittances are computed, i.e. the region between the last index of the S subregion and the surface.

- H_{unity} is a point corresponding to the closest tangent altitude to the unity altitude, i.e. the altitude below which atmospheric absorption is occurring (this altitude is wavenumber dependent).
- R is the subregion of T containing all spectra with tangent altitudes above H_{unity}. This subregion is used to check that the linear regression calculated in S continues to fit the data above the atmosphere.
- E is the subregion of T containing the spectra where the tangent altitudes are under the unity altitude. Absorption occurs at these corresponding tangent altitudes.
- U is the umbra region defined above. It extends between the tangent altitude of approximately 0 km and the lowest tangent altitude where a measurement was done (typically 0 km + 30 seconds). The U region is used for the noise calculation and is not converted to transmittance.

In the first iteration, the linear regression from S is calculated using all available spectra above S_{min}. The linear fit is extrapolated into the region E, where atmospheric absorptions are present. Transmittances are calculated by dividing the spectra measured in the T region by the extrapolated line, with several checks performed to ensure that the linear regression is correct; if not, S_{max} is reduced and the checks are performed again. If S_{max} is reduced so much that there are now less than 20 spectra in the S region, S_{min} is reduced and the S_{max} region is iterated until the criteria being checked are met. If no acceptable fit is found, and S_{min} is reduced until there fewer than 20 spectra in the R region, then all spectra from that bin are rejected.

In cases where the signal is too low to perform the extrapolation, or if there are insufficient points in a region to perform the calculation, as above, the spectra in that bin are completely removed from the file. This is an extreme case, and generally only occurs if either there is a problem with the measurement parameters or spacecraft, or for particular types of observations e.g. grazing occultations where the tangent altitude never reaches the low atmosphere. If all bins are removed then the observation cannot be calibrated and the PSA product will not be generated.

Spectra can also be rejected if certain criteria are not met: if the transmittance in the R region is too low with respect the **Transmittance error** or standard deviation, or if the SNR is too low overall. In this case, the transmittance is calculated and will appear in the PSA product.

The transmittance noise, stored in the field **Transmittance error**, is calculated for all pixel of all spectra in the T region, using the standard deviation of the signal in the U and S regions, when the spectra have been normalised to reduce systematic errors (see Trompet et al. 2016 for full details).

At the time of writing, H_{unity} is set to the values in Table 18. These may be refined further when the data has been analysed more thoroughly. Note that, as the transmittance is calculated for all values in the T region, the highest altitude at which the observation begins/ends is not constant, and is dependent on diffraction order. During the iterative fitting process, S_{min} can also be reduced further, meaning that some observations will have different starting/ending altitudes even when measuring the same diffraction order. Care should be taken to use the correct tangent altitude for each spectrum in the .TAB product.

Diffraction order range	H_{unity} (km)	S_{min} (km)
110-145	120	150
146-154	160	200
155-157	180	220
158-166	200	230
167	160	200
168-200	120	150

Table 18: Starting altitudes for the SO channel occultation subregions. During the iterative fit, S_{min} may be reduced to satisfy the required criteria, hence the highest altitude in the file may vary between different observations.

Note that, whilst it is possible for the LNO channel to perform solar occultations, this is not currently envisaged unless there is a problem with the SO channel.

3.3.20 Level 1.0A – UVIS occultation transmittance calibration

UVIS solar occultation observations are calibrated in the similar way to the SO and LNO channels, except for the following differences:

- As UVIS does not measure diffraction orders, only one value for H_{unity} and S_{min} are needed. These are currently 120 km and 150 km respectively
- No extrapolation is performed from the S region to the R and E regions. Instead, each spectrum is divided by the mean of all S region spectra.

3.3.21 Level 1.0A - LNO nadir reflectance factor calibration

Two reflectance factor datasets are provided in the LNO nadir PSA products, following the two radiometric calibrations that were performed. The first is detailed in Thomas et al. 2022 [RD.15]. Dayside nadir observation spectra are converted to reflectance factor using solar calibration observations, where spectra are taken of all diffraction orders in the LNO channel spectral range. Using multiple different observations, where NOMAD is operating at different temperatures, allows a temperature-dependent model of the solar spectrum to be built. From this, for every nadir observation, a solar spectrum is generated for the same instrument temperature, and therefore the conversion to reflectance factor is as follows:

$$REFF = \pi \frac{ADU_{nadir}(T)}{ADU_{solar}(T)\, S\, cos(SZA)}$$

Where ADU is the analogue-to-digital units (counts) of the nadir and solar observations at instrument temperature T, normalised to counts per pixel per second; SZA is the solar zenith angle of the nadir observation; and S is the solar-to-nadir scaling factor. The last parameter is related to rsun, the radius of the Sun, and dsun, the distance between the Sun and Mars (accounting for the non-circular orbit of Mars around the Sun):

$$S = \pi \left(\frac{r_{sun}}{d_{sun}}\right)^2$$

The SZA used here is calculated as the mean of the real incidence angles (taking into account surface slopes) of the ten geometry points: the centre and the four corners of the FOV at the start and end of the acquisition. Reflectance factor per pixel is stored in the group field **Reflectance factor**. At present no error is calculated; when ready, values will be stored in the fields **Reflectance factor error**, with equal units to the radiance factor values above.

The second radiometric calibration method is described in Cruz Mermy et al. 2022 [RD.16]. This method starts from basic principles, calculating the instrument throughput from calibration observations and applying the results to the nadir spectra. The output is again reflectance factor per pixel, stored in the group field **Reflectance factor (baseline removed).**

Both methods are valid, however the latter uses a baseline correction method to remove oscillations from the nadir spectra. The result may be more useful for those analysing narrow gaseous absorption lines, as the continuum has been already flattened. However care should be taken when analysing wider spectral features such as those associated with surface composition, ice, or aerosols; as the baseline correction will remove these features from the

spectra. In these cases, only the **Reflectance factor** dataset should be used.

3.3.22 Level 1.0A - UVIS nadir radiance calibration

Convert detector pixel counts into radiance (W/m2/nm/sr) by multiplying the straylight corrected raw data by the instrumental function (determined during the ground calibration campaign). Spectra are stored in the group file Radiance. The radiance error on each pixel, stored in the group field **Radiance error,** is calculated by considering the errors accumulated throughout the calibration including straylight removal.

3.4 Validation

The following sections describe the process by which the data products are validated.

3.4.1 Instrument Team Validation

Various consistency checks will be performed on the data, as described below.

3.4.1.1 Consistency Check 1

The engineering team at BIRA-IASB and the OU check the incoming housekeeping data to ensure that the values received are within acceptable limits. Large anomalies will be dealt with through ESA, while small instrument issues are flagged in the pipeline through the use of quality flags.

3.4.1.2 Consistency Check 2

A consistency check is performed on the calibrated PDS4 products prior to delivery to the SOC. The check ensures that the pipeline has been correctly implemented and that the science results are accurate and sensible.

3.4.2 Peer Review

The SGS has conducted a full peer review of all of the data types that the NOMAD team intends to archive. The review data consists of fully formed bundles populated with candidate final versions of the data and other products and the associated metadata.

3.5 Data Delivery Schedule

Deliverables	Schedule
Corrected TM122 and TM125 binary raw data in .EXM format	Immediately* delivered to the ESA PSA.
Raw data in PDS4 format	Immediately converted by SOC to PDS4 format
Partially processed data in PDS4 format	Immediately converted by SOC to PDS4 format
Calibrated PDS4 data with supporting geometry (Level 1.0)	Immediately* delivered to the ESA PSA. Data will be made available via the PSA once the initial embargo is lifted.
Retrieved atmospheric profiles in PDS4 format (Level 2.0)	When data is ready and validated, up to a maximum of 12 months after generation of Level 1.0 data
Gridded maps and correlations in PDS4 format (Level 3.0)	When data is ready and validated, up to a maximum of 12 months after generation of Level 2.0 data

*Table 19: List of deliverables with corresponding delivery schedule (to the ESA PSA). * When fully operational, the interface between NOMAD and SOC will operate in near real time. Once all the required data for a given observation has arrived from the ESA PSA, a product is made by NOMAD rapidly (<24 hours) and will be immediately transferred to the ESA PSA where it is then prepared for delivery to the PSA. Delays will be incurred only if suspect or corrupted data is discovered.*

4 DATA ORGANISATION AND CONTENTS

This section describes the basic organization of a NOMAD bundle, and the naming conventions used for the products, collections and bundle, collection, and basic product filenames.

4.1 Format and Conventions

4.2 Bundle Content and Structure

The bundle structure is defined by the SOC, and is shown in Figure 2931.

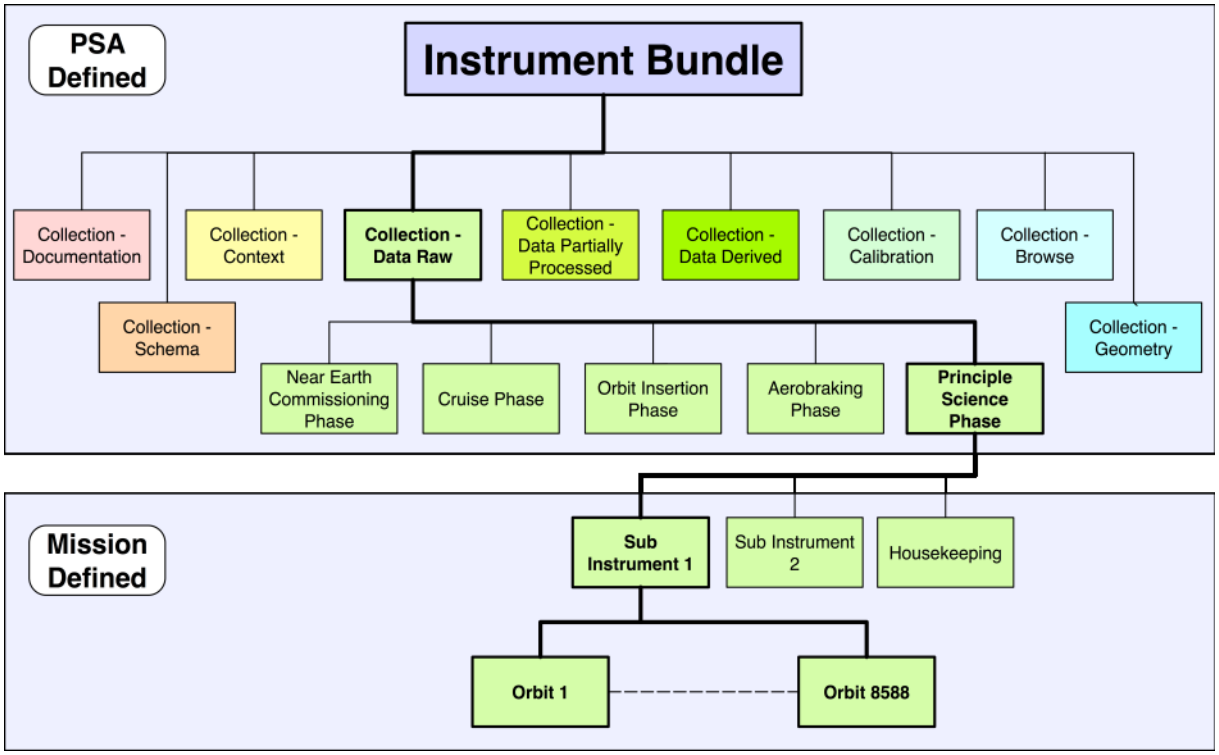

Figure 29: Instrument bundle structure in the PSA. Note that lowest level is subject to further subdivisions not shown here.

4.3 Data Directory Naming Convention

The subdivisions of the data_raw, data_partially_processed and data_calibrated directories is shown in Figure 3032, and depends on the mission phase. The data is divided by sub instrument between mission phase and the time/orbit subdivisions shown here, as follows:

- Data (data_raw, data_partially_processed, data_calibrated, etc.)
    - Mission phase (Near_Earth_Commissioning, Cruise, etc.)
        - Orbit range (in groups of 100 orbits, if applicable for the phase)
            - Orbit number (if applicable for the phase)

The sub level(s) vary depending on the mission phase:

- Near Earth Commissioning and Mid-Cruise Checkout: split by xxx
- Cruise phase: split by week
- Mars Capture Orbit: split by orbit
- Aerobraking: split by 100 orbits
- Science phase: split by 100 orbits, then split by orbit within that.

Where an observation spans multiple orbits, the time that the TC20 was executed in UTC is used to decide which directory the whole observation is placed in.

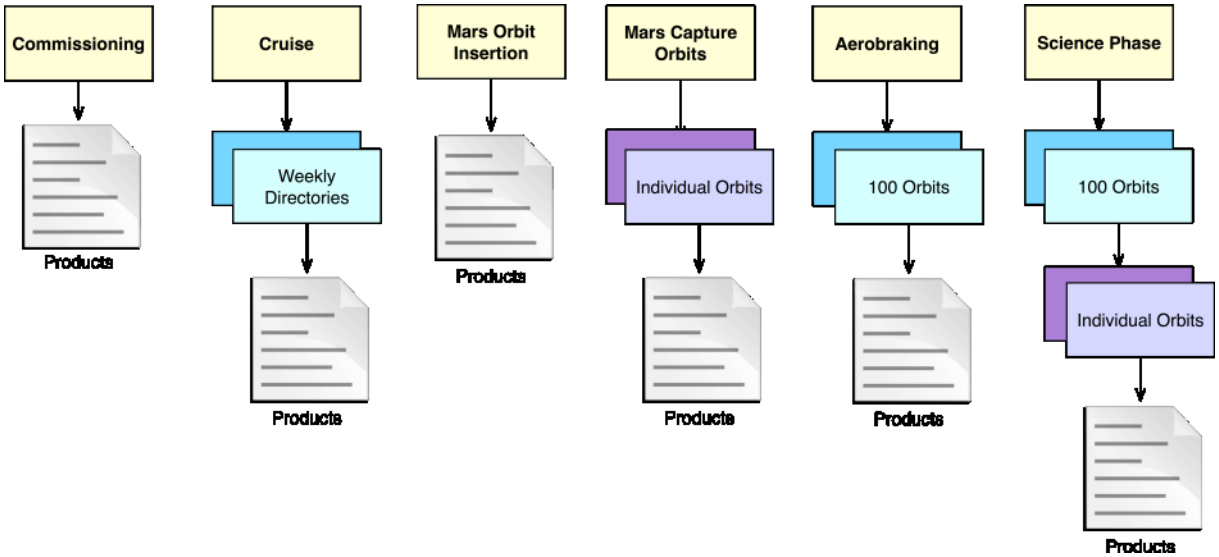

Figure 30: Separation of the data directories into further subdivisions. The number and type of separation depends on the mission phase.

The number and type of products contained within each orbit will depend on the mission phase and observations made within that orbit. One observation, as defined as one TC20 telecommand, will be split as shown in Figure 3133. Products vary by channel and observation type, therefore multiple branches are required. SO/LNO products are further split into one product per diffraction order.

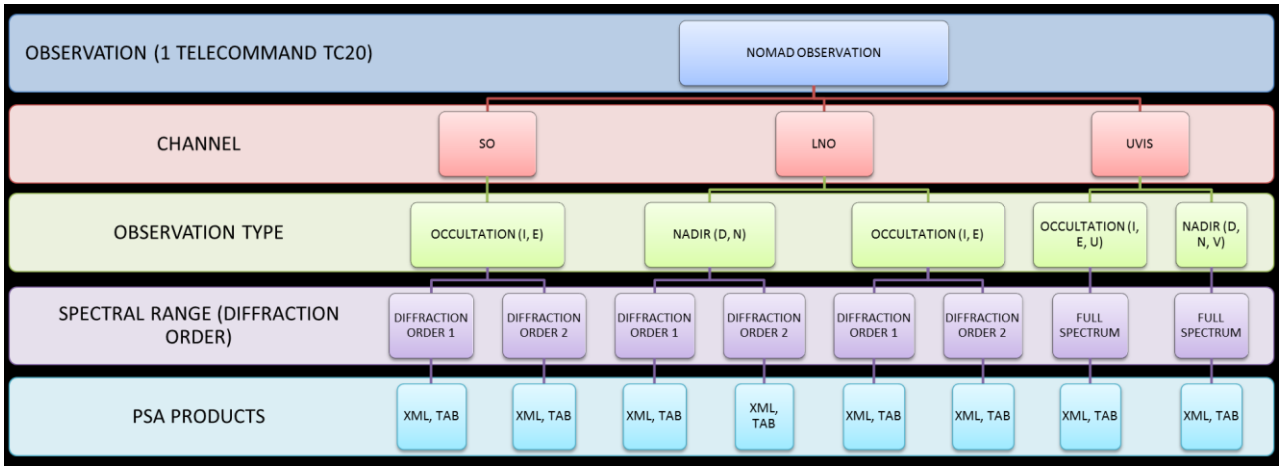

Figure 31: PSA product tree, showing how one nominal science observation is split by channel, observation type and diffraction order (if applicable) into multiple PDS4 products. SO and LNO can measure up to 6 diffraction orders, plus the 6 orders can be changed during a single observation – hence there could be 12 XML and TAB products generated from a single SO/LNO observation.

4.4 File Naming Convention

4.4.1 Raw and Partially Processed Products

Raw and partially processed products, as stored on the ESA PSA and PI institute filesystems, are named as follows:

nmd_<level>_<comm_type>_<pkt_type>_<YYYYMMDD1>T<hhmmss1>-<YYYYMMDD2>T<hhmmss2>-<pkt_type_no>-<orbit_no>-<obs_number>

where:

- *<level>* is the PSA data level, e.g. raw, par (for partially_processed).
- *<comm_type>* is the communication type used by NOMAD. "hk" designates packets sent via the 1553 connection, and "sc" for packets sent via SpaceWire.
- *<pkt_type>* is the packet type sent by NOMAD. This is “so” for the SO channel science data, “lno” for LNO data, “uvis” for UVIS data, “hk1” and “hk2” for housekeeping packets and “Sinbad” for data from SINBAD.
- *<YYYYMMDD1>T<hhmmss1>* is the observation start time in years, months, days, hours, minutes and seconds respectively.
- *<YYYYMMDD2>T<hhmmss2>* is the observation end time in years, months, days, hours, minutes and seconds respectively.
- *<pkt_type_no>* is the NOMAD packet type number as described in section 2.6.3.1 and RD10. For example, SO science data is sent in packets of type 22 or 122, LNO are types 25 or 125, etc. This has been implemented for UVIS in particular, which has three packet types (27, 28 and 29) all sent via Spacewire.
- *<orbit_no>* is the TGO orbit number. 0 = cruise phase
- *<obs_no>* is the observation number within the given orbit.

Note that when the products are delivered to the archive, the version number is appended. Therefore a typical sent product would be named as follows:
nmd_par_sc_lno_20161120T235932-20161121T004931-25-9999-3_2.0.xml
nmd_par_sc_lno_20161120T235932-20161121T004931-25-9999-3_2.0.tab

The version number is removed when delivered to the PSA archive, therefore archived products would be renamed to:
nmd_par_sc_lno_20161120T235932-20161121T004931-25-9999-3.xml
nmd_par_sc_lno_20161120T235932-20161121T004931-25-9999-3.tab

4.4.2 Calibrated Products

PDS4 calibrated products have a different naming convention, with more detail concerning the observation type and spectral range where appropriate:

- For solar occultation observations with SO or LNO:

  nmd_cal_sc_<channel>_<YYYYMMDD1>T<hhmmss1>-<YYYYMMDD2>T<hhmmss2>-<altitude_type>-<obs_type>-<diffraction_order>

- For nadir observations with LNO:

  nmd_cal_sc_lno_<YYYYMMDD1>T<hhmmss1>-<YYYYMMDD2>T<hhmmss2>-<obs_number>-<obs_type>-<diffraction_order>

- For UVIS observations:

  nmd_cal_sc_uvis_<YYYYMMDD1>T<hhmmss1>-<YYYYMMDD2>T<hhmmss2>-<obs_type>

Where:

- *<channel>* is “so” for the SO channel science data, “lno” for LNO data, or “uvis” for UVIS data.
- *<YYYYMMDD1>T<hhmmss1>* is the observation start time in years, months, days, hours, minutes and seconds respectively.
- *<YYYYMMDD2>T<hhmmss2>* is the observation end time in years, months, days, hours, minutes and seconds respectively.
- *<altitude_type>* denotes whether the given diffraction order was measured continuously throughout the occultation, or if it was switched at 50km (see section 3.3.7.1). The three options are: H=measured only at high altitudes; L=measured only at low altitudes; and A=measured at all altitudes. The latter is by far the most common.
- *<obs_number>* is a special flag for LNO, as it is theoretically possible that each nadir observation can be split into two halves, with a different set of diffraction orders used for each half. The number will be set to 1 for diffraction orders measured during the entire or first half of the nadir; or will be set to 2 for those measured during the second half of the nadir observation. At the time of writing this splitting has never been used, so only values of 1 will be present in the archive.
- *<obs_type>* is the observation type, e.g. I=occultation ingress, E=occultation egress, etc. These are defined in section 2.8.

- *<diffraction_order>* is the observed SO/LNO diffraction order, in the range 90-225, if appropriate.

4.4.3 Calibrated Browse Products

Browse products have a similar naming convention to the data products as follows:

- For solar occultation observations with SO or LNO:

  nmd_cal_sc_browse_<YYYYMMDD1>T<hhmmss1>-<YYYYMMDD2>T<hhmmss2>-<altitude_type>-<obs_type>-<diffraction_order>-<channel>

- For nadir observations with LNO:

  nmd_cal_sc_browse_<YYYYMMDD1>T<hhmmss1>-<YYYYMMDD2>T<hhmmss2>-<obs_number>-<obs_type>-<diffraction_order>-lno

- For UVIS observations:

  nmd_cal_sc_browse_<YYYYMMDD1>T<hhmmss1>-<YYYYMMDD2>T<hhmmss2>-<obs_type>-uvis

4.5 Logical Identifier Formation

The logical identifiers (LID) are defined below:

- The bundle LID for NOMAD is: urn:esa:psa:em16_tgo_nmd
- The raw data collection LID is: urn:esa:psa:em16_tgo_nmd:data_raw
- The partially processed data collection LID is: urn:esa:psa:em16_tgo_nmd:data_partially_processed
- The calibrated data collection LID is: urn:esa:psa:em16_tgo_nmd:data_calibrated

Product LIDs are defined as the collection LID + : + product name (section 4.4). For example:
urn:esa:psa:em16_tgo_nmd:data_calibrated:nmd_cal_sc_so_20180421t202111-20180421t203543-a-e-165

Is a calibrated NOMAD SO product, measuring diffraction order 165 during an egress occultation on 21st April 2018 at 20:21:11. The browse product LIDs are also defined in the same way.

4.6 Examples of Product Filenames

Table 1 contains examples of filenames for data and browse products that have been delivered to the PSA; one row is given for each observation type.

Observation Type	Example data and browse label filenames (replace .xml by .tab and .png for data table and browse image filenames)
SO occultation	nmd_cal_sc_so_20180422T120404-20180422T121838-a-e-190_3.0.xml nmd_cal_sc_browse_20180422T120404-20180422T121838-a-e-190-so_3.0.xml
UVIS occultation	nmd_cal_sc_uvis_20180422T001650-20180422T003123-e_3.0.xml nmd_cal_sc_browse_20180422T001650-20180422T003123-e-uvis_3.0.xml
UVIS grazing occultation	nmd_cal_sc_uvis_20180507T165516-20180507T173940-gi_3.0.xml nmd_cal_sc_browse_20180507T165516-20180507T173940-gi-uvis_3.0.xml
SO fullscan occultation	nmd_cal_sc_so_20180424T111248-20180424T112733-e-s_3.0.xml nmd_cal_sc_browse_20180424T111248-20180424T112733-e-s-so_3.0.xml
LNO fullscan occultation	nmd_cal_sc_lno_20181129T223804-20181129T225514-i-s_3.0.xml nmd_cal_sc_browse_20181129T223804-20181129T225514-i-s-lno_3.0.xml
LNO day nadir	nmd_cal_sc_lno_20180422T003456-20180422T013736-d-169_3.0.xml nmd_cal_sc_browse_20180422T003456-20180422T013736-d-169-lno_3.0.xml
UVIS day nadir	nmd_cal_sc_uvis_20180422T065058-20180422T071128-d_3.0.xml nmd_cal_sc_browse_20180422T065058-20180422T071128-d-uvis_3.0.xml
UVIS night nadir	nmd_cal_sc_uvis_20181009T194356-20181009T202049-n_3.0.xml nmd_cal_sc_browse_20181009T194356-20181009T202049-n-uvis_3.0.xml
UVIS day limb	nmd_cal_sc_uvis_20210408T135810-20210408T151105-l_3.0.xml nmd_cal_sc_browse_20210408T135810-20210408T151105-l-uvis_3.0.xml
UVIS night limb	nmd_cal_sc_uvis_20210404T065052-20210404T072557-o_3.0.xml nmd_cal_sc_browse_20210404T065052-20210404T072557-o-uvis_3.0.xml
SO solar line scan calibration	nmd_cal_sc_so_20180428T023343-20180428T032553-cl_3.0.xml nmd_cal_sc_browse_20180428T023343-20180428T032553-cl-so_3.0.xml
LNO solar line scan calibration	nmd_cal_sc_lno_20180619T020651-20180619T030101-cl_3.0.xml nmd_cal_sc_browse_20180619T020651-20180619T030101-cl-lno_3.0.xml
UVIS solar line scan calibration	nmd_cal_sc_uvis_20180522T221149-20180522T230359-cl_3.0.xml nmd_cal_sc_browse_20180522T221149-20180522T230359-cl-uvis_3.0.xml
SO solar fullscan calibration	nmd_cal_sc_so_20180702T104832-20180702T112342-cf_3.0.xml nmd_cal_sc_browse_20180702T104832-20180702T112342-cf-so_3.0.xml
LNO solar fullscan calibration	nmd_cal_sc_lno_20180702T112352-20180702T115902-cf_3.0.xml nmd_cal_sc_browse_20180702T112352-20180702T115902-cf-lno_3.0.xml
SO solar miniscan calibration	nmd_cal_sc_so_20180715T232121-20180716T000701-1-cm_3.0.xml nmd_cal_sc_so_20180715T232121-20180716T000701-2-cm_3.0.xml

	nmd_cal_sc_browse_20180715T232121-20180716T000701-1-cm-so_3.0.xml nmd_cal_sc_browse_20180715T232121-20180716T000701-2-cm-so_3.0.xml
LNO solar miniscan calibration	nmd_cal_sc_lno_20180912T082502-20180912T090802-1-cm_3.0.xml nmd_cal_sc_lno_20180912T082502-20180912T090802-2-cm_3.0.xml nmd_cal_sc_browse_20180912T082502-20180912T090802-1-cm-lno_3.0.xml nmd_cal_sc_browse_20180912T082502-20180912T090802-2-cm-lno_3.0.xml
UVIS solar stare calibration	nmd_cal_sc_uvis_20180702T104832-20180702T112342-cs_3.0.xml nmd_cal_sc_browse_20180702T104832-20180702T112342-cs-uvis_3.0.xml

Table 20: Examples of data and browse product filenames for all observation types delivered to the PSA

4.7 Data volume estimation

Data volume estimates for NOMAD, running in E-IRD compliant mode, are given in Table 2120.

When the data rate is high, UVIS will operate regularly in full frame mode, therefore these values will increase significantly for nadir observations to fill the volume allocated to NOMAD by the SOC. Due to the high data rate throughout the mission so far, UVIS had been able to operate mainly in full frame mode, therefore the values below will be an underestimate.

Data Level	Channel	Total data volume
EDDS Data Volume	All	18.7 Mb per orbit
		0.22 Gb per day
		6.73 Gb per MTP
PSA Raw Data Volume	All	40 Mb per orbit
		0.48 Gb per day
		14.4 Gb per MTP
PSA Partially Processed Data Volume	All	40 mb per orbit
		0.48 Gb per day
		14.4 Gb per MTP
PSA Calibrated Data Volume	SO Occ	65.0 mb per orbit
	LNO Nadir	8.7 mb per orbit
	UVIS Occ	31.9 mb per orbit
	UVIS Nadir	7.1 mb per orbit

	All	112.7 mb per orbit
		1.4 Gb per day
		40.6 Gb per MTP

Table 21: Data volume estimates for NOMAD

The ESA PSA volume is dynamically allocated at ESAC and can be adjusted to the needs of each mission as the mission progresses. The extent to which this allocation is used is routinely monitored and a request for additional space can be actioned within hours.

4.8 NOMAD Science Data Organisation

The NOMAD science data is organised into 1 instrument bundle listed in Table 2221. The following sections describe the contents of each of these bundles in more detail.

Bundle Title	***Bundle Logical Identifier***	***Description***
NOMAD Instrument Bundle	em16_tgo_nom	Master Bundle for NOMAD Instrument data

Table 22: NOMAD data bundle

4.8.1 NOMAD Bundle 1

High-level description of the bundle and bundle content, including responsibility for the generation of specific products.

Collection Logical ID	***Description***
context	Mission and Observation Aims
xml_schema	PDS format conventions
document	Ancillary documents describing NOMAD
calibration	Products containing calibration coefficients
data_raw	Raw data (generated by SOC)
data_partially_processed	Partially processed data (generated by SOC)
data_calibrated	Calibrated data (delivered by NOMAD team)
data_derived	Derived data (delivered by NOMAD team; TBD)

Table 23: NOMAD Bundle 1 Content

5 DATA PRODUCT FORMATS

NOMAD data products are formatted in accordance with the PDS4 specifications (see [AD.03], [AD.04] and [AD.05]) following the rules in the ExoMars 2016 Archiving Guide [AD.02]. This section provides details on the formats used for each of the products included in the NOMAD science data.

5.1 Primary Products Formats

This section describes the format and record structure of each of the data file types. The generated products are separated into the following collections:

- documentation
  - Information to understand and use the data products, e.g.
    - Interface control document for NOMAD archive (this document)
    - Descriptions of calibration pipelines
    - Published technical papers describing the instrument, functions, studies and science objectives, subject to publishers' rules.
- schema
  - Documents describing file structure and PDS4/PSA conventions
- context
  - Documents containing PDS4 registration data e.g. mission and instrument information
- data_raw
  - Raw data, as returned from the spacecraft
- data_partially_processed
  - Partially processed data, with housekeeping converted to physical units
- data_calibrated
  - Calibrated data, with housekeeping and science data converted to physical units with geometry and other parameters added.
- data_derived
  - TBD: Derived data e.g. gridded maps and other higher-level products
- calibration:
  - Calibration observation products and products containing AOTF functions, bad pixel maps, etc. derived from ground and inflight calibration campaigns

5.2 Raw Data Products

Conversion from EDDS to PDS4 raw data products is performed by the SOC. Detailed descriptions of each parameter are given below, separated by product type.

5.2.1 NOMAD Housekeeping 1 Product

Product Field Name	Description	Data Type	Data Units
PACKET TYPE 23	0 = no packet data, 23 = data in packet	Integer	None
PACKET SIZE 23	size of packet	Integer	Bytes
COARSE TIME STAMP 23	packet timestamp coarse	Integer	None
FINE TIME STAMP 23	packet timestamp fine	Integer	None
TM COUNT 23	packet number (of this type)	Integer	None
+12V_SO_CCC (raw/pp)	+12 V measured on CCC board of SO	Integer (raw)/ float (pp)	None (raw)/ volts (pp)
-12V_SO_CCC (raw/pp)	-12 V measured on CCC board of SO	Integer (raw)/ float (pp)	None (raw)/ volts (pp)
+8.5V_SO_HSK (raw/pp)	+8.5 V measured on HSK board of SO	Integer (raw)/ float (pp)	None (raw)/ volts (pp)
-8.5V_SO_HSK (raw/pp)	-8.5 V measured on HSK board of SO	Integer (raw)/ float (pp)	None (raw)/ volts (pp)
+3.3V_SO_CCC (raw/pp)	+3.3 V measured on CCC board of SO	Integer (raw)/ float (pp)	None (raw)/ volts (pp)
+2.5V_SO_CCC (raw/pp)	+2.5 V measured on CCC board of SO	Integer (raw)/ float (pp)	None (raw)/ volts (pp)
+5V_SO_HSK (raw/pp)	+5 V measured on HSK board of SO	Integer (raw)/ float (pp)	None (raw)/ volts (pp)
-5V_SO_HSK (raw/pp)	-5 V measured on HSK board of SO	Integer (raw)/ float (pp)	None (raw)/ volts (pp)
FPA1_FULL_SCALE_TEMP_SO (raw/pp)	SO focal plane array full scale temperature	Integer (raw)/ float (pp)	None (raw)/ kelvin (pp)
FPA2_ZOOMED_TEMP_SO (raw/pp)	SO focal plane array zoomed temperature	Integer (raw)/ float (pp)	None (raw)/ kelvin (pp)
SENSOR_1_TEMP_SO (raw/pp)	temperature sensor 1 near SO AOTF housing	Integer (raw)/ float (pp)	None (raw)/ Celsius (pp)
SENSOR_2_TEMP_SO (raw/pp)	temperature sensor 2 near SO grating structure	Integer (raw)/ float (pp)	None (raw)/ Celsius (pp)
SENSOR_3_TEMP_SO (r	temperature sensor 3 near SO	Integer (raw)/ float	None (raw)/ Celsius

aw/pp)	detector structure	(pp)	(pp)
AOTF_TEMP_SO (raw/pp)	temperature inside SO AOTF box	Integer (raw)/ float (pp)	None (raw)/ Celsius (pp)
RF_AMPLITUDE_SO (raw/pp)	RF amplitude of SO AOTF driver	Integer (raw)/ float (pp)	None (raw)/ volts (pp)
GROUND_POTENTIAL_SO_HSK (raw/pp)	ground potential measured on SO HSK board	Integer (raw)/ float (pp)	None (raw)/ volts (pp)
MOTOR_POWER_DAC_CODE_SO (raw/pp)	SO cooler motor power DAC control	Integer	None (raw)/ ADU (pp)
CHECKSUM 23	packet checksum	Hexadecimal	None
PACKET TYPE 26	0 = no packet data, 26 = data in packet	Integer	None
PACKET SIZE 26	size of packet	Integer	Bytes
COARSE TIME STAMP 26	packet timestamp coarse	Integer	None
FINE TIME STAMP 26	packet timestamp fine	Integer	None
TM COUNT 26	packet number (of this type)	Integer	None
+12V_LNO_CCC (raw/pp)	+12 V measured on CCC board of LNO	Integer (raw)/ float (pp)	None (raw)/ volts (pp)
-12V_LNO_CCC (raw/pp)	-12 V measured on CCC board of LNO	Integer (raw)/ float (pp)	None (raw)/ volts (pp)
+8.5V_LNO_HSK (raw/pp)	+8.5 V measured on HSK board of LNO	Integer (raw)/ float (pp)	None (raw)/ volts (pp)
-8.5V_LNO_HSK (raw/pp)	-8.5 V measured on HSK board of LNO	Integer (raw)/ float (pp)	None (raw)/ volts (pp)
+3.3V_LNO_CCC (raw/pp)	+3.3 V measured on CCC board of LNO	Integer (raw)/ float (pp)	None (raw)/ volts (pp)
+2.5V_LNO_CCC (raw/pp)	+2.5 V measured on CCC board of LNO	Integer (raw)/ float (pp)	None (raw)/ volts (pp)
+5V_LNO_HSK (raw/pp)	+5 V measured on HSK board of LNO	Integer (raw)/ float (pp)	None (raw)/ volts (pp)
-5V_LNO_HSK (raw/pp)	-5 V measured on HSK board of LNO	Integer (raw)/ float (pp)	None (raw)/ volts (pp)
FPA1_FULL_SCALE_TEMP_LNO (raw/pp)	LNO focal plane array full scale temperture	Integer (raw)/ float (pp)	None (raw)/ kelvin (pp)
FPA2_ZOOMED_TEMP_LNO (raw/pp)	LNO focal plane array zoomed temperature	Integer (raw)/ float (pp)	None (raw)/ kelvin (pp)
SENSOR_1_TEMP_LNO (raw/pp)	temperature sensor 1 near LNO AOTF housing	Integer (raw)/ float (pp)	None (raw)/ Celsius (pp)
SENSOR_2_TEMP_LNO (raw/pp)	temperature sensor 2 near LNO grating structure	Integer (raw)/ float (pp)	None (raw)/ Celsius (pp)
SENSOR_3_TEMP_LNO (raw/pp)	temperature sensor 3 near LNO detector structure	Integer (raw)/ float (pp)	None (raw)/ Celsius (pp)

AOTF_TEMP_LNO (raw/ pp)	temperature inside LNO AOTF box	Integer (raw)/ float (pp)	None (raw)/ Celsius (pp)
RF_AMPLITUDE_LNO (raw/pp)	RF amplitude of LNO AOTF driver	Integer (raw)/ float (pp)	None (raw)/ volts (pp)
GROUND_POTENTIAL_ LNO_HSK (raw/pp)	ground potential measured on LNO HSK board	Integer (raw)/ float (pp)	None (raw)/ volts (pp)
MOTOR_POWER_DAC_ CODE_LNO (raw/pp)	LNO cooler motor power DAC control	Integer	None (raw)/ ADU (pp)
CHECKSUM 26	packet checksum	Hexadecimal	None
PACKET TYPE 29	0 = no packet data, 29 = data in packet	Integer	None
PACKET SIZE 29	size of packet	Integer	Bytes
COARSE TIME STAMP 29	packet timestamp coarse	Integer	None
FINE TIME STAMP 29	packet timestamp fine	Integer	None
TM COUNT 29	packet number (of this type)	Integer	None
+10V_RAIL_VOLTAGE (raw/pp)	+10 V measured on UVIS board	Integer (raw)/ float (pp)	None (raw)/ volts (pp)
-10V_RAIL_VOLTAGE (raw/pp)	-10 V measured on UVIS board	Integer (raw)/ float (pp)	None (raw)/ volts (pp)
+5V_RAIL_VOLTAGE (raw/pp)	+5 V measured on UVIS board	Integer (raw)/ float (pp)	None (raw)/ volts (pp)
-5V_RAIL_VOLTAGE (raw/pp)	-5 V measured on UVIS board	Integer (raw)/ float (pp)	None (raw)/ volts (pp)
+12V_RAIL_CURRENT (raw/pp)	+12V rail current	Integer (raw)/ float (pp)	None (raw)/ milliamps (pp)
-12V_RAIL_CURRENT (raw/pp)	-12V rail current	Integer (raw)/ float (pp)	None (raw)/ milliamps (pp)
+5V_RAIL_CURRENT (raw/pp)	+5V rail current	Integer (raw)/ float (pp)	None (raw)/ milliamps (pp)
-5V_RAIL_CURRENT (raw/pp)	-5V rail current	Integer (raw)/ float (pp)	None (raw)/ milliamps (pp)
CCD_IMAGE_CLOCK_HIGH (raw/pp)	CCD image clock HI	Integer (raw)/ float (pp)	None (raw)/ volts (pp)
CCD_IMAGE_CLOCK_LOW (raw/pp)	CCD image clock LO	Integer (raw)/ float (pp)	None (raw)/ volts (pp)
CCD_READOUT_REG_ HIGH (raw/pp)	CCD readout register HI	Integer (raw)/ float (pp)	None (raw)/ volts (pp)
CCD_READOUT_REG_LOW (raw/pp)	CCD readout register LO	Integer (raw)/ float (pp)	None (raw)/ volts (pp)

SUBSTRATE_VOLTAGE_VSS (raw/pp)	Substrate Voltage (VSS)	Integer (raw)/ float (pp)	None (raw)/ volts (pp)
OUTPUT_GATE_VOLTAGE_VOG (raw/pp)	Output gate voltage (VOG)	Integer (raw)/ float (pp)	None (raw)/ volts (pp)
OUTPUT_DRAIN_VOLTAGE_VOD (raw/pp)	Output drain voltage (VOD)	Integer (raw)/ float (pp)	None (raw)/ volts (pp)
RESET_DRAIN_VOLTAGE_VRD (raw/pp)	Reset transistor drain voltage (VRD)	Integer (raw)/ float (pp)	None (raw)/ volts (pp)
DIODE_DRAIN_VOLTAGE_VDD (raw/pp)	Diode drain voltage (VDD)	Integer (raw)/ float (pp)	None (raw)/ volts (pp)
TEMP_1_PROXIMITY_BOARD (raw/pp)	Temp 1 (Proximity Board)	Integer (raw)/ float (pp)	None (raw)/ Celsius (pp)
TEMP_2_CCD (raw/pp)	Temp 2 (CCD)	Integer (raw)/ float (pp)	None (raw)/ Celsius (pp)
TEMP_3_DETECTOR_BOARD (raw/pp)	Temp 3 (Detector Board)	Integer (raw)/ float (pp)	None (raw)/ celsius (pp)
MOTOR_CURRENT_A (raw/pp)	Motor current	Integer (raw)/ float (pp)	None (raw)/ milliamps (pp)
CHECKSUM 29	packet checksum	Hexadecimal	None

Table 24: NOMAD HSK 1 raw and partially processed (pp) PDS4 product fields

5.2.2 NOMAD Housekeeping 2 Product

The housekeeping 2 product is purely for engineering purposes and contains no useful information for PSA users.

5.2.3 NOMAD SO 22 and 122 Science Product

Product Field Name	Description	Data Type	Data Units
PACKET_SIZE	size of packet	Integer	Bytes
TIMESTAMP COARSE	packet timestamp coarse	Integer	None
TIMESTAMP FINE	packet timestamp fine	Integer	None
TM COUNT	packet number (of this type)	Integer	None
TC_EXECUTION_TIMESTAMP COARSE	packet timestamp coarse	Integer	None
TC_EXECUTION_TIMESTAMP FINE	packet timestamp fine	Integer	None
CHANNEL_ID	1= SO, 2= LNO	Integer	None

FLIP_MIRROR_INFO	0= contingency position (solar), 1= default position (nadir), 255= unknown position	Integer	None
HSK_TIMESTAMP COARSE	housekeeping packet timestamp coarse	Integer	None
HSK_TIMESTAMP FINE	housekeeping packet timestamp fine	Integer	None
HSK_TM_COUNT	packet number (of this type)	Integer	None
+12V_SO_CCC (raw/pp)	+12 V measured on CCC board of SO	Integer (raw)/ float (pp)	None (raw)/ volts (pp)
-12V_SO_CCC (raw/pp)	-12 V measured on CCC board of SO	Integer (raw)/ float (pp)	None (raw)/ volts (pp)
+8.5V_SO_HSK (raw/pp)	+8.5 V measured on HSK board of SO	Integer (raw)/ float (pp)	None (raw)/ volts (pp)
-8.5V_SO_HSK (raw/pp)	-8.5 V measured on HSK board of SO	Integer (raw)/ float (pp)	None (raw)/ volts (pp)
+3.3V_SO_CCC (raw/pp)	+3.3 V measured on CCC board of SO	Integer (raw)/ float (pp)	None (raw)/ volts (pp)
+2.5V_SO_CCC (raw/pp)	+2.5 V measured on CCC board of SO	Integer (raw)/ float (pp)	None (raw)/ volts (pp)
+5V_SO_HSK (raw/pp)	+5 V measured on HSK board of SO	Integer (raw)/ float (pp)	None (raw)/ volts (pp)
-5V_SO_HSK (raw/pp)	-5 V measured on HSK board of SO	Integer (raw)/ float (pp)	None (raw)/ volts (pp)
FPA1_FULL_SCALE_TEMP_SO (raw/pp)	SO focal plane array full scale temperature	Integer (raw)/ float (pp)	None (raw)/ kelvin (pp)
FPA2_ZOOMED_TEMP_SO (raw/pp)	SO focal plane array zoomed temperature	Integer (raw)/ float (pp)	None (raw)/ kelvin (pp)
SENSOR_1_TEMP_SO (raw/pp)	temperature sensor 1 near SO AOTF housing	Integer (raw)/ float (pp)	None (raw)/ Celsius (pp)
SENSOR_2_TEMP_SO (raw/pp)	temperature sensor 2 near SO grating structure	Integer (raw)/ float (pp)	None (raw)/ Celsius (pp)
SENSOR_3_TEMP_SO (raw/pp)	temperature sensor 3 near SO detector structure	Integer (raw)/ float (pp)	None (raw)/ Celsius (pp)
AOTF_TEMP_SO (raw/pp)	temperature inside SO AOTF box	Integer (raw)/ float (pp)	None (raw)/ Celsius (pp)
RF_AMPLITUDE_SO (raw/pp)	RF amplitude of SO AOTF driver	Integer (raw)/ float (pp)	None (raw)/ volts (pp)

GROUND_POTENTIAL_SO_HSK (raw/pp)	ground potential measured on SO HSK board	Integer (raw)/ float (pp)	None (raw)/ volts (pp)
MOTOR_POWER_DAC_CODE_SO (raw/pp)	SO cooler motor power DAC control	Integer	None (raw)/ ADU (pp)
SIZE_OF_TC_COPY	Size of "LAST_TELECOMMAND" parameter. Equal to (number of subdomains measured)*25	Integer	Bytes
SIZE_OF_SCIENCE_DATA	Size of "SO_SCIENCE_DATA" parameter. Equal to 16+480* (number of spectra returned)	Integer	Bytes
LAST_TELECOMMAND	See section 5.2.7.1	Hexadecimal	None
SO_SCIENCE_DATA	See section 5.2.7.2	Hexadecimal	None

Table 25: NOMAD SO raw and partially processed (pp) PDS4 product fields

5.2.4 NOMAD LNO 25 and 125 Science Product

Product Field Name	Description	Data Type	Data Units
PACKET_SIZE	size of packet	Integer	Bytes
TIMESTAMP COARSE	packet timestamp coarse	Integer	None
TIMESTAMP FINE	packet timestamp fine	Integer	None
TM COUNT	packet number (of this type)	Integer	None
TC_EXECUTION_TIMESTAMP COARSE	packet timestamp coarse	Integer	None
TC_EXECUTION_TIMESTAMP FINE	packet timestamp fine	Integer	None
CHANNEL_ID	1= SO, 2= LNO	Integer	None
FLIP_MIRROR_INFO	0= contingency position (solar), 1= default position (nadir), 255= unknown position	Integer	None
HSK_TIMESTAMP COARSE	housekeeping packet timestamp coarse	Integer	None
HSK_TIMESTAMP FINE	housekeeping packet timestamp fine	Integer	None
HSK_TM_COUNT	packet number (of this type)	Integer	None

+12V_LNO_CCC (raw/pp)	+12 V measured on CCC board of LNO	Integer (raw)/ float (pp)	None (raw)/ volts (pp)
-12V_LNO_CCC (raw/pp)	-12 V measured on CCC board of LNO	Integer (raw)/ float (pp)	None (raw)/ volts (pp)
+8.5V_LNO_HSK (raw/pp)	+8.5 V measured on HSK board of LNO	Integer (raw)/ float (pp)	None (raw)/ volts (pp)
-8.5V_LNO_HSK (raw/pp)	-8.5 V measured on HSK board of LNO	Integer (raw)/ float (pp)	None (raw)/ volts (pp)
+3.3V_LNO_CCC (raw/pp)	+3.3 V measured on CCC board of LNO	Integer (raw)/ float (pp)	None (raw)/ volts (pp)
+2.5V_LNO_CCC (raw/pp)	+2.5 V measured on CCC board of LNO	Integer (raw)/ float (pp)	None (raw)/ volts (pp)
+5V_LNO_HSK (raw/pp)	+5 V measured on HSK board of LNO	Integer (raw)/ float (pp)	None (raw)/ volts (pp)
-5V_LNO_HSK (raw/pp)	-5 V measured on HSK board of LNO	Integer (raw)/ float (pp)	None (raw)/ volts (pp)
FPA1_FULL_SCALE_TEMP_LNO (raw/pp)	LNO focal plane array full scale temperature	Integer (raw)/ float (pp)	None (raw)/ kelvin (pp)
FPA2_ZOOMED_TEMP_LNO (raw/pp)	LNO focal plane array zoomed temperature	Integer (raw)/ float (pp)	None (raw)/ kelvin (pp)
SENSOR_1_TEMP_LNO (raw/pp)	temperature sensor 1 near LNO AOTF housing	Integer (raw)/ float (pp)	None (raw)/ Celsius (pp)
SENSOR_2_TEMP_LNO (raw/pp)	temperature sensor 2 near LNO grating structure	Integer (raw)/ float (pp)	None (raw)/ Celsius (pp)
SENSOR_3_TEMP_LNO (raw/pp)	temperature sensor 3 near LNO detector structure	Integer (raw)/ float (pp)	None (raw)/ Celsius (pp)
AOTF_TEMP_LNO (raw/pp)	temperature inside LNO AOTF box	Integer (raw)/ float (pp)	None (raw)/ Celsius (pp)
RF_AMPLITUDE_LNO (raw/pp)	RF amplitude of LNO AOTF driver	Integer (raw)/ float (pp)	None (raw)/ volts (pp)
GROUND_POTENTIAL_LNO_HSK (raw/pp)	ground potential measured on LNO HSK board	Integer (raw)/ float (pp)	None (raw)/ volts (pp)
MOTOR_POWER_DAC_CODE_LNO (raw/pp)	LNO cooler motor power DAC control	Integer	None (raw)/ ADU (pp)
SIZE_OF_TC_COPY	Size of "LAST_TELECOMMAND" parameter. Equal to (number of subdomains measured)*25	Integer	Bytes
SIZE_OF_SCIENCE_DATA	Size of "LNO_SCIENCE_DATA"	Integer	Bytes

	parameter. Equal to 16+480* (number of spectra returned)		
LAST_TELECOMMAND	See section 5.2.7.1	Hexadecimal	None
LNO_SCIENCE_DATA	See section 5.2.7.2	Hexadecimal	None

Table 26: NOMAD LNO raw and partially processed (pp) PDS4 product fields

5.2.5 NOMAD UVIS 27 Science Product

Product Field Name	Description	Data Type	Data Units
PACKET_SIZE	size of packet	Integer	Bytes
TIMESTAMP_SECONDS	packet timestamp coarse	Integer	None
TIMESTAMP_MICROSECONDS	packet timestamp fine	Integer	None
TM_COUNT	packet number (of this type)	Integer	None
UVIS_RESET_SELECTOR	selector mechanism reset flag	Integer	None
MODE	Functional mode for this set of scans (1 = SO, 2 = Nadir, 3=Calibration Selector, 5 = Cruise Checkout Test Card)	Integer	None
ACQUISITION_MODE	CCD readout mode (0 = Full CCD, 1 = Vertical Binning)	Integer	None
BIAS_AVERAGE	Number of 'Bias' scans to average.	Integer	None
DARK_AVERAGE	Number of 'Dark' scans to average.	Integer	None
SCIENCE_AVERAGE	Number of 'Science' scans to average.	Integer	None
V_START	Top Right Corner, Y - Coordinate	Integer	None
V_END	Bottom Left Corner, Y - Coordinate	Integer	None
H_START	Top Right Corner, X - Coordinate	Integer	None
H_END	Bottom Left Corner, X - Coordinate	Integer	None
VOD_VALUE	Value to apply to VOD DAC	Integer	ADU
VRD_VALUE	Value to apply to VRD DAC	Integer	ADU
START_DELAY	Delay from start command (Number of 5 millisecond increments to pause between receipt of start command and actual acquisition.)	Integer	None

ACQUISITION_DELAY	Delay between two successive acquisitions (Number of 5 millisecond increments to pause between receipt of start command and actual acquisition.)	Integer	None
INTEGRATION_TIME	Exposure delay before the CCD readout starts. (Time to accumulate image prior to readout). 0<value<20000: 0 to 20000 ms in 1 ms increments; 20000<value<21600: 20 to 180 s in 0.1 s increments	Integer	None
NUMBER_OF_ACQUISITIONS	Number of acquistions to return in current sweep	Integer	None
NUMBER_OF_FLUSHES	Number of flush operations to carry out	Integer	None
DARK_TO_OBSERVATION_STEPS	Steps to drive motor from dark to observation mode	Integer	None
OBSERVATION_TO_DARK_STEPS	Steps to drive motor from observation mode to dark	Integer	None
MOTOR_DELAY	Sets stepper motor drive frequency	Integer	None
MOTOR_START_POSITION	Sets the starting pole position for the SO and NADIR motor sequences	Integer	None
B7_SET_ON_OFF_CHIP_BINNING	0 = Binning is performed in the FPGA, 1 = Binning is perform on chip	Integer	None
B6_MOTOR_HOLD	0 = No motor hold, 1 = default = active motor hold to accurately keep the fixed measurement position.	Integer	None
B5_LED	0 = default = LED Off (always off for inflight), 1 = LED On for ground testing.	Integer	None
B4_LOCATE_DARK	0 = default = don't sweep the motor from Dark->SO->Dark->ND. 1 = do a full sweep to reset motor position.	Integer	None
B3_SCI_HK	0 = default = not to include the full HK in sci packets (but include the three Temperatures); 1= full HK in sci pckts	Integer	None
B2_INTEGRATION_TIME_INCREMENT	Integration time increment, 0 = no increments, 1 = causes the sequencer to increase the integration time after each pair of acquisitions in a way that is useful for photon transfer curve measurement, resulting in times that increase by a factor of 1,1, 2,2, 3,3, 4,4, 5,5 etc	Integer	None
B1_LOOP_DARK	Loop Dark is for alternating between Dark & Science measurements. 0 = no loop (but still do the first and last dark scans), 1 = loop Dark--> Obs	Integer	None
B0_LED_CONTROL	bit 0 (Lsb) = LED permanently ON (for cal);	Integer	None
HORIZONTAL_AND_COMBINED_	Number of columns for Horizontal binning, or size of side for square "super pixels" for Combined binning.	Integer	None

BINNING_SIZE			
CONTROL_BITS	Bit 0: 1 to inhibit Noise measurement. Bit 1: 0 for Reverse clocking in Noise measurement, 1 for Forward clocking. Bit 2: 0 for two rows of Noise measurement, 1 for one row. Bit 3: 1 to inhibit Leading Bias. Bit 4: 1 to inhibit Leading Dark. Bit 5: 1 to inhibit Science. Bit 6: 1 to inhibit Trailing Bias. Bit 7: 1 to inhibit Trailing Dark. Bit 8: 1 to inhibit Sweep While Flush (R-clocks dis/en-abled with 3us period). Bit 9: 1 for Synthetic Data Bit 11: 1 = HK inhibited (TM29 HK o/p supressed, used during full frames / SINBAD comms tests) , 0=HK TM29 output at defined rates (1 per sec in SO and 1 per 15 seconds in ND) Bits 15..12 I-clock timing adjustment	Integer	None

Table 27: NOMAD UVIS TM(27) raw and partially processed (pp) PDS4 product fields

5.2.6 NOMAD UVIS 28 Science Product

Product Field Name	Description	Data Type	Data Units
PACKET_SIZE	size of packet	Integer	Bytes
TIMESTAMP COARSE	packet timestamp coarse	Integer	None
TIMESTAMP FINE	packet timestamp fine	Integer	None
TM_COUNT	packet number (of this type)	Integer	None
MODE	Functional mode for this set of scans (1 = SO, 2 = Nadir, 3=Calibration Selector, 5 = Cruise Checkout Test Card)	Integer	None
ACQUISITION_MODE	CCD readout mode (0 = Full CCD, 1 = Vertical Binning)	Integer	None
BIAS_AVERAGE	Number of 'Bias' scans to average.	Integer	None
DARK_AVERAGE	Number of 'Dark' scans to average.	Integer	None
SCIENCE_AVERAGE	Number of 'Science' scans to average.	Integer	None
V_START	Top Right Corner, Y - Coordinate	Integer	None
V_END	Bottom Left Corner, Y - Coordinate	Integer	None
H_START	Top Right Corner, X - Coordinate	Integer	None

H_END	Bottom Left Corner, X - Coordinate	Integer	None
VOD_VALUE	Value to apply to VOD DAC	Integer	ADU
VRD_VALUE	Value to apply to VRD DAC	Integer	ADU
START_DELAY	Delay from start command (Number of 5 millisecond increments to pause between receipt of start command and actual acquisition.)	Integer	None
ACQUISITION_DELAY	Delay between two successive acquisitions (Number of 5 millisecond increments to pause between receipt of start command and actual acquisition.)	Integer	None
INTEGRATION_TIME	Exposure delay before the CCD readout starts. (Time to accumulate image prior to readout). 0<value<20000: 0 to 20000 ms in 1 ms increments; 20000<value<21600: 20 to 180 s in 0.1 s increments	Integer	None
NUMBER_OF_ACQUISITIONS	Number of acquistions to return in current sweep	Integer	None
NUMBER_OF_FLUSHES	Number of flush operations to carry out	Integer	None
DARK_TO_OBSERVATION_STEPS	Steps to drive motor from dark to observation mode	Integer	None
OBSERVATION_TO_DARK_STEPS	Steps to drive motor from observation mode to dark	Integer	None
MOTOR_DELAY	Sets stepper motor drive frequency	Integer	None
MOTOR_START_POSITION	Sets the starting pole position for the SO and NADIR motor sequences	Integer	None
B7_SET_ON_OFF_CHIP_BINNING	0 = Binning is performed in the FPGA, 1 = Binning is perform on chip	Integer	None
B6_MOTOR_HOLD	0 = No motor hold, 1 = default = active motor hold to accurately keep the fixed measurement position.	Integer	None
B5_LED	0 = default = LED Off (always off for inflight), 1 = LED On for ground testing.	Integer	None
B4_LOCATE_DARK	0 = default = don't sweep the motor from Dark->SO->Dark->ND. 1 = do a full sweep to reset motor position.	Integer	None
B3_SCI_HK	0 = default = not to include the full HK in sci packets (but include the three Temperatures); 1= full HK in sci pckts	Integer	None
B2_INTEGRATION_TIME_I	Integration time increment, 0 = no	Integer	None

NCREMENT	increments, 1 = causes the sequencer to increase the integration time after each pair of acquisitions in a way that is useful for photon transfer curve measurement, resulting in times that increase by a factor of 1,1, 2,2, 3,3, 4,4, 5,5 etc		
B1_LOOP_DARK	Loop Dark is for alternating between Dark & Science measurements. 0 = no loop (but still do the first and last dark scans), 1 = loop Dark--> Obs	Integer	None
B0_LED_CONTROL	bit 0 (Lsb) = LED permanently ON (for cal);	Integer	None
HORIZONTAL_AND_COMBINED_BINNING_SIZE	Number of columns for Horizontal binning, or size of side for square "super pixels" for Combined binning.	Integer	None
CONTROL_BITS	Bit 0: 1 to inhibit Noise measurement. Bit 1: 0 for Reverse clocking in Noise measurement, 1 for Forward clocking. Bit 2: 0 for two rows of Noise measurement, 1 for one row. Bit 3: 1 to inhibit Leading Bias. Bit 4: 1 to inhibit Leading Dark. Bit 5: 1 to inhibit Science. Bit 6: 1 to inhibit Trailing Bias. Bit 7: 1 to inhibit Trailing Dark. Bit 8: 1 to inhibit Sweep While Flush (R-clocks dis/en-abled with 3us period). Bit 9: 1 for Synthetic Data Bit 11: 1 = HK inhibited (TM29 HK o/p supressed, used during full frames / SINBAD comms tests) , 0=HK TM29 output at defined rates (1 per sec in SO and 1 per 15 seconds in ND) Bits 15..12 I-clock timing adjustment	Integer	None
REVERSE_FLAG_AND_DATA_TYPE_FLAG_REGISTER	Transmit the Reverse flag to show which data packet contains reverse clocked data: b(0) - 0 = normal data, 1 = reverse clocked data. Next two bits define data type: 00 = Dark Scan, 01 = Bias Scan, 10 = Science Data	Integer	None
POSITIVE_10_V_RAIL_VO	+10 V measured on UVIS board	Integer (raw)/	None (raw)/

LTAGE (raw/pp)		float (pp)	volts (pp)
NEGATIVE_10_V_RAIL_VOLTAGE (raw/pp)	-10 V measured on UVIS board	Integer (raw)/ float (pp)	None (raw)/ volts (pp)
POSITIVE_5_V_RAIL_VOLTAGE (raw/pp)	+5 V measured on UVIS board	Integer (raw)/ float (pp)	None (raw)/ volts (pp)
NEGATIVE_5_V_RAIL_VOLTAGE (raw/pp)	-5 V measured on UVIS board	Integer (raw)/ float (pp)	None (raw)/ volts (pp)
POSITIVE_12_V_RAIL_CURRENT (raw/pp)	+12V rail current	Integer (raw)/ float (pp)	None (raw)/ milliamps (pp)
NEGATIVE_12_V_RAIL_CURRENT (raw/pp)	-12V rail current	Integer (raw)/ float (pp)	None (raw)/ milliamps (pp)
POSITIVE_5_V_RAIL_CURRENT (raw/pp)	+5V rail current	Integer (raw)/ float (pp)	None (raw)/ milliamps (pp)
NEGATIVE_5_V_RAIL_CURRENT (raw/pp)	-5V rail current	Integer (raw)/ float (pp)	None (raw)/ milliamps (pp)
CCD_IMAGE_CLOCK_HIGH (raw/pp)	CCD image clock HI	Integer (raw)/ float (pp)	None (raw)/ volts (pp)
CCD_IMAGE_CLOCK_LOW (raw/pp)	CCD image clock LO	Integer (raw)/ float (pp)	None (raw)/ volts (pp)
CCD_READOUT_REGISTER_HIGH (raw/pp)	CCD readout register HI	Integer (raw)/ float (pp)	None (raw)/ volts (pp)
CCD_READOUT_REGISTER_LOW (raw/pp)	CCD readout register LO	Integer (raw)/ float (pp)	None (raw)/ volts (pp)
SUBSTRATE_VOLTAGE_VSS (raw/pp)	Substrate Voltage (VSS)	Integer (raw)/ float (pp)	None (raw)/ volts (pp)
OUTPUT_GATE_VOLTAGE_VOG (raw/pp)	Output gate voltage (VOG)	Integer (raw)/ float (pp)	None (raw)/ volts (pp)
OUTPUT_DRAIN_VOLTAGE_VOD (raw/pp)	Output drain voltage (VOD)	Integer (raw)/ float (pp)	None (raw)/ volts (pp)
RESET_TRANSISTOR_DRAIN_VOLTAGE_VRD (raw/pp)	Reset transistor drain voltage (VRD)	Integer (raw)/ float (pp)	None (raw)/ volts (pp)
DIODE_DRAIN_VOLTAGE_VDD (raw/pp)	Diode drain voltage (VDD)	Integer (raw)/ float (pp)	None (raw)/ volts (pp)
TEMPERATURE_1 (raw/pp)	Temp 1 (Proximity Board)	Integer (raw)/ float (pp)	None (raw)/ Celsius (pp)
TEMPERATURE_2 (raw/pp)	Temp 2 (CCD)	Integer (raw)/ float (pp)	None (raw)/ Celsius (pp)

TEMPERATURE_3 (raw/pp)	Temp 3 (Detector Board)	Integer (raw)/ float (pp)	None (raw)/ celsius (pp)
MOTOR_CURRENT_A (raw /pp)	Motor current	Integer (raw)/ float (pp)	None (raw)/ milliamps (pp)
UVIS_SCIENCE_DATA	See section 5.2.7.3	Hexadecimal	ADU

Table 28: NOMAD UVIS TM(28) raw and partially processed (pp) PDS4 product fields

5.2.7 NOMAD UVIS 29 Science Product

Product Field Name	Description	Data Type	Data Units
PACKET_SIZE	size of packet	Integer	Bytes
TIMESTAMP_SECONDS	packet timestamp coarse	Integer	None
TIMESTAMP_MICROSECONDS	packet timestamp fine	Integer	None
TM_COUNT	packet number (of this type)	Integer	None
+10V_RAIL_VOLTAGE (raw/pp)	+10 V measured on UVIS board	Integer (raw)/ float (pp)	None (raw)/ volts (pp)
-10V_RAIL_VOLTAGE (raw/pp)	-10 V measured on UVIS board	Integer (raw)/ float (pp)	None (raw)/ volts (pp)
+5V_RAIL_VOLTAGE (raw/pp)	+5 V measured on UVIS board	Integer (raw)/ float (pp)	None (raw)/ volts (pp)
-5V_RAIL_VOLTAGE (raw/pp)	-5 V measured on UVIS board	Integer (raw)/ float (pp)	None (raw)/ volts (pp)
+12V_RAIL_CURRENT (raw/pp)	+12V rail current	Integer (raw)/ float (pp)	None (raw)/ milliamps (pp)
-12V_RAIL_CURRENT (raw/pp)	-12V rail current	Integer (raw)/ float (pp)	None (raw)/ milliamps (pp)
+5V_RAIL_CURRENT (raw/pp)	+5V rail current	Integer (raw)/ float (pp)	None (raw)/ milliamps (pp)
-5V_RAIL_CURRENT (raw/pp)	-5V rail current	Integer (raw)/ float (pp)	None (raw)/ milliamps (pp)
CCD_IMAGE_CLOCK_HIGH (raw/ pp)	CCD image clock HI	Integer (raw)/ float (pp)	None (raw)/ volts (pp)
CCD_IMAGE_CLOCK_LOW (raw/p p)	CCD image clock LO	Integer (raw)/ float (pp)	None (raw)/ volts (pp)
CCD_READOUT_REG_HIGH (raw/ pp)	CCD readout register HI	Integer (raw)/ float (pp)	None (raw)/ volts (pp)
CCD_READOUT_REG_LOW (raw/ pp)	CCD readout register LO	Integer (raw)/ float (pp)	None (raw)/ volts (pp)

SUBSTRATE_VOLTAGE_VSS (raw/pp)	Substrate Voltage (VSS)	Integer (raw)/ float (pp)	None (raw)/ volts (pp)
OUTPUT_GATE_VOLTAGE_VOG (raw/pp)	Output gate voltage (VOG)	Integer (raw)/ float (pp)	None (raw)/ volts (pp)
OUTPUT_DRAIN_VOLTAGE_VOD (raw/pp)	Output drain voltage (VOD)	Integer (raw)/ float (pp)	None (raw)/ volts (pp)
RESET_DRAIN_VOLTAGE_VRD (raw/pp)	Reset transistor drain voltage (VRD)	Integer (raw)/ float (pp)	None (raw)/ volts (pp)
DIODE_DRAIN_VOLTAGE_VDD (raw/pp)	Diode drain voltage (VDD)	Integer (raw)/ float (pp)	None (raw)/ volts (pp)
TEMP_1_PROXIMITY_BOARD (raw/pp)	Temp 1 (Proximity Board)	Integer (raw)/ float (pp)	None (raw)/ Celsius (pp)
TEMP_2_CCD (raw/pp)	Temp 2 (CCD)	Integer (raw)/ float (pp)	None (raw)/ Celsius (pp)
TEMP_3_DETECTOR_BOARD (raw/pp)	Temp 3 (Detector Board)	Integer (raw)/ float (pp)	None (raw)/ celsius (pp)
MOTOR_CURRENT_A (raw/pp)	Motor current	Integer (raw)/ float (pp)	None (raw)/ milliamps (pp)

Table 29: NOMAD UVIS TM(29) raw and partially processed (pp) PDS4 product fields

5.2.7.1 SO/LNO Last Telecommand Parameters

The SO or LNO channels' telecommand parameters are recorded for each subdomain measured during an observation, consisting of 25 bytes per subdomain.

Parameter name	**Byte number**	**Size (bits)**	**Description**
spare	0	5	spare
AOTF power cmd		1	AOTF power command flag
write cooler parameters		1	write coolers parameter flag
start accumulation		1	start accumulations flag
force AOTF enable	1	1	force AOTF enable flag
hsk enable		1	housekeeping enable flag
DEGF		1	detector gain flag
DVAF		1	detector video amplifier flag
force size AB		1	force size A/B flag

prog enable		1	programming enable flag
SBSF		1	spectral background subtraction flag
detector enable		1	detector enable flag
NRACC	2	8	number of accumulations
DWNL	3	8	height of detector window (i.e. number of lines in detector window)
DWYA	4	8	number of first line in detector window
BF	5	8	binning factor
DEIT	6	24	detector integration time
	7		
	8		
spare	9	5	spare
DS		1	detector supply flag
DDS		1	data source flag
DVS		1	data valid source flag
spare	10	8	spare
spare	11	1	spare
TGA		7	AOTF delay
AOPS	12	8	AOTF power setting
AOFS	13	32	AOTF frequency setting
	14		
	15		
	16		
spare	17	8	spare
spare	18	4	spare
PFCM		1	closed loop flag
CED1		1	cooler enable flag 1
CED2		1	cooler enable flag 2
CED3		1	cooler enable flag 3
spare	19+20	3	spare
PCP		13	cooler set point (target temperature)
spare	21	8	spare
C1	22	4	cooler closed loop coefficient 1
spare		4	spare
spare	23	2	spare

C2		4	cooler closed loop coefficient 2
spare		2	spare
spare	24	4	spare
C3		4	cooler closed loop coefficient 3

Table 30: SO or LNO last telecommand parameters in the raw and partial processed PDS4 products

5.2.7.2 SO/LNO Science Data

SO and LNO science data is transmitted as lines of spectra, with one measurement typically consisting of 24 lines by 320 pixels each. The data is stored as 14-bit numbers, consisting of a 2 bit exponent (one value per line of spectra) and 12 bits of data per individual pixel. For each subdomain, a timetag is also stored, to indicate the relative timing of the subdomain measurement w.r.t. the execution time recorded in the packet. As shown in Figure 10, subdomains are measured consecutively, not simultaneously, and so the timetag for the 6th subdomain (if present) will be greater than the timetag for the 1st subdomain. The exponent and timetag data is contained within 16 bytes which are always present irrespective of number of subdomains. This is followed by the 320 x 12bit (1.5 byte) detector pixel readouts x number of lines of spectra recorded (up to a maximum of 16+320*1.5*24 = 11536 bytes).

Byte	Bit	Field	Comments
0	7	0	
	6	0	
	5	Exponent 6	equals 11111 if no subdomain 6 is present
	4		
	3		
	2		
	1		
	0	Exponent 5	equals 11111 if no subdomain 5 is present
1	7		
	6		
	5		
	4		
	3	Exponent 4	equals 11111 if no subdomain 4 is present
	2		

	1		
	0		
2	7		
	6	Exponent 3	equals 11111 if no subdomain 3 is present
	5		
	4		
	3		
	2		
	1	Exponent 2	equals 11111 if no subdomain 2 is present
	0		
3	7		
	6		
	5		
	4	Exponent 1	equals 11111 if no subdomain 1 is present
	3		
	2		
	1		
	0		
4	15	Time Tag 6	Time Tag for subdomain 6 Equals FFFF when no subdomain 6 is present
	14		
	13		
	12		
	11		
	10		
	9		
	8		
5	7		
	6		
	5		
	4		
	3		
	2		
	1		
	0		
6-7	15	Time Tag 5	Time Tag for subdomain 5 Equals FFFF when no subdomain 5 is present
	…		
	0		
8-9	15	Time Tag 4	Time Tag for subdomain 4 Equals FFFF when no subdomain 4 is present
	…		

	0		
10-11	15	Time Tag 3	Time Tag for subdomain 3 Equals FFFF when no subdomain 3 is present
Etc.			
16	7	Pixel 0 value	Detector data
	6		
	5		
	4		
	3		
	2		
	1		
	0		
17	7		
	6		
	5		
	4		
	3	Pixel 1 value	Detector data
	2		
	1		
	0		
18	7		
	6		
	5		
	4		
	3		
	2		
	1		
	0		
Etc.			

Table 31: SO or LNO detector data in the raw and partial processed PDS4 products

5.2.7.3 UVIS Science Data

UVIS can perform in 16-bit or 20-bit mode, depending on the settings used. Typically, if the detector data is vertically binned then each spectral point is recorded as 20bits (however 16bit is possible); if running in unbinned mode then only 16bits can be recorded per pixel.

The packet data size depends on the number of lines of spectra (N) and the number of pixels per line, up to a maximum of 90 bytes + 15 lines * 1048 pixels * 2 bytes in unbinned mode where N=15. In 20bit mode, the maximum size per packet is 90 bytes + 3 lines * 1048 * 2.5 bytes (where N=3 here). N=1,2,3 for normal science; N>3 is used only for downloading full frames. The first UVIS science packet of each observation has a size of 4282 bytes where N=2 i.e. 90 + 2 lines * 1048 pixels * 2 bytes.

5.3 Partially Processed Data Products

Conversion to partially processed data products is performed by the SOC. As can be seen in the above tables, the partially processed data products contain the same fields as the raw data, except that housekeeping temperatures and voltages have been converted into physical units e.g. Celsius, Volts, Amps, etc.

Science data, including attributes LAST_TELECOMMAND_SUBDOMAIN_1 to 6 have been left unchanged. Detailed descriptions of each parameter are given above and conversion formulae can be found in the appendix; further details are included in the NOMAD Data Operations Handbook [RD10].

5.4 Calibrated Data Products

As shown in Figure 13, the pipeline is split between channel (SO/LNO and UVIS) and observation type (nadir and solar occultation). There are also calibration observations that do not pass through either pipeline, and are instead used only to derive the calibrated products.

5.4.1 Data Collections

The outputs of both are quite different, as the former will produce calibrated atmospheric transmittances (with values ranging from 0 to 1); while the latter will produce spectra with units of radiance factor i.e. a ratio between the signal reflected from Mars and the signal coming directly from the Sun. Both pipelines will also provide a spectral calibration axis, in nanometres for UVIS and wavenumbers for SO/LNO. In addition to this, calibrated data products will contain geolocation data, as derived from the SPICE kernels; however the types of location data will differ for occultation and nadir. Some auxiliary housekeeping products, such as temperatures and voltages, are not included, while some observation parameters are expanded and included as separate fields in the PDS4 products. A particular example of this is the LAST_TELECOMMAND_SUBDOMAIN attribute: in the raw and partially processed collections, this data is encoded in a hexadecimal format; whereas here it will be expanded to

provide human-readable values of interest to scientists. Also, a best estimate of the measurement error is added as an attribute, and the quality flags are included in the metadata. Some parameters will be promoted to metadata to allow PSA users to search for specific datasets based on supplied keywords.

Details of the contents of the PDS4 TAB and XML products are grouped into the following general groups:

- Telecommand information
- Instrument details
- Quality flags
- Measurement parameters
- Geometry parameters
- Science data
- Additional information

These are described in the following sections below, starting with the XML metadata fields

5.4.1.1 XML telecommand information

Product Field Name	Data Type	Data Units
so_start_time	Integer	Seconds
so_start_science1	Integer	Seconds
so_start_science2	Integer	Seconds
so_duration_reference1	Integer	Seconds
so_duration_reference2	Integer	Seconds
so_duration_time	Integer	Seconds
so_cop_general	Integer	No Units
so_cop_precooling	Integer	No Units
so_cop_science1	Integer	No Units
so_cop_science2	Integer	No Units
lno_start_time	Integer	Seconds
lno_start_science1	Integer	Seconds
lno_start_science2	Integer	Seconds
lno_duration_reference1	Integer	Seconds
lno_duration_reference2	Integer	Seconds
lno_duration_time	Integer	Seconds
lno_cop_general	Integer	No Units

lno_cop_precooling	Integer	No Units
lno_cop_science1	Integer	No Units
lno_cop_science2	Integer	No Units
uvis_start_time	Integer	Seconds
uvis_duration_time	Integer	Seconds
uvis_cop_row	Integer	No Units

Table 32: TC20 telecommand parameters

5.4.1.2 XML instrument details

Product Field Name	Description	Data Type	Data Units
cop_table_version	Version of the COP table in instrument	String	No Units
xcalib_ref	Reference to the calibration procedure used to calibrate the X axis	String	No Units
ycalib_ref	Reference to the calibration procedure used to calibrate the Y axis	String	No Units
yerror_ref	Reference to the procedure used to calculate the error on the Y axis	String	No Units
observation_mode	Description of observation mode, e.g. fullscan, calibration, nominal science, etc.	String	No Units
geometry	Geometry description	String	No Units
desc	Measurement description based on COP row executed	String	No Units
channel_name	Name of the channel and telescope used, and number of sciences (if applicable)	String	No Units
nspec	Number of spectra in the file. 1 subdomain = 1 spectrum	Integer	No Units
nsubdomain	Number of subdomains (SO/LNO only)	String	No Units
datecreated	Date the file was made	String	No Units
observation_type	Letter taken from ITL file descriptor e.g. C = calibration, I = ingress occultation, E = egress, N = nadir, etc.	String	No Units

Table 33: Instrument description metadata

5.4.1.3 XML quality flags

Product Field Name	Description	Data Type	Data Units
hsk_disturbed	Housekeeping values are disturbed (e.g. by electrical interference). Not yet implemented	Integer	No Units
hsk_out_of_bounds	Housekeeping values are out of bounds	Integer	No Units
discarded_packets	Packet(s) were discarded during this observation	Integer	No Units
bad_pixels_hinterpolated	Bad pixels have been removed by horizontal interpolation	Integer	No Units
bad_pixels_vinterpolated	Bad pixels have been removed by vertical interpolation	Integer	No Units
bad_pixels_masked	Bad pixels have been removed by masking	Integer	No Units
detector_saturated	Detector saturated during measurement (N/A for calibrations)	Integer	No Units
lno_straylight	LNO geometric straylight detected in 1 or more frames	Integer	No Units
high_instrument_temperature	Channel temperature exceeds normal operating temperature (LNO: 10C on baseplate)	Integer	No Units
pointing_error	Pointing is not correct or perturbation detected. Not yet implemented	Integer	No Units
uvis_occ_boresight	UVIS solar occultation boresight was used instead of default SO	Integer	No Units
lno_occ_boresight	LNO solar occultation boresight was used instead of default SO	Integer	No Units
mir_occ_boresight	ACS MIR solar occultation boresight was used instead of default SO	Integer	No Units
tirvim_occ_boresight	ACS TIRVIM solar occultation boresight was used instead of default SO	Integer	No Units

Table 34: List of quality flags present in the metadata.

5.4.1.4 XML SO/LNO measurement parameters

Measurement parameters vary by channel, hence there are two tables: one for SO/LNO and one for UVIS

Product Field Name	Description	Data Type	Data Units
aotf_frequency	AOTF frequency used for this spectrum	Float	Kilohertz
diffraction_order	Measured diffraction order	Integer	No Units
number_of_accumulations	Number of detector accumulations in measurement	Integer	No Units
spectral_resolution	Spectral resolution of each pixel in wavenumbers	Float	Wavenumbers
integration_time	Detector integration time	Float	Milliseconds

Table 35: Infrared metadata measurement parameters

5.4.1.5 XML UVIS measurement parameters

Product Field Name	Description	Data Type	Data Units
Mode	1 = SO; 2 = Nadir; 3=Calibration Selector; 5 = Cruise Checkout Test Card	Integer	No Units
AcquisitionMode	0 = Full CCD, 1 = Vertical Binning, 3 Stepper calibration, 5 - test card	Integer	No Units
BiasAverage	0=1 frame per acquisition; 1=2 frames per acquisition, etc.	Integer	No Units
DarkAverage	0=1 frame per acquisition; 1=2 frames per acquisition, etc.	Integer	No Units
ScienceAverage	0=1 frame per acquisition; 1=2 frames per acquisition, etc.	Integer	No Units
VStart	Detector starting row number	Integer	No Units
VEnd	Detector ending row number	Integer	No Units
HStart	Detector ending column number	Integer	No Units
HEnd	Detector starting column number	Integer	No Units
StartDelay	Number of 5 millisecond increments to pause between receipt of start command and actual acquisition.	Integer	No Units

AcquisitionDelay	Number of 5 millisecond increments to pause between receipt of start command and actual acquisition.	Integer	No Units
IntegrationTime	Detector integration time	Integer	Milliseconds
NumberOfAcquisitions	If B1LoopDark=0, then this parameter is the number of acquisitions to perform before doing a dark measurement	Integer	No Units
NumberOfFlushes	Bits 0 to 3: number of flushes to perform to remove charge accumulated on detector Bits 4 to 7: number of purges to perform to remove charge accumulated on detector	Integer	No Units
DarkToObservationSteps	Number of steps to drive motor from dark to observation position	Integer	No Units
ObservationToDarkSteps	Number of steps to drive motor from observaton to dark position	Integer	No Units
MotorDelay	Motor delay resolution: If Bit 7=0: Bits 0 to 6 give motor delay of 1 to 127ms in steps of 1ms; if Bit 7=1: Bits 0 to 6 give motor delay of 8 to 1016ms in steps of 8ms	Integer	No Units
MotorStartPosition	Define starting pole position for driving the motor to occultation and nadir positions	Integer	No Units
B0LEDControl	LED permanently ON (for cal)	Integer	No Units
B1LoopDark	Alternate between dark and science measurements. 0 = no loop (but still do the first and last dark scans), 1 = run dark frames	Integer	No Units
B2IntegrationTimeIncrement	Integration time increment: 0 = no increments, 1 = causes the sequencer to increase integration time after each pair of acquisitions (increasing by a factor of 1,1, 2,2, 3,3, 4,4, 5,5 etc.)	Integer	No Units
B3SciHSK	0 = default = not to include the full HSK in science packets (but include the 3 temperatures); 1= full HSK in science packets	Integer	No Units
B4LocateDark	0 = default = don't sweep the motor from dark-occultation-dark-nadir. 1 = do a full sweep to reset motor position	Integer	No Units
B5LED	0 = default = LED Off (always off for	Integer	No Units

	inflight); 1 = LED On for ground testing		
B6MotorHold	0 = No motor hold; 1 = default = active motor hold to accurately keep the fixed measurement position	Integer	No Units
B7SetOnOffChipBinning	0 = Binning is performed in the FPGA, 1 = Binning is perform on chip	Integer	No Units
HorizontalAnd CombinedBinningSize	Bits 0 to 3: values 0 to 15 indicate a horizontal binning factor of 1 to 16; Bit 7: 1 to enable combined binning (with square super-pixels)	Integer	No Units
ControlBits	Bit 0: 1=inhibit noise frame; Bit 1: 0=reverse clock noise measurement, 1=forward clock; Bit 2: 0=2 rows of noise frames, 1=1 row; Bit 3: 1=inhibit leading bias; Bit 4: 1=inhibit leading dark; Bit 5: 1=inhibit science; Bit 6: 1=inhibit trailing bias; Bit 7: 1=inhibit trailing dark; Bit 8: 1=inhibit sweep while flush; Bit 9: 1=synthetic data; Bit 11: 1=suppress TM29 packets, 0=output TM29 packets at 1 per sec in occultation and 1 per 15 seconds in nadir; Bits 12 to 15: I-clock timing adjustment	Integer	No Units

Table 36: UVIS metadata measurement parameters.

5.4.1.6 XML nadir geometry parameters

Metadata geometry parameters are provided to ease the user in finding relevant observation data. A single observation can cover a large swath of the surface, and so parameters can vary greatly between the start, centre and end, particularly for those observations that pass near the poles. Therefore minimum/maximum/first/last values are provided where appropriate. In the case of latitude and longitude, mean values are also included as these provide a practical way to determine the approximate location of each observation.

Product Field Name	**Description**	**Data Type**	**Data Units**
first_lon	First surface longitude of the observation	Float	Degrees
last_lon	Last surface longitude of the observation	Float	Degrees

min_lon	Minimum surface longitude of the observation	Float	Degrees
max_lon	Maximum surface longitude of the observation	Float	Degrees
first_lat	First surface latitude of the observation	Float	Degrees
last_lat	Last surface latitude of the observation	Float	Degrees
min_lat	Minimum surface latitude of the observation	Float	Degrees
max_lat	Maximum surface latitude of the observation	Float	Degrees
first_lst	First local solar time of surface point of the observation	Float	Hours
last_lst	Last local solar time of surface point of the observation	Float	Hours
first_incidence_angle	First solar incidence angle of the observation	Float	Degrees
last_incidence_angle	Last solar incidence angle of the observation	Float	Degrees
min_incidence_angle	Minimum solar incidence angle of the observation	Float	Degrees
max_incidence_angle	Maximum solar incidence angle of the observation	Float	Degrees
first_emission_angle	First emission angle of the observation	Float	Degrees
last_emission_angle	Last emission angle of the observation	Float	Degrees
min_emission_angle	Minimum emission angle of the observation	Float	Degrees
max_emission_angle	Maximum emission angle of the observation	Float	Degrees
first_phase_angle	First phase angle of the observation	Float	Degrees
last_phase_angle	Last phase angle of the observation	Float	Degrees
min_phase_angle	Minimum phase angle of the observation	Float	Degrees
max_phase_angle	Maximum phase angle of the observation	Float	Degrees
first_sub_obs_lon	First sub-satellite longitude of the observation	Float	Degrees
last_sub_obs_lon	Last sub-satellite longitude of the observation	Float	Degrees
min_sub_obs_lon	Minimum sub-satellite longitude of the observation	Float	Degrees
max_sub_obs_lon	Maximum sub-satellite longitude of the observation	Float	Degrees
first_sub_obs_lat	First sub-satellite latitude of the observation	Float	Degrees
last_sub_obs_lat	Last sub-satellite latitude of the observation	Float	Degrees
min_sub_obs_lat	Minimum sub-satellite latitude of the observation	Float	Degrees
max_sub_obs_lat	Maximum sub-satellite latitude of the observation	Float	Degrees
first_lsubs	First planetocentric longitude of the observation	Float	Degrees
last_lsubs	Last planetocentric longitude of the observation	Float	Degrees
first_sub_sol_lon	First sub-solar longitude of the observation	Float	Degrees
last_sub_sol_lon	Last sub-solar longitude of the observation	Float	Degrees
first_sub_sol_lat	First sub-solar latitude of the observation	Float	Degrees
last_sub_sol_lat	Last sub-solar latitude of the observation	Float	Degrees

Table 37: Nadir geometry metadata

5.4.1.7 XML solar occultation geometry parameters

Product Field Name	Description	Data Type	Data Units
first_lon	First tangent point longitude of the observation	Float	Degrees
last_lon	Last tangent point longitude of the observation	Float	Degrees
min_lon	Minimum tangent point longitude of the observation	Float	Degrees
max_lon	Maximum tangent point longitude of the observation	Float	Degrees
first_lat	First tangent point latitude of the observation	Float	Degrees
last_lat	Last tangent point latitude of the observation	Float	Degrees
min_lat	Minimum tangent point latitude of the observation	Float	Degrees
max_lat	Maximum tangent point latitude of the observation	Float	Degrees
first_lst	First local solar time of tangent point of the observation	Float	Hours
last_lst	Last local solar time of tangent point of the observation	Float	Hours
first_alt	First tangent point altitude above the Mars areoid of the observation	Float	Kilometres
last_alt	Last tangent point altitude above the Mars areoid of the observation	Float	Kilometres
first_slant_path_dist	First distance between satellite and tangent point	Float	Kilometres
last_slant_path_dist	Last distance between satellite and tangent point	Float	Kilometres
first_sub_obs_lon	First sub-satellite longitude of the observation	Float	Degrees
last_sub_obs_lon	Last sub-satellite longitude of the observation	Float	Degrees
min_sub_obs_lon	Minimum sub-satellite longitude of the observation	Float	Degrees
max_sub_obs_lon	Maximum sub-satellite longitude of the observation	Float	Degrees
first_sub_obs_lat	First sub-satellite latitude of the observation	Float	Degrees
last_sub_obs_lat	Last sub-satellite latitude of the observation	Float	Degrees
min_sub_obs_lat	Minimum sub-satellite latitude of the observation	Float	Degrees
max_sub_obs_lat	Maximum sub-satellite latitude of the observation	Float	Degrees
first_lsubs	First planetocentric longitude of the observation	Float	Degrees
last_lsubs	Last planetocentric longitude of the observation	Float	Degrees

first_sub_sol_lon	First sub-solar longitude of the observation	Float	Degrees
last_sub_sol_lon	Last sub-solar longitude of the observation	Float	Degrees
first_sub_sol_lat	First sub-solar latitude of the observation	Float	Degrees
last_sub_sol_lat	Last sub-solar latitude of the observation	Float	Degrees
min_pointing_deviation	Minimum pointing deviation from centre of solar disk	Float	Arcminutes
max_pointing_deviation	Maximum pointing deviation from centre of solar disk	Float	Arcminutes

Table 38: Occultation geometry metadata

5.4.1.8 XML additional information

Some calibrated data fields are populated using data taken from the raw and partially processed products generated by the SOC. Hence these parameters are defined by ESA rather than the NOMAD team.

Product Field Name	Description	Data Type	Data Units
target/name	Name of target (Mars or Sun)	String	No units
target/type	Type of target (planet or sun)	String	No units
mission_phase_name	Phase of mission	String	No units
mission_phase_identifier	Phase of mission (short form)	String	No units
start_orbit_number	Orbit in which observation starts	Integer	No units

Table 39: Addition metadata in the XML products

The TAB products contain the full dataset, with each row of the table corresponding to a single spectrum. When operating in normal science mode, UVIS nadir/occultation (observation modes D, N, U, V) and LNO nadir (D, N) output one spectrum per measurement. SO/LNO in occultation mode (I, E) have several detector bins, and can return multiple spectra per measurement (each with a different FOV).

5.4.1.9 TAB SO/LNO nadir measurement parameters

Product Field Name	Description	Data Type	Data Units
ObservationDatetimeStart	UTC start datetime of spectrum acquisition	String	No Units
ObservationDatetimeEnd	UTC end datetime of spectrum acquisition	String	No Units
AOTFFrequency	AOTF frequency used for this spectrum (can vary for fullscan measurements)	Float	Kilohertz
BinTop	Detector starting row number (all bins)	Integer	No Units
BinHeight	Detector row height (all bins)	Integer	No Units
BinStart	Starting row of given detector bin	Integer	No Units
BinEnd	End row of given detector bin	Integer	No Units
DiffractionOrder	Measured diffraction order (can vary for fullscan measurements)	Integer	No Units
Exponent	Exponent value for each spectrum. See 5.2.7.2.	Integer	No Units
InstrumentTemperature	Temperature of instrument	Float	Celsius

DetectorTemperature	Temperature of detector	Float	Kelvin

Table 40: Infrared calibrated nadir science parameters.

5.4.1.10 TAB UVIS nadir measurement parameters

Product Field Name	Description	Data Type	Data Units
ObservationDatetimeStart	UTC start datetime of spectrum acquisition	String	No Units
ObservationDatetimeEnd	UTC end datetime of spectrum acquisition	String	No Units
DetectorTemperature	Temperature of detector during observation	Float	Celsius

Table 41: UVIS calibrated nadir science parameters

5.4.1.11 TAB nadir geometry parameters

Product Field Name	Description	Data Type	Data Units
StartObsAlt	Starting altitude of observer above centre of Mars	Float	Kilometres
EndObsAlt	Ending altitude of observer above centre of Mars	Float	Kilometres
StartSubObsLon	Starting sub-satellite longitude	Float	Degrees
EndSubObsLon	Ending sub-satellite longitude	Float	Degrees
StartSubObsLat	Starting sub-satellite latitude	Float	Degrees
EndSubObsLat	Ending sub-satellite latitude	Float	Degrees
StartLSubS	Starting planetocentric longitude Ls	Float	Degrees
EndLSubS	Ending planetocentric longitude Ls	Float	Degrees
StartSubSolLon	Starting sub-solar longitude	Float	Degrees
EndSubSolLon	Ending sub-solar longitude	Float	Degrees
StartSubSolLat	Starting sub-solar latitude	Float	Degrees
EndSubSolLat	Ending sub-solar latitude	Float	Degrees
PointXN (where N=geometry point number)	Relative X position of point w.r.t. bin or slit, where -1 to 1 define edges	Float	No Units
PointYN (where N=geometry point number)	Relative Y position of point w.r.t. bin or slit, where -1 to 1 define edges	Float	No Units
LonStartN (where N=geometry point number)	Starting surface latitude for this point (-999 = invalid value)	Float	Degrees
LonEndN (where N=geometry point number)	Ending surface latitude for this point (-999 = invalid value)	Float	Degrees

LatStartN (where N=geometry point number)	Starting surface latitude for this point (-999 = invalid value)	Float	Degrees
LatEndN (where N=geometry point number)	Ending surface latitude for this point (-999 = invalid value)	Float	Degrees
LSTStartN (where N=geometry point number)	Starting local solar time of surface point (-999 = invalid value)	Float	Hours
LSTEndN (where N=geometry point number)	Ending local solar time of surface point (-999 = invalid value)	Float	Hours
IncidenceAngleStartN (where N=geometry point number)	Starting incidence angle for this point (-999 = invalid value)	Float	Degrees
IncidenceAngleEndN (where N=geometry point number)	Ending incidence angle for this point (-999 = invalid value)	Float	Degrees
EmissionAngleStartN (where N=geometry point number)	Starting emission angle for this point (-999 = invalid value)	Float	Degrees
EmissionAngleEndN (where N=geometry point number)	Ending emission angle for this point (-999 = invalid value)	Float	Degrees
PhaseAngleStartN (where N=geometry point number)	Starting phase angle for this point (-999 = invalid value)	Float	Degrees
PhaseAngleEndN (where N=geometry point number)	Ending phase angle for this point (-999 = invalid value)	Float	Degrees
SurfaceAltAreoidStartN (where N=geometry point number)	Starting height of the DSK surface above the areoid for this point (-999 = invalid value)	Float	Kilometres
SurfaceAltAreoidEndN (where N=geometry point number)	Ending height of the DSK surface above the areoid for this point (-999 = invalid value)	Float	Kilometres
SurfaceRadiusStartN (where N=geometry point number)	Starting DSK surface radius for this point (-999 = invalid value)	Float	Kilometres
SurfaceRadiusEndN (where N=geometry point number)	Ending DSK surface radius for this point (-999 = invalid value)	Float	Kilometres

Table 42: Calibrated nadir geometry parameters

5.4.1.12 TAB solar occultation geometry parameters

Product Field Name	Description	Data Type	Data Units
StartObsAlt	Starting altitude of observer above centre of Mars	Float	Kilometres

EndObsAlt	Ending altitude of observer above centre of Mars	Float	Kilometres
StartSubObsLon	Starting sub-satellite longitude	Float	Degrees
EndSubObsLon	Ending sub-satellite longitude	Float	Degrees
StartSubObsLat	Starting sub-satellite latitude	Float	Degrees
EndSubObsLat	Ending sub-satellite latitude	Float	Degrees
StartLSubS	Starting planetocentric longitude Ls	Float	Degrees
EndLSubS	Ending planetocentric longitude Ls	Float	Degrees
StartSubSolLon	Starting sub-solar longitude	Float	Degrees
EndSubSolLon	Ending sub-solar longitude	Float	Degrees
StartSubSolLat	Starting sub-solar latitude	Float	Degrees
EndSubSolLat	Ending sub-solar latitude	Float	Degrees
StartPointingDeviation	Starting pointing deviation from centre of solar disk	Float	Arcminutes
EndPointingDeviation	Ending pointing deviation from centre of solar disk	Float	Arcminutes
PointXN	Relative X position of point w.r.t. bin or slit, where -1 to 1 define edges	Float	No Units
PointYN	Relative Y position of point w.r.t. bin or slit, where -1 to 1 define edges	Float	No Units
LonStartN	Starting tangent point longitude for this point (-999 = invalid value)	Float	Degrees
LonEndN	Ending tangent point longitude for this point (-999 = invalid value)	Float	Degrees
LatStartN	Starting tangent point latitude for this point (-999 = invalid value)	Float	Degrees
LatEndN	Ending tangent point latitude for this point (-999 = invalid value)	Float	Degrees
LSTStartN	Starting local solar time of tangent (-999 = invalid value)	Float	Hours
LSTEndN	Ending local solar time of tangent (-999 = invalid value)	Float	Hours
TangentAltEllipsoidStartN	Starting tangent point altitude above the Mars ellipsoid for this point (-999 = invalid value)	Float	Kilometres
TangentAltEllipsoidEndN	Ending tangent point altitude above the Mars ellipsoid for this point (-999 = invalid value)	Float	Kilometres
TangentAltAreoidStart	Starting tangent point altitude above the Mars areoid for this point (-999 = invalid	Float	Kilometres

	value)		
TangentAltAreoidEnd	Ending tangent point altitude above the Mars areoid for this point (-999 = invalid value)	Float	Kilometres
TangentAltSurfaceStart	Starting tangent point altitude above the Mars DSK surface for this point (-999 = invalid value)	Float	Kilometres
TangentAltSurfaceEnd	Ending tangent point altitude above the Mars DSK surface for this point (-999 = invalid value)	Float	Kilometres
SlantPathDistanceStart	Starting distance between satellite and tangent point (-999 = invalid value)	Float	Kilometres
SlantPathDistanceEnd	Ending distance between satellite and tangent point (-999 = invalid value)	Float	Kilometres

Table 43: Calibrated solar occultation geometry parameters

5.4.1.13 TAB science data

There is one wavelength/wavenumber (X), radiance/transmittance (Y) and radiance/transmittance error (YError) value for every pixel.

Product Field Name	**Description**	**Data Type**	**Data Units**
PixelN (where N=pixel number)	Spectral values	Float	cm^{-1} (SO/LNO) nm (UVIS)
PixelN transmittance/radiance (where N=pixel number)	Calibrated transmittances (occultation) or radiances nadir. Values are set to -999 if error.	Float	No units (occultation) W/cm2/sr/cm-1 (nadir)
PixelN transmittance/radiance error (where N=pixel number)	Error on transmittances (occ) or radiances (nadir). Values are set to -999n if error.	Float	No units (occultation) W/cm2/sr/cm-1 (nadir)
PixelN Mask (where N=pixel number)	UVIS only: flag to specify if pixel is good (=0) or bad (=1).	Integer	No units

Table 44: Calibrated science data.

Some of the parameters above are described in more detail below, including the point geometry and how it relates to the fields of view of the channels.

5.4.2 *Example TAB products*

5.4.2.1 SO occultation TAB product

ObservationDatetimeStart	2018-04-21T20:31:48.577Z
ObservationDatetimeEnd	2018-04-21T20:31:48.693Z
AOTFFrequency	22384.00
BinTop	120
BinHeight	15
BinStart	124
BinEnd	127
DiffractionOrder	165
InstrumentTemperature	-7.82E+00
DetectorTemperature	8.50E+01
YValidFlag	1
StartObsAlt	
EndObsAlt	
StartSubObsLon	-34.77
EndSubObsLon	-34.76
StartSubObsLat	54.55
EndSubObsLat	54.56
StartLSubS	163.12
EndLSubS	163.12
StartSubSolLon	133.35
EndSubSolLon	133.35
StartSubSolLat	7.1
EndSubSolLat	7.1
StartPointingDeviation	0.032
EndPointingDeviation	0.031
PointX0	0
PointY0	0
LonStart0	0.73
LonEnd0	0.74
LatStart0	79.44
LatEnd0	79.44
LSTStart0	3.16

LSTEnd0	3.16
TangentAltEllipsoidStart0	-4.36
TangentAltEllipsoidEnd0	-4.19
TangentAltAreoidStart0	-1.23
TangentAltAreoidEnd0	-1.04
TangentAltSurfaceStart0	-2.93
TangentAltSurfaceEnd0	-2.79
SlantPathDistanceStart0	1234.56
SlantPathDistanceEnd0	1235.67
PointX1	1
PointY1	1
LonStart1	0.56
LonEnd1	0.57
LatStart1	79.42
LatEnd1	79.42
LSTStart1	3.15
LSTEnd1	3.15
TangentAltEllipsoidStart1	-4.36
TangentAltEllipsoidEnd1	-4.19
TangentAltAreoidStart1	-1.23
TangentAltAreoidEnd1	-1.04
TangentAltSurfaceStart1	-2.93
TangentAltSurfaceEnd1	-2.79
SlantPathDistanceStart1	1234.56
SlantPathDistanceEnd1	1235.67
PointX2	-1
PointY2	1
LonStart2	0.63
LonEnd2	0.64
LatStart2	79.41
LatEnd2	79.41
LSTStart2	3.15
LSTEnd2	3.15
TangentAltEllipsoidStart2	-4.36
TangentAltEllipsoidEnd2	-4.19
TangentAltAreoidStart2	-1.23

TangentAltAreoidEnd2	-1.04
TangentAltSurfaceStart2	-2.93
TangentAltSurfaceEnd2	-2.79
SlantPathDistanceStart2	1234.56
SlantPathDistanceEnd2	1235.67
PointX3	-1
PointY3	-1
LonStart3	0.9
LonEnd3	0.9
LatStart3	79.46
LatEnd3	79.46
LSTStart3	3.17
LSTEnd3	3.17
TangentAltEllipsoidStart3	-4.36
TangentAltEllipsoidEnd3	-4.19
TangentAltAreoidStart3	-1.23
TangentAltAreoidEnd3	-1.04
TangentAltSurfaceStart3	-2.93
TangentAltSurfaceEnd3	-2.79
SlantPathDistanceStart3	1234.56
SlantPathDistanceEnd3	1235.
PointX4	1
PointY4	-1
LonStart4	0.83
LonEnd4	0.84
LatStart4	79.47
LatEnd4	79.47
LSTStart4	3.17
LSTEnd4	3.17
TangentAltEllipsoidStart4	-4.36
TangentAltEllipsoidEnd4	-4.19
TangentAltAreoidStart4	-1.23
TangentAltAreoidEnd4	-1.04
TangentAltSurfaceStart4	-2.93
TangentAltSurfaceEnd4	-2.79
SlantPathDistanceStart4	1234.56

SlantPathDistanceEnd4	1235.
Pixel0	3708.063
Pixel1	3708.155
…	…
Pixel318	3737.525
Pixel319	3737.619
Pixel0 transmittance	9.99214E-01
Pixel1 transmittance	9.99697E-01
…	…
Pixel318 transmittance	9.88854E-01
Pixel319 transmittance	9.90563E-01
Pixel0 transmittance error	1.18302E-03
Pixel1 transmittance error	1.33528E-03
…	…
Pixel318 transmittance error	1.65930E-03
Pixel319 transmittance error	1.46070E-03

5.4.2.2 Example UVIS occultation TAB product

ObservationDatetimeStart	2018-04-22T00:28:44.313Z
ObservationDatetimeEnd	2018-04-22T00:28:44.343Z
DetectorTemperature	-8.302
YValidFlag	1
StartObsAlt	3804.72
EndObsAlt	3804.74
StartSubObsLon	-89.405
EndSubObsLon	-89.403
StartSubObsLat	57.953
EndSubObsLat	57.955
StartLSubS	163.209
EndLSubS	163.209
StartSubSolLon	75.697
EndSubSolLon	7.57E+01
StartSubSolLat	7.06E+00

EndSubSolLat	7.064
StartPointingDeviation	0.032
EndPointingDeviation	0.031
PointX0	0
PointY0	0
LonStart0	-54.194
LonEnd0	-54.193
LatStart0	78.785
LatEnd0	78.785
LSTStart0	3.341
LSTEnd0	3.341
TangentAltEllipsoidStart0	-4.36
TangentAltEllipsoidEnd0	-4.19
TangentAltAreoidStart0	-1.23
TangentAltAreoidEnd0	-1.04
TangentAltSurfaceStart0	-2.93
TangentAltSurfaceEnd0	-2.79
SlantPathDistanceStart0	1234.56
SlantPathDistanceEnd0	1235.
PointX1	0
PointY1	1
LonStart1	-54.755
LonEnd1	-54.754
LatStart1	78.899
LatEnd1	78.899
LSTStart1	3.303
LSTEnd1	3.303
TangentAltEllipsoidStart1	-4.36
TangentAltEllipsoidEnd1	-4.19
TangentAltAreoidStart1	-1.23
TangentAltAreoidEnd1	-1.04
TangentAltSurfaceStart1	-2.93
TangentAltSurfaceEnd1	-2.79
SlantPathDistanceStart1	1234.56
SlantPathDistanceEnd1	1235.
PointX2	0.707

PointY2	0.707
LonStart2	-53.582
LonEnd2	-53.58
LatStart2	79.034
LatEnd2	79.034
LSTStart2	3.382
LSTEnd2	3.382
TangentAltEllipsoidStart2	-4.36
TangentAltEllipsoidEnd2	-4.19
TangentAltAreoidStart2	-1.23
TangentAltAreoidEnd2	-1.04
TangentAltSurfaceStart2	-2.93
TangentAltSurfaceEnd2	-2.79
SlantPathDistanceStart2	1234.56
SlantPathDistanceEnd2	1235.
PointX3	1
PointY3	0
LonStart3	-52.756
LonEnd3	-52.755
LatStart3	79.019
LatEnd3	79.018
LSTStart3	3.437
LSTEnd3	3.437
TangentAltEllipsoidStart3	-4.36
TangentAltEllipsoidEnd3	-4.19
TangentAltAreoidStart3	-1.23
TangentAltAreoidEnd3	-1.04
TangentAltSurfaceStart3	-2.93
TangentAltSurfaceEnd3	-2.79
SlantPathDistanceStart3	1234.56
SlantPathDistanceEnd3	1235.
PointX4	0.707
PointY4	-0.707
LonStart4	-52.796
LonEnd4	-52.794
LatStart4	78.867

LatEnd4	78.866
LSTStart4	3.434
LSTEnd4	3.434
TangentAltEllipsoidStart4	-4.36
TangentAltEllipsoidEnd4	-4.19
TangentAltAreoidStart4	-1.23
TangentAltAreoidEnd4	-1.04
TangentAltSurfaceStart4	-2.93
TangentAltSurfaceEnd4	-2.79
SlantPathDistanceStart4	1234.56
SlantPathDistanceEnd4	1235.
PointX5	0
PointY5	-1
LonStart5	-53.652
LonEnd5	-53.651
LatStart5	78.669
LatEnd5	78.668
LSTStart5	3.377
LSTEnd5	3.377
TangentAltEllipsoidStart5	-4.36
TangentAltEllipsoidEnd5	-4.19
TangentAltAreoidStart5	-1.23
TangentAltAreoidEnd5	-1.04
TangentAltSurfaceStart5	-2.93
TangentAltSurfaceEnd5	-2.79
SlantPathDistanceStart5	1234.56
SlantPathDistanceEnd5	1235.
PointX6	-0.707
PointY6	-0.707
LonStart6	-54.794
LonEnd6	-54.792
LatStart6	78.536
LatEnd6	78.536
LSTStart6	3.301
LSTEnd6	3.301
TangentAltEllipsoidStart6	-4.36

TangentAltEllipsoidEnd6	-4.19
TangentAltAreoidStart6	-1.23
TangentAltAreoidEnd6	-1.04
TangentAltSurfaceStart6	-2.93
TangentAltSurfaceEnd6	-2.79
SlantPathDistanceStart6	1234.56
SlantPathDistanceEnd6	1235.
PointX7	-1
PointY7	0
LonStart7	-55.574
LonEnd7	-55.573
LatStart7	78.545
LatEnd7	78.544
LSTStart7	3.249
LSTEnd7	3.249
TangentAltEllipsoidStart7	-4.36
TangentAltEllipsoidEnd7	-4.19
TangentAltAreoidStart7	-1.23
TangentAltAreoidEnd7	-1.04
TangentAltSurfaceStart7	-2.93
TangentAltSurfaceEnd7	-2.79
SlantPathDistanceStart7	1234.56
SlantPathDistanceEnd7	1235.
PointX8	-0.707
PointY8	0.707
LonStart8	-55.567
LonEnd8	-55.565
LatStart8	78.694
LatEnd8	78.694
LSTStart8	3.249
LSTEnd8	3.249
TangentAltEllipsoidStart8	-4.36
TangentAltEllipsoidEnd8	-4.19
TangentAltAreoidStart8	-1.23
TangentAltAreoidEnd8	-1.04
TangentAltSurfaceStart8	-2.93

TangentAltSurfaceEnd8	-2.79
SlantPathDistanceStart8	1234.56
SlantPathDistanceEnd8	1235.
Pixel0	198.9783
Pixel1	199.4513
…	…
Pixel1022	653.6765
Pixel1023	654.0835
Pixel0 transmittance	1.1373E+00
Pixel1 transmittance	9.6926E-01
…	…
Pixel1022 transmittance	1.0334E+00
Pixel1023 transmittance	1.0723E+00
Pixel0 transmittance error	1.0487E-03
Pixel1 transmittance error	2.9914E-03
…	…
Pixel1022 transmittance error	3.3783E-03
Pixel1023 transmittance error	4.1872E-03
Pixel0 Mask	0
Pixel1 Mask	0
…	…
Pixel1022 Mask	0
Pixel1023 Mask	0

5.4.2.3 Example UVIS nadir TAB product

ObservationDatetimeStart	2018-04-21T20:40:13.591Z
ObservationDatetimeEnd	2018-04-21T20:40:33.591Z
DetectorTemperature	-9.473
YValidFlag	1
StartObsAlt	3804.32
EndObsAlt	3804.36
StartSubObsLon	6.818
EndSubObsLon	9.893
StartSubObsLat	72.373

EndSubObsLat	72.707
StartLSubS	163.125
EndLSubS	163.125
StartSubSolLon	131.301
EndSubSolLon	1.31E+02
StartSubSolLat	7.10E+00
EndSubSolLat	7.098
PointX0	0
PointY0	0
LonStart0	13.581
LonEnd0	16.813
LatStart0	73.635
LatEnd0	73.834
LSTStart0	4.152
LSTEnd0	4.373
IncidenceAngleStart0	64.894
IncidenceAngleEnd0	63.517
EmissionAngleStart0	0.498
EmissionAngleEnd0	0.342
PhaseAngleStart0	64.415
PhaseAngleEnd0	63.448
SurfaceAltAreoidStart0	-4.321
SurfaceAltAreoidEnd0	-4.245
SurfaceRadiusStart0	3377.92
SurfaceRadiusEnd0	3378.22
PointX1	0
PointY1	1
LonStart1	13.5
LonEnd1	16.74
LatStart1	73.678
LatEnd1	73.878
LSTStart1	4.147
LSTEnd1	4.368
IncidenceAngleStart1	64.894
IncidenceAngleEnd1	63.517
EmissionAngleStart1	0.498
EmissionAngleEnd1	0.342
PhaseAngleStart1	64.415
PhaseAngleEnd1	63.448

SurfaceAltAreoidStart1	-4.321
SurfaceAltAreoidEnd1	-4.245
SurfaceRadiusStart1	3377.92
SurfaceRadiusEnd1	3378.22
PointX2	0.707
PointY2	0.707
LonStart2	13.41
LonEnd2	16.643
LatStart2	73.648
LatEnd2	73.85
LSTStart2	4.141
LSTEnd2	4.362
IncidenceAngleStart2	64.894
IncidenceAngleEnd2	63.517
EmissionAngleStart2	0.498
EmissionAngleEnd2	0.342
PhaseAngleStart2	64.415
PhaseAngleEnd2	63.448
SurfaceAltAreoidStart2	-4.321
SurfaceAltAreoidEnd2	-4.245
SurfaceRadiusStart2	3377.92
SurfaceRadiusEnd2	3378.22
PointX3	1
PointY3	0
LonStart3	13.42
LonEnd3	16.647
LatStart3	73.611
LatEnd3	73.812
LSTStart3	4.141
LSTEnd3	4.362
IncidenceAngleStart3	64.894
IncidenceAngleEnd3	63.517
EmissionAngleStart3	0.498
EmissionAngleEnd3	0.342
PhaseAngleStart3	64.415
PhaseAngleEnd3	63.448
SurfaceAltAreoidStart3	-4.321
SurfaceAltAreoidEnd3	-4.245
SurfaceRadiusStart3	3377.92

SurfaceRadiusEnd3	3378.22
PointX4	0.707
PointY4	-0.707
LonStart4	13.525
LonEnd4	16.747
LatStart4	73.588
LatEnd4	73.788
LSTStart4	4.148
LSTEnd4	4.369
IncidenceAngleStart4	64.894
IncidenceAngleEnd4	63.517
EmissionAngleStart4	0.498
EmissionAngleEnd4	0.342
PhaseAngleStart4	64.415
PhaseAngleEnd4	63.448
SurfaceAltAreoidStart4	-4.321
SurfaceAltAreoidEnd4	-4.245
SurfaceRadiusStart4	3377.92
SurfaceRadiusEnd4	3378.22
PointX5	0
PointY5	-1
LonStart5	13.662
LonEnd5	16.887
LatStart5	73.592
LatEnd5	73.79
LSTStart5	4.158
LSTEnd5	4.378
IncidenceAngleStart5	64.894
IncidenceAngleEnd5	63.517
EmissionAngleStart5	0.498
EmissionAngleEnd5	0.342
PhaseAngleStart5	64.415
PhaseAngleEnd5	63.448
SurfaceAltAreoidStart5	-4.321
SurfaceAltAreoidEnd5	-4.245
SurfaceRadiusStart5	3377.92
SurfaceRadiusEnd5	3378.22
PointX6	-0.707
PointY6	-0.707

LonStart6	13.753
LonEnd6	16.984
LatStart6	73.622
LatEnd6	73.818
LSTStart6	4.164
LSTEnd6	4.384
IncidenceAngleStart6	64.894
IncidenceAngleEnd6	63.517
EmissionAngleStart6	0.498
EmissionAngleEnd6	0.342
PhaseAngleStart6	64.415
PhaseAngleEnd6	63.448
SurfaceAltAreoidStart6	-4.321
SurfaceAltAreoidEnd6	-4.245
SurfaceRadiusStart6	3377.92
SurfaceRadiusEnd6	3378.22
PointX7	-1
PointY7	0
LonStart7	13.743
LonEnd7	16.981
LatStart7	73.66
LatEnd7	73.856
LSTStart7	4.163
LSTEnd7	4.384
IncidenceAngleStart7	64.894
IncidenceAngleEnd7	63.517
EmissionAngleStart7	0.498
EmissionAngleEnd7	0.342
PhaseAngleStart7	64.415
PhaseAngleEnd7	63.448
SurfaceAltAreoidStart7	-4.321
SurfaceAltAreoidEnd7	-4.245
SurfaceRadiusStart7	3377.92
SurfaceRadiusEnd7	3378.22
PointX8	-0.707
PointY8	0.707
LonStart8	13.638
LonEnd8	16.88
LatStart8	73.683

LatEnd8	73.881
LSTStart8	4.156
LSTEnd8	4.377
IncidenceAngleStart8	64.894
IncidenceAngleEnd8	63.517
EmissionAngleStart8	0.498
EmissionAngleEnd8	0.342
PhaseAngleStart8	64.415
PhaseAngleEnd8	63.448
SurfaceAltAreoidStart8	-4.321
SurfaceAltAreoidEnd8	-4.245
SurfaceRadiusStart8	3377.92
SurfaceRadiusEnd8	3378.22
Pixel0	198.9783
Pixel1	199.4513
…	…
Pixel1022	653.6765
Pixel1023	654.0835
Pixel0 radiance	5.3344E-04
Pixel1 radiance	5.0467E-04
…	…
Pixel1022 radiance	5.6583E-04
Pixel1023 radiance	2.9324E-04
Pixel0 radiance error	5.8477E-06
Pixel1 radiance error	4.3502E-06
…	…
Pixel1022 radiance error	3.7036E-06
Pixel1023 radiance error	3.5719E-06
Pixel0 Mask	0
Pixel1 Mask	0
…	…
Pixel1022 Mask	0
Pixel1023 Mask	0

5.5 Calibration collection

5.5.1 SO and LNO

Calibration products are available containing coefficients and bad pixel maps for the infrared channels:

- nmd_cal_calib_coefficients contains various AOTF and spectral calibration coefficients. A description of each is given in the product
- nmd_cal_lno_bad_pixel contains a map of the bad pixels in the LNO channel as a function of detector row
- nmd_cal_so_bad_pixel contains a map of the bad pixels in the SO channel as a function of detector row

The optimum calibration coefficients will change over time, therefore new coefficients will be issued as the mission progresses either via reference to published works or through the creation of new PDS4 calibration products.

If the new parameter affects the data and reflects an improvement over a previous calibration, the PDS products will be regenerated and redelivered to the PSA. If the new parameter reflects a change in instrument behaviour, the change will be applied only to new products from that date forward.

5.5.2 UVIS

UVIS calibration is ongoing, but in future we expect to provide:

- Coefficients for pixel-wavelength calibration
- A matrix of 1048 x 1048 coefficients for visible straylight calibration
- 8 straylight spectra, 8 transmission filters spectra and the radiometric calibration of the lamp used for IR straylight calibration
- An instrumental function of 1024 points for the radiance conversion

5.6 Browse Collection

5.6.1 SO Nominal Science Solar Occultation

The browse collection contains thumbnail images showing how the signal level on a pixel is extrapolated to perform the calibration and how the signal varies as the field of view passes through the atmosphere. Features in the atmosphere that reduce the signal are visible in the images.

A browse product is created for the bins of every diffraction order. An example is given in Figure 3234.

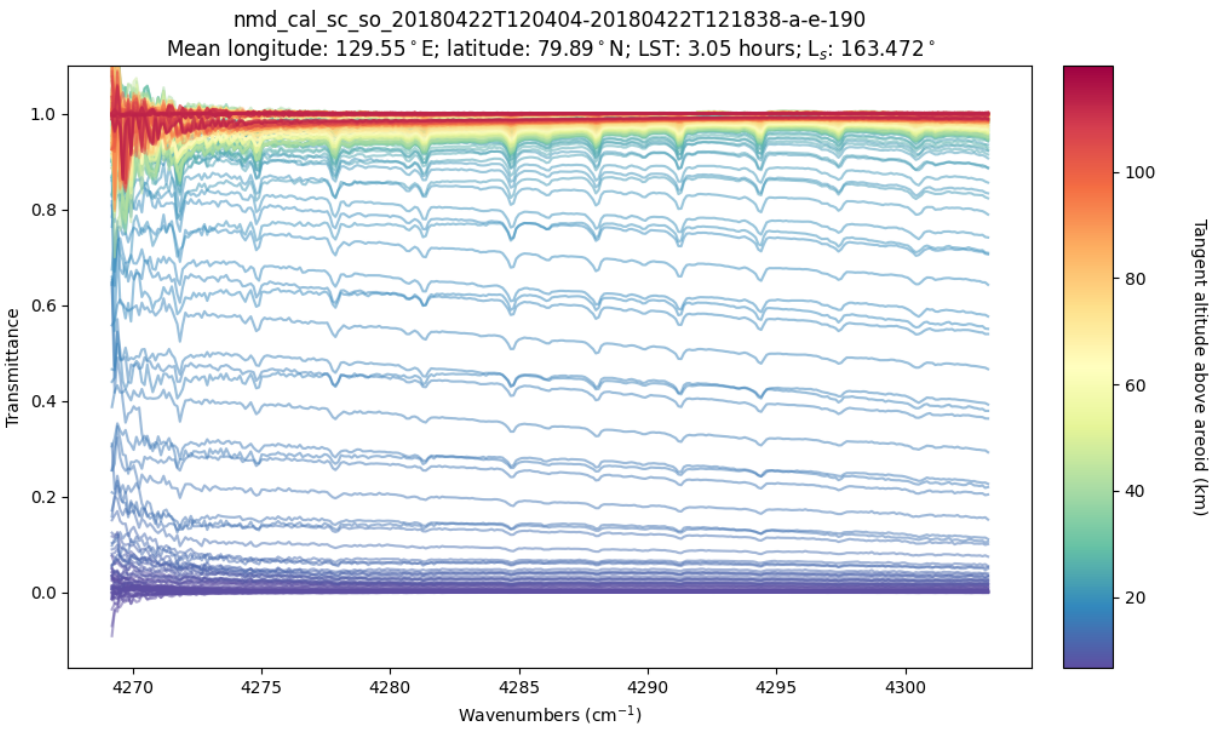

Figure 32: An example of an SO browse product, showing the signal versus altitude for the accepted bins of one diffraction order. The colour denotes the tangent altitude above the Areoid model. Mean geometric parameters are given the title.

5.6.2 UVIS Solar Occultation

A browse product is created showing how the transmittance spectra change with tangent altitude from the top of the atmosphere to the surface. An example is given in Figure 37.

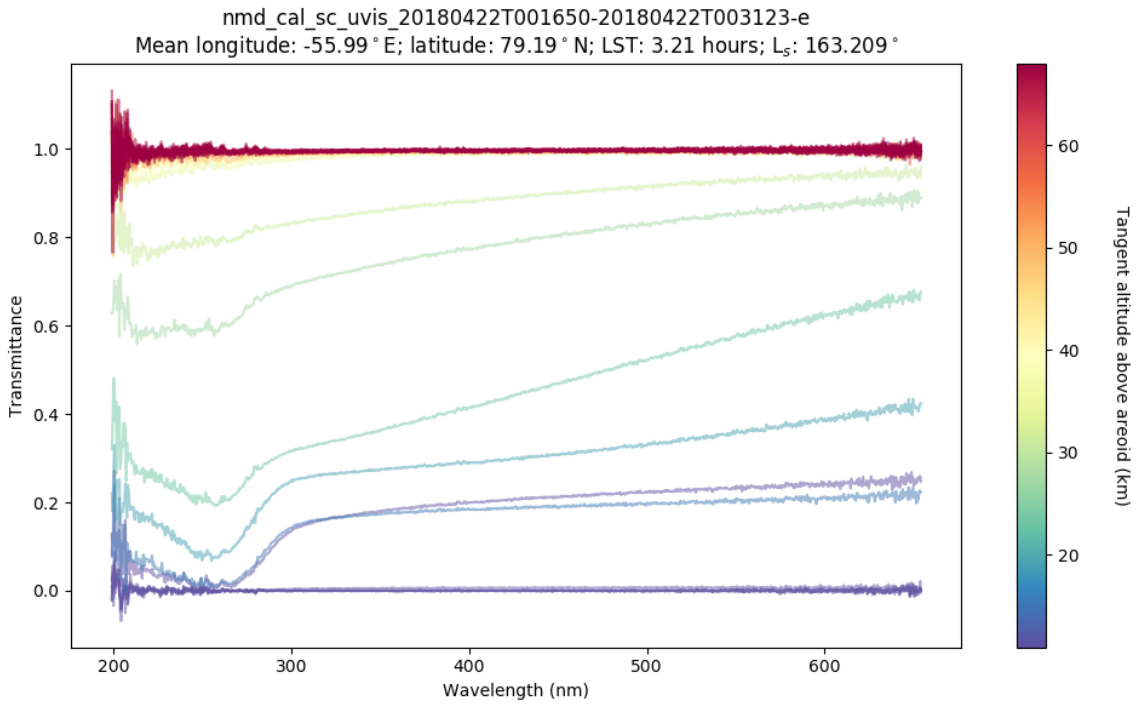

Figure 33: An example of a UVIS browse product, showing the signal versus altitude. The colour denotes the tangent altitude above the Areoid model. Mean geometric parameters are given the title.

5.6.3 SO Fullscan Solar Occultation

Unlike nominal solar occultations, the spectra for all measured diffraction orders are recorded in the same product for fullscan observations, so the browse product contains all spectra for a wide spectral region spanning multiple diffraction orders.

Two examples are shown here, one where all diffraction orders are measured (Figure 34) and one where a reduced set of orders are measured (Figure 35).

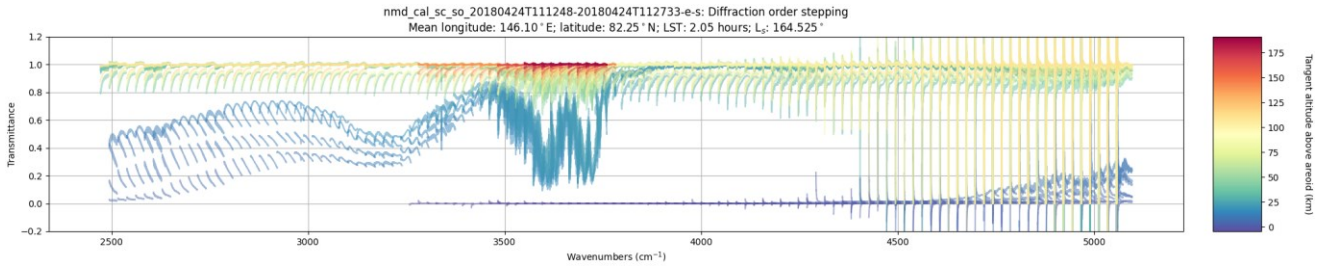

Figure 34: SO channel solar occultation fullscan (diffraction order stepping across full spectral range)

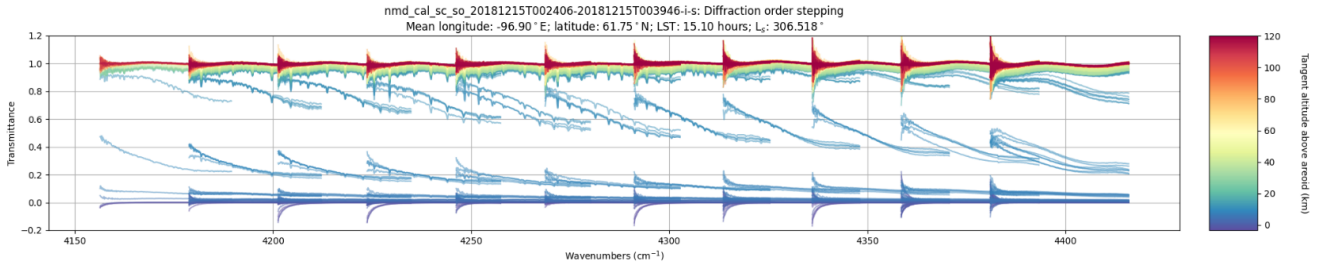

Figure 35: SO channel solar occultation fullscan (diffraction order stepping across limited spectral range)

5.6.4 LNO Fullscan Solar Occultation

Unlike nominal solar occultations, the spectra for all measured diffraction orders are recorded in the same product for fullscan observations, so the browse product contains all spectra for a wide spectral region spanning multiple diffraction orders.

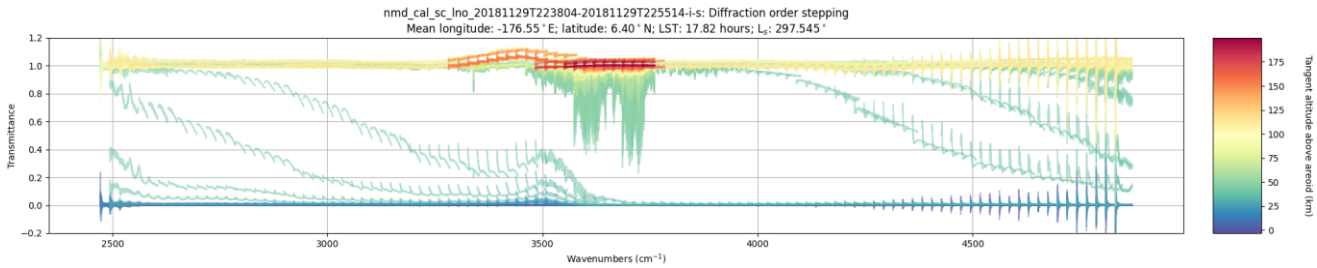

Figure 36: LNO channel solar occultation fullscan (diffraction order stepping)

5.6.5 LNO Nominal Science Dayside Nadir

A 2D image of wavenumber vs time, where the reflectance factor is denoted by the colour of each pixel, is generated for each diffraction order of a nadir observation. An example is given in Figure 3735. Note that the browse image is made from the first calibration method i.e. the dataset **Reflectance factor**.

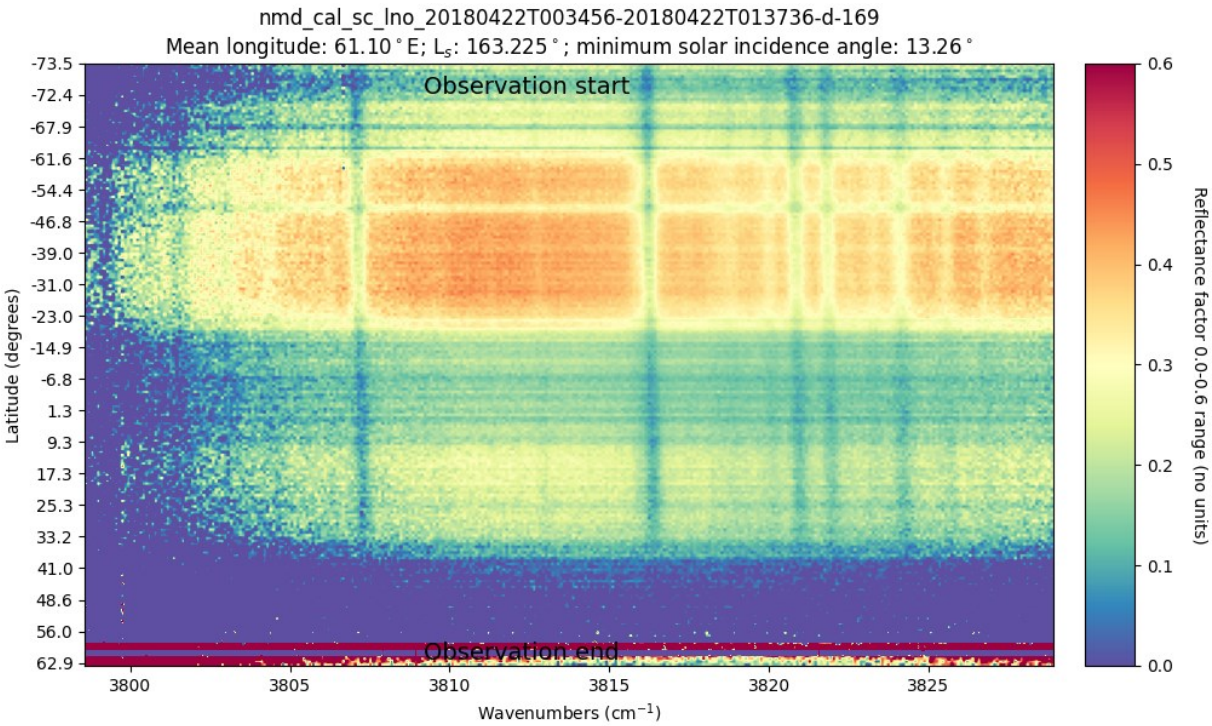

Figure 37: An example of an LNO nadir browse product, where the colour denotes the signal throughout the given observation for every pixel (when the LNO calibration is complete we expect this to be improved.). The faint vertical bands are atmospheric absorption lines present in the data. Mean geometric parameters are given the title. The x axis shows the observed latitude, from start of the observation (bottom line) to end (top line)

5.6.6 UVIS Dayside Nadir

A 2D image of wavelength (x axis) vs time (y axis), where the radiance is denoted by the colour of each image pixel, is generated for each nadir observation. An example is given in Figure 3836.

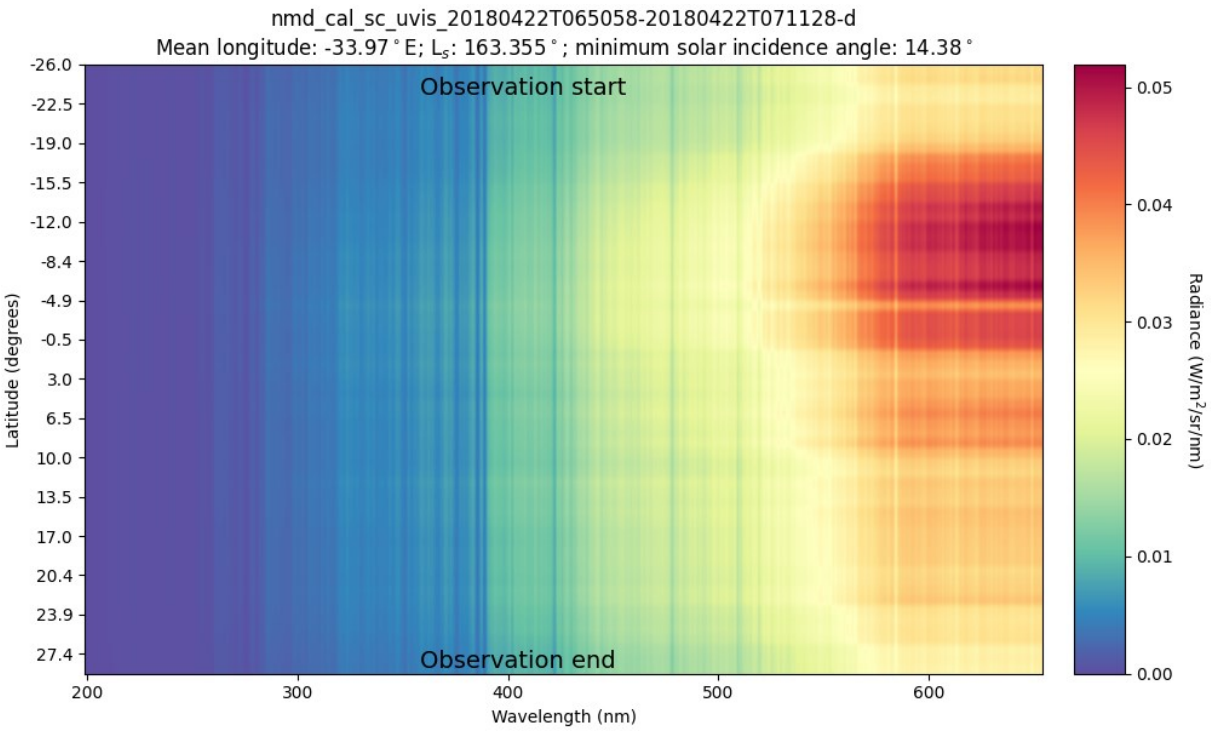

Figure 38 : Example of an UVIS nadir browse product, showing the radiance evolution during one observation. Mean geometric parameters are given the title. The x axis shows the observed latitude, from start of the observation (bottom line) to end (top line).

5.6.7 UVIS Nightside Nadir

A 2D image of wavelength (x axis) vs time (y axis), where the radiance is denoted by the colour of each image pixel, is generated for each nadir observation.

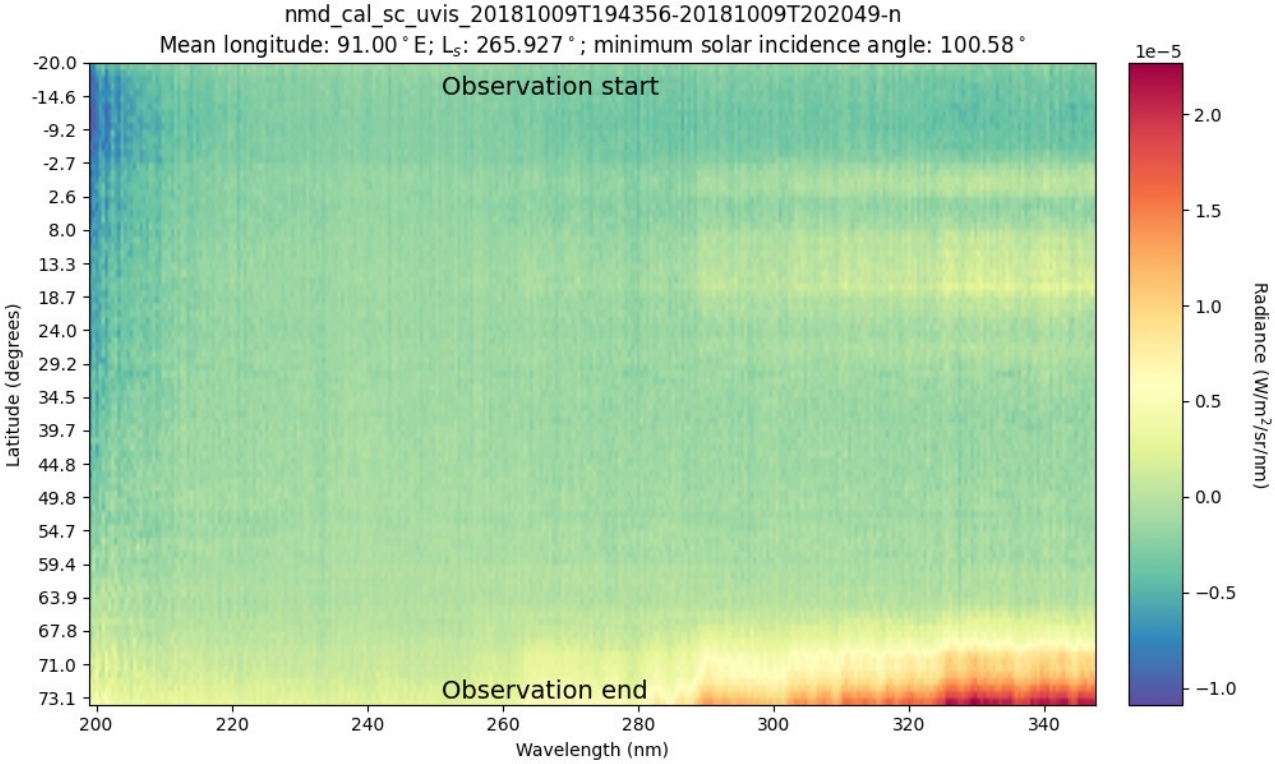

Figure 39: UVIS channel night nadir

5.6.8 UVIS Dayside Limb

This browse product consists of two subplots: a line chart showing the evolution of the tangent altitude (altitude of the centre of the FOV above the closest point on the surface); and a 2D image of wavelength (x axis) vs time (y axis), where the radiance is denoted by the colour of each image pixel. The tangent point is on the dayside of the planet during the observation.

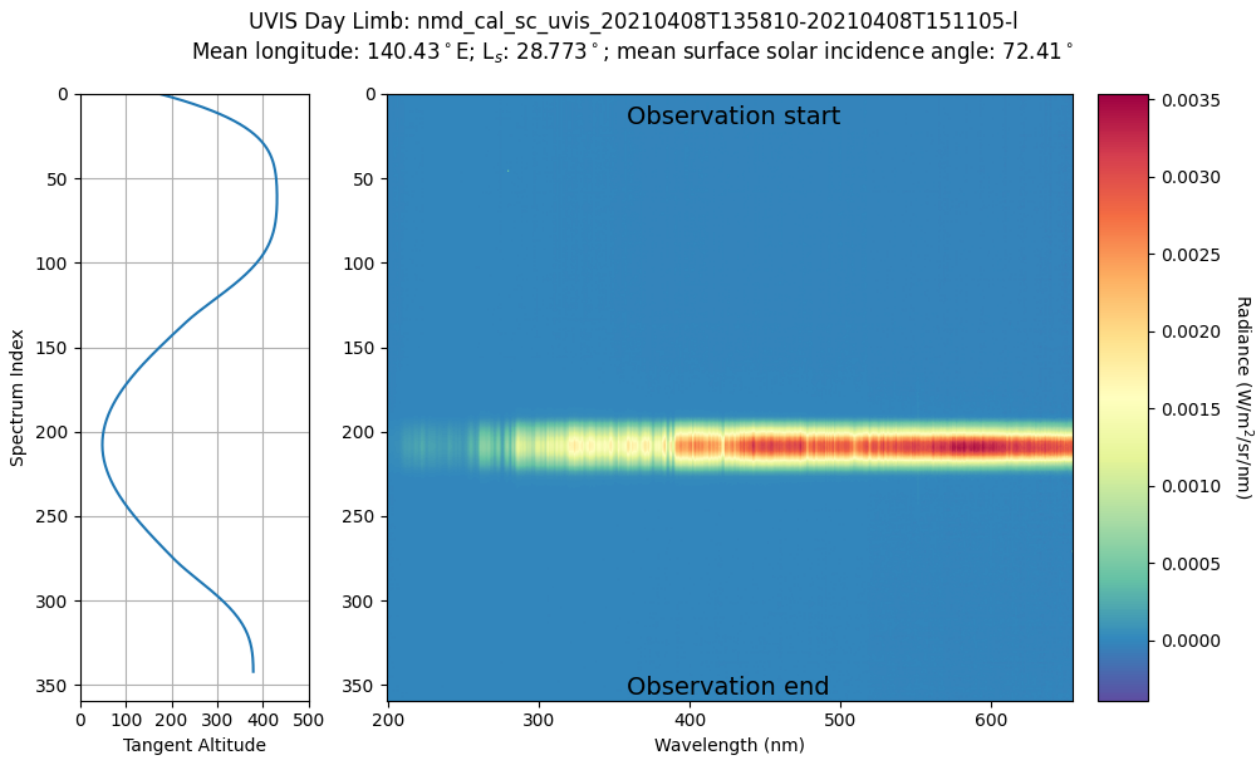

Figure 40: UVIS channel day limb

5.6.9 UVIS Nightside Limb

This browse product consists of two subplots: a line chart showing the evolution of the tangent altitude (altitude of the centre of the FOV above the closest point on the surface); and a 2D image of wavelength (x axis) vs time (y axis), where the radiance is denoted by the colour of each image pixel. The tangent point is on the nightside of the planet during the observation.

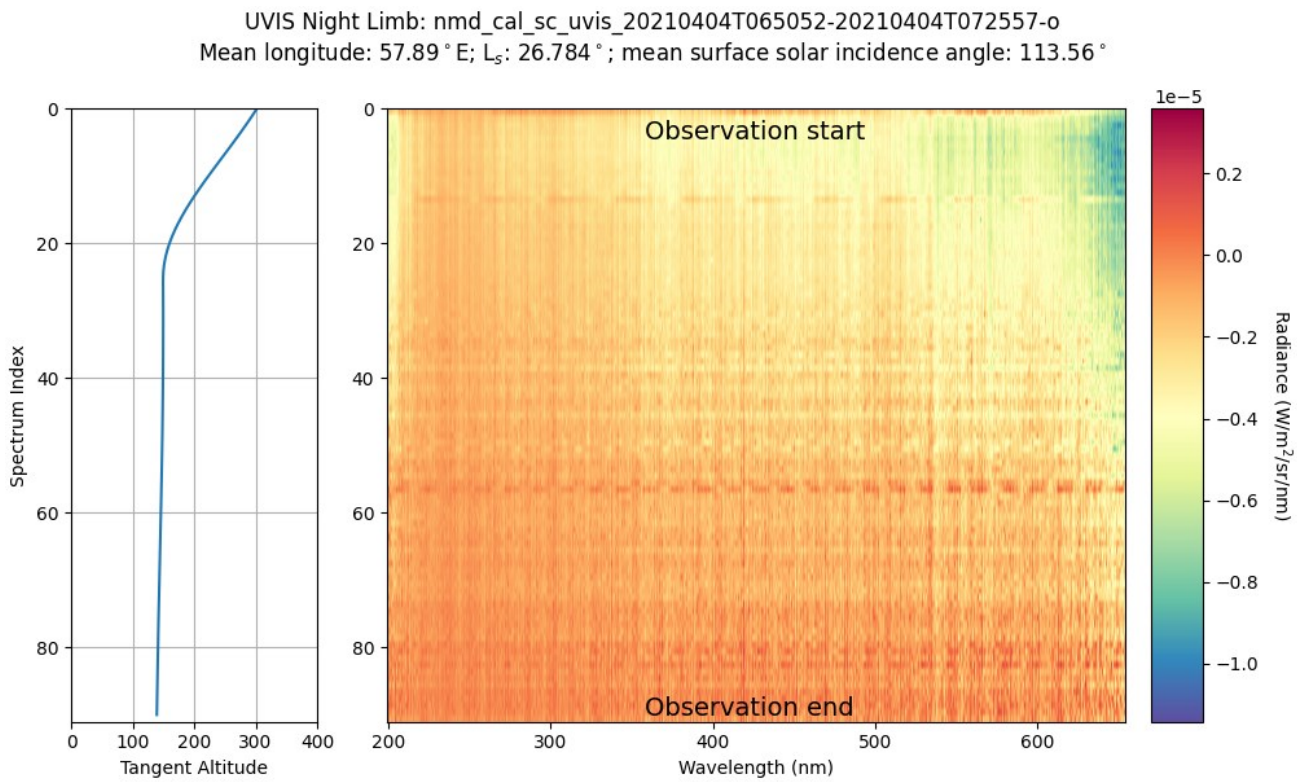

Figure 41: UVIS channel night limb

5.6.10 SO Line Scan (FOV) Calibration

A 2D image of wavenumber (x axis) vs time (y axis) is provided, where the colour denotes the raw counts for each pixel in the detector row at the centre of the detector. Here the FOV is scanned over the solar disk and the surrounding dark space, and so the signal recorded on the detector changes dramatically.

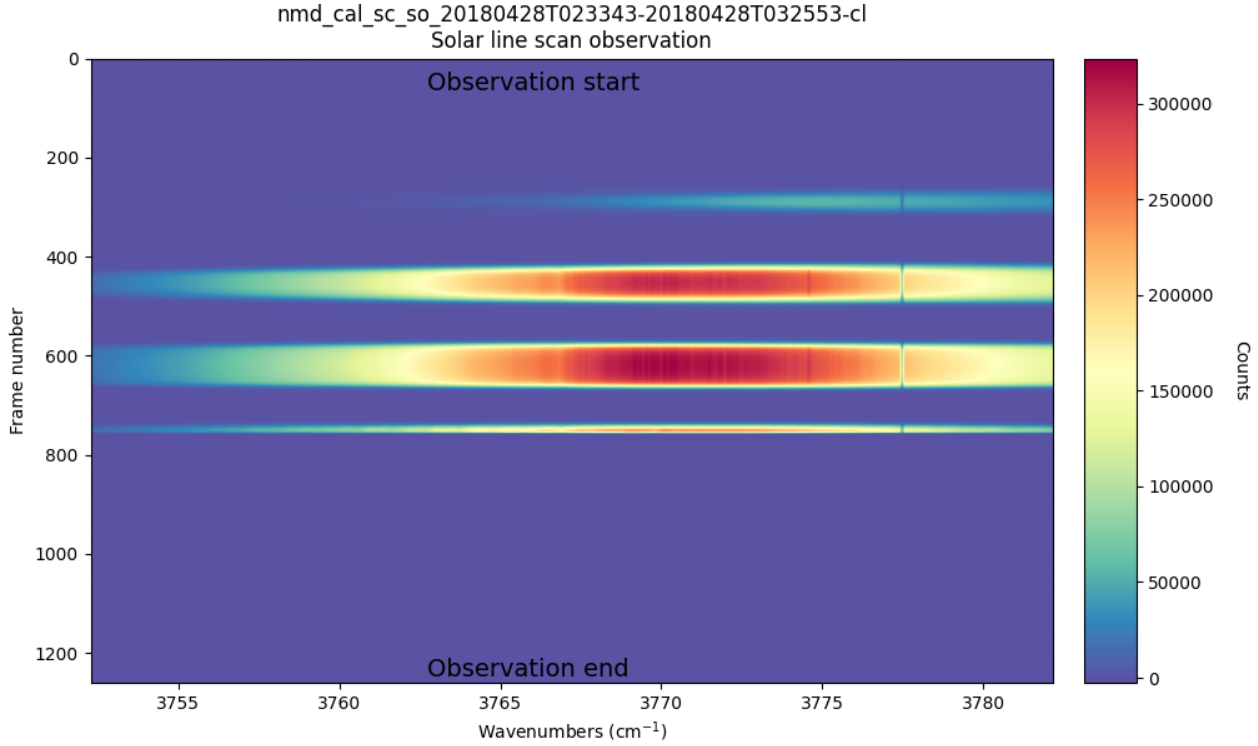

Figure 42: SO channel solar line scan calibration

5.6.11 LNO Line Scan (FOV) Calibration

A 2D image of wavenumber (x axis) vs time (y axis) is provided, where the colour denotes the raw counts for each pixel in the detector row at the centre of the detector. Here the FOV is scanned over the solar disk and the surrounding dark space, and so the signal recorded on the detector changes dramatically.

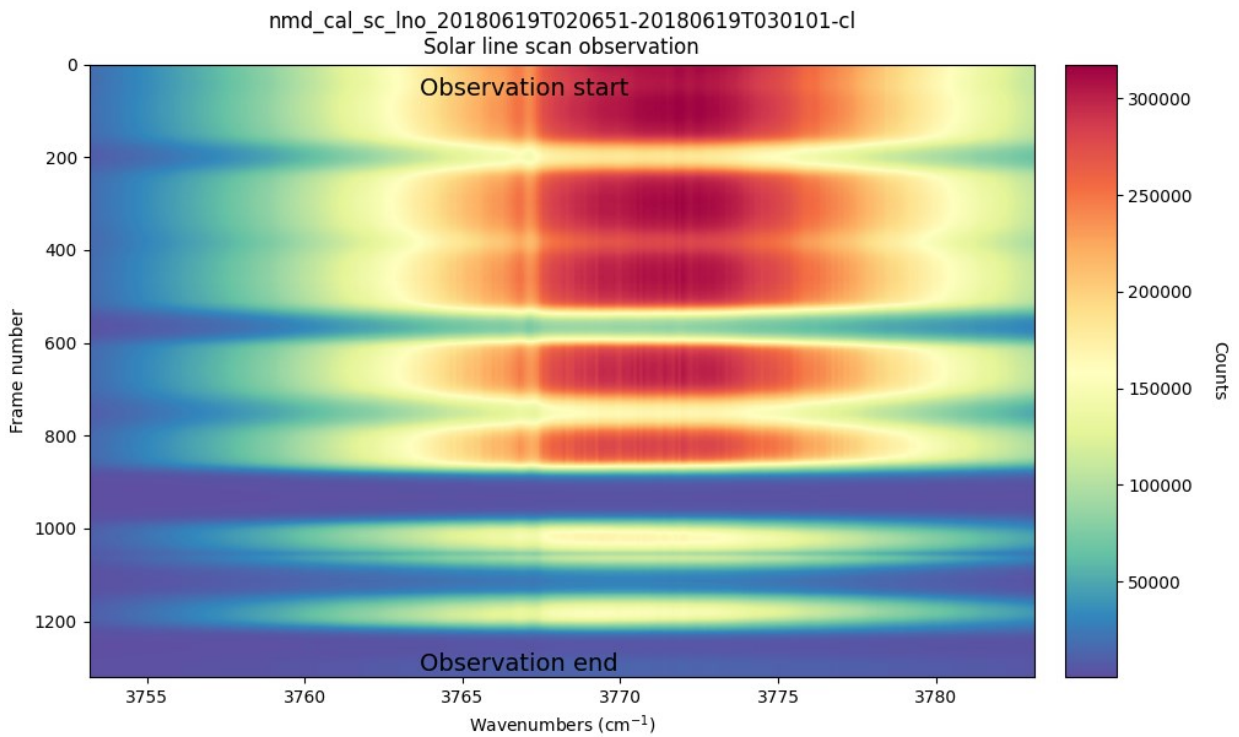

Figure 43: LNO channel solar line scan calibration

5.6.12 UVIS Line Scan (FOV) Calibration

A 2D image of wavenumber (x axis) vs time (y axis) is provided, where the colour denotes the raw counts for each detector column. Here the FOV is scanned over the solar disk and the surrounding dark space, and so the signal recorded on the detector changes dramatically.

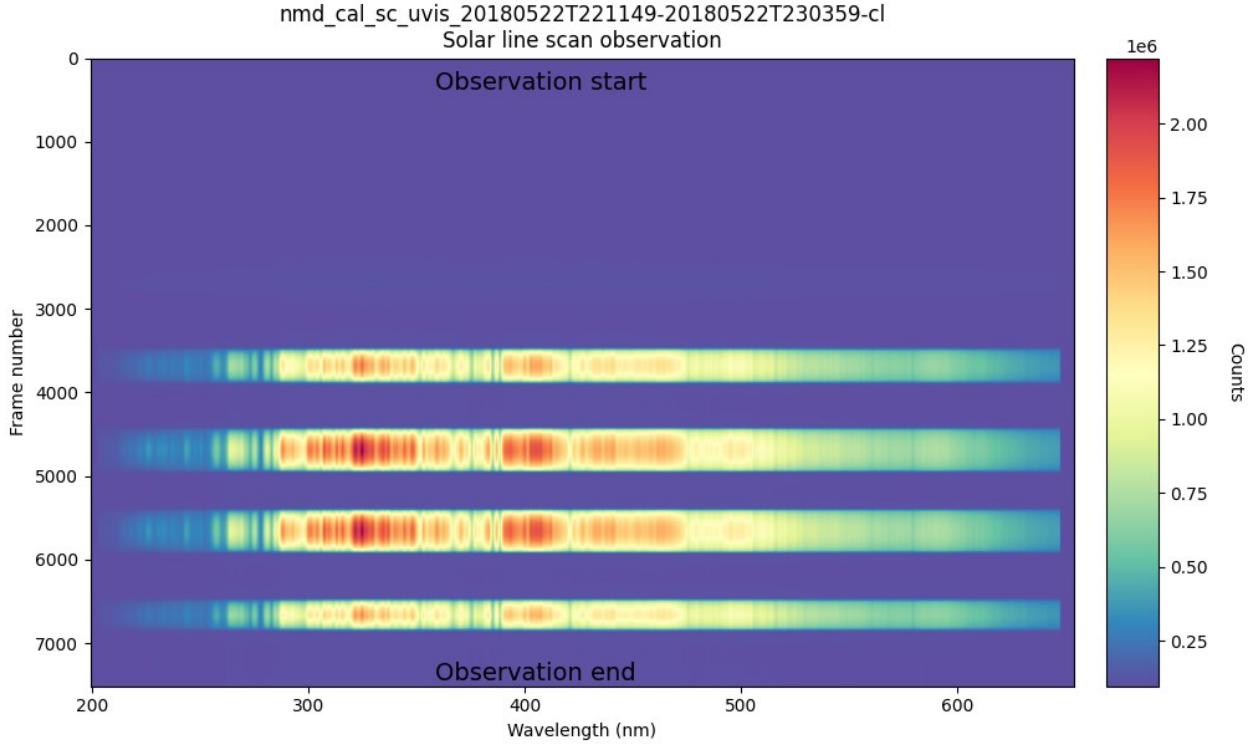

Figure 44: UVIS channel solar line scan calibration

5.6.13 SO Fullscan Solar Calibration

During a fullscan, spectra for all measured diffraction orders are recorded in the same product, so the browse product contains spectra of the central detector row for a wide spectral region spanning multiple diffraction orders. This is a calibration fullscan, so the FOV remains centred on the solar disk throughout the observation (without observing the Martian atmosphere).

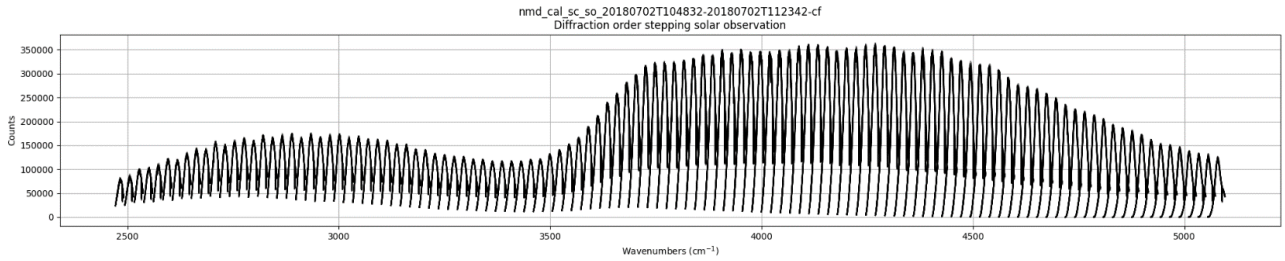

Figure 45: SO channel solar fullscan calibration (diffraction order stepping)

5.6.14 LNO Fullscan Solar Calibration

During a fullscan, spectra for all measured diffraction orders are recorded in the same product, so the browse product contains spectra of the central detector row for a wide spectral region spanning multiple diffraction orders. This is a calibration fullscan, so the FOV remains centred on the solar disk throughout the observation (without observing the Martian atmosphere).

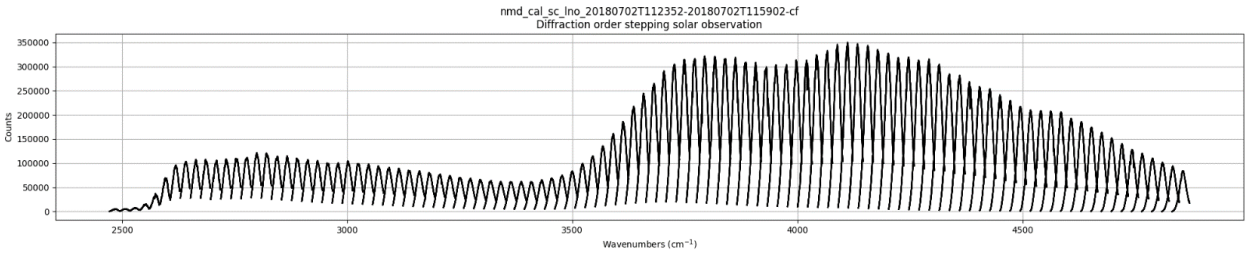

Figure 46: LNO channel solar fullscan calibration (diffraction order stepping)

5.6.15 SO Miniscan Solar Calibration

During a miniscan, the AOTF frequency is increased in steps (either 1, 2, 4 or 8 kHz per step), up to 256 steps. The measurement then repeats from the first AOTF frequency, covering many diffraction orders multiple times. This is a calibration fullscan, so the FOV remains centred on the solar disk throughout the observation (without observing the Martian atmosphere). The browse product contains a 2D array of pixel number (x axis) vs time (y axis), where the colour denotes the raw counts for the central row of the detector.

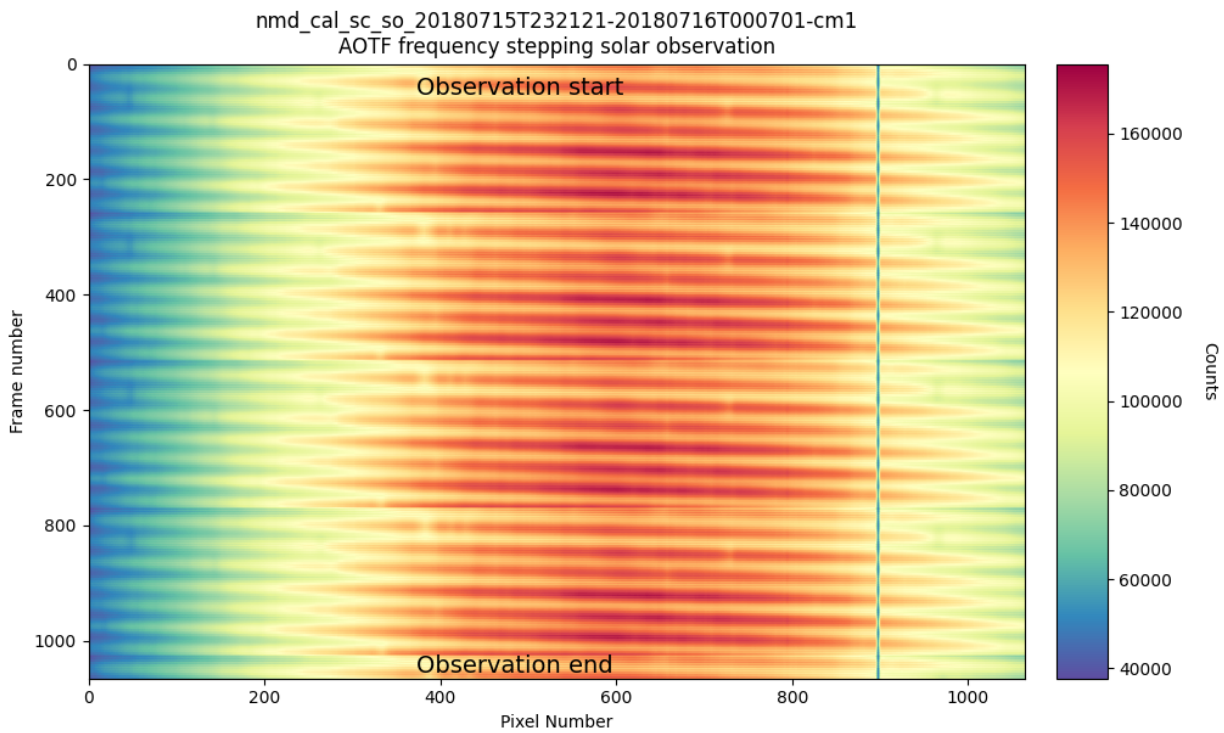

Figure 47: SO channel solar miniscan calibration (AOTF frequency stepping)

5.6.16 LNO Miniscan Solar Calibration

During a miniscan, the AOTF frequency is increased in steps (either 1, 2, 4 or 8 kHz per step), up to 256 steps. The measurement then repeats from the first AOTF frequency, covering many diffraction orders multiple times. This is a calibration fullscan, so the FOV remains centred on the solar disk throughout the observation (without observing the Martian atmosphere). The browse product contains a 2D array of pixel number (x axis) vs time (y axis), where the colour denotes the raw counts for the central row of the detector.

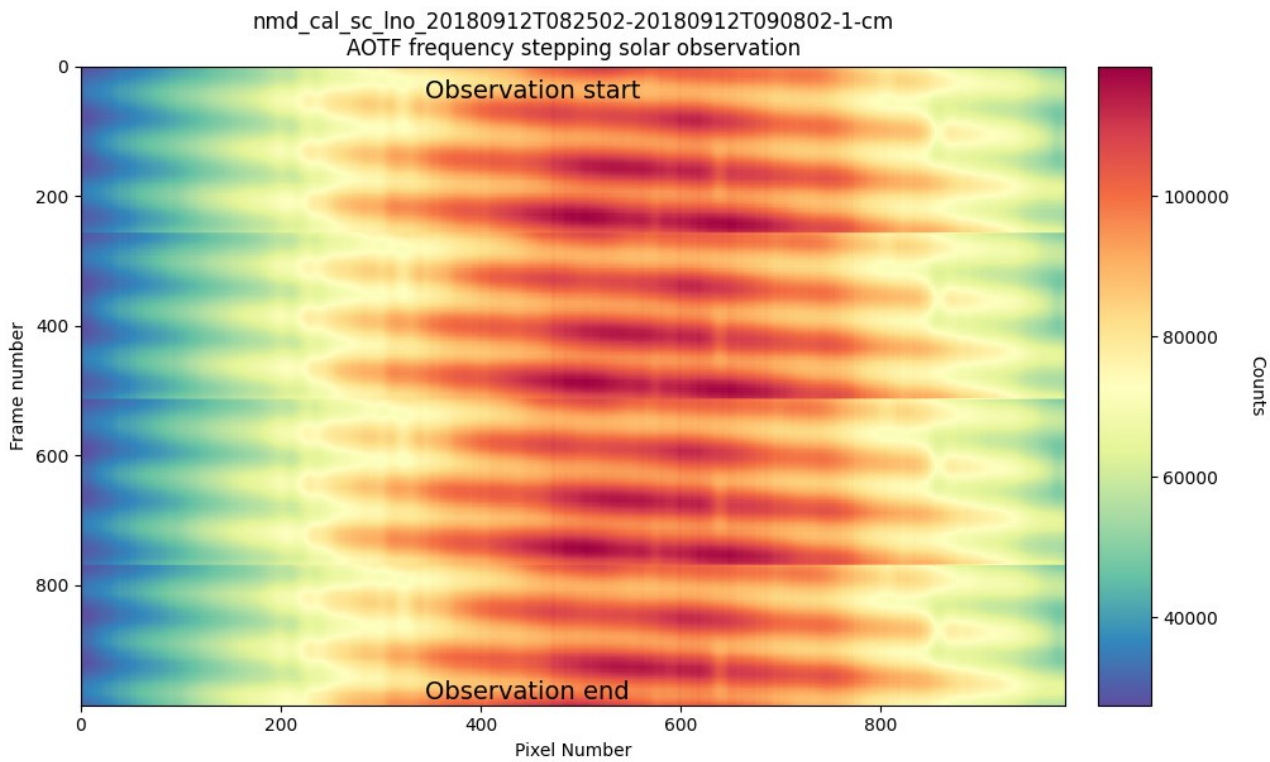

Figure 48: LNO channel solar miniscan calibration (AOTF frequency stepping)

5.6.17 UVIS Solar Stare Calibration

During a solar stare calibration, the FOV remains centred on the solar disk (without observing the Martian atmosphere) and multiple spectra are recorded. The browse product contains the raw detector column spectra for each observation type measured – solar, dark and bias.

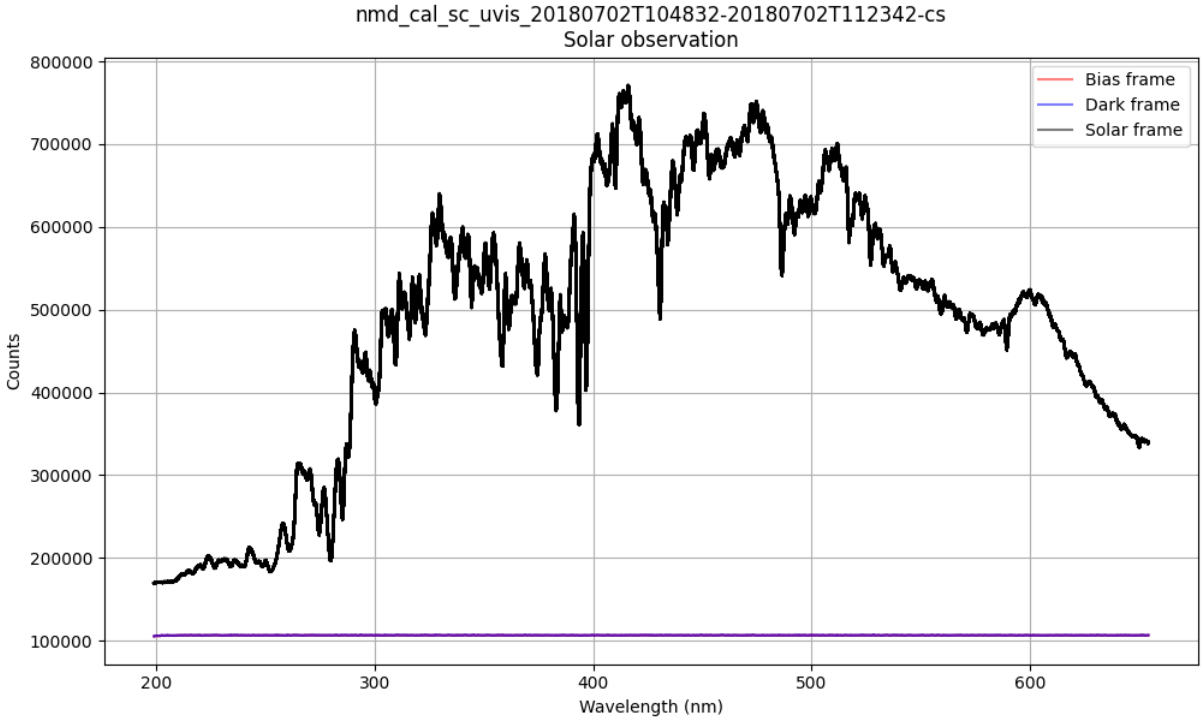

Figure 49: UVIS channel solar stare calibration

5.7 Derived Data Products

Derived data will contain gas species abundances, initially in the form of a vertical profile (for solar occultations) or as a nadir swath (for nadir). Later derived products will be in the form of gridded datasets, as a function of latitude, longitude and altitude above the Martian surface. These datasets will be provided in PDS4 format at regular intervals once the higher level analysis pipeline is complete and has been verified.

The exact structure of the products is to be determined still, however we expect that it will be similar to the calibrated data products.

5.8 Supplementary Products Formats

Auxilliary spacecraft data e.g. housekeeping, operational heater currents, etc., TGO SPICE kernels, and uploaded telecommand data will be required by NOMAD. These will be archived by the SOC independently of the NOMAD team.

6 APPENDIX

6.1 Temperature Sensors on NOMAD

A list of available temperature sensors in NOMAD is given in Table 4544. Those named ANC_* are monitored by the TGO spacecraft, and hence are read out continuously, even when NOMAD is switched off.

TGO data is archived separately to NOMAD products. More details to be provided by the SOC.

Instrument Part/Channel	Name	Description
NOMAD	ANC 1 NOMINAL	SO channel temperature, as monitored by the TGO spacecraft
NOMAD	ANC 1 REDUNDANT	SO channel temperature, as monitored by the TGO spacecraft
NOMAD	ANC 2 NOMINAL	LNO channel temperature, as monitored by the TGO spacecraft
NOMAD	ANC 2 REDUNDANT	LNO channel temperature, as monitored by the TGO spacecraft
~~NOMAD~~	~~ANC 3 NOMINAL~~	~~UVIS Channel (Spacecraft monitoring).~~ Due to a wiring issue on the spacecraft, this monitoring sensor is not available in flight.
NOMAD	ANC 3 REDUNDANT	UVIS channel temperature, as monitored by the TGO spacecraft
SINBAD	DC_DC_MODULE_TEMPERATURE	Temperature of DC/DC module
SINBAD	POWER_BOARD_TEMPERATURE	Temperature of POW board
SINBAD	LNO_DETECTOR_TEMPERATURE	Temperature of LNO cold section
SINBAD	LNO_TEMPERATURE	Temperature of LNO
SINBAD	UVIS_TEMPERATURE	Temperature of UVIS
SINBAD	SO_TEMPERATURE	Temperature of SO
SO	FPA_1_FULL_SCALE_TEMPERATURE _SO	SO focal plane array full scale temperature
SO	FPA_2_ZOOMED_TEMPERATURE_SO	SO focal plane array zoomed temperature
SO	SENSOR_1_TEMPERATURE_SO	Temperature sensor 1 near SO AOTF housing
SO	SENSOR_2_TEMPERATURE_SO	Temperature sensor 2 near SO grating structure
SO	SENSOR_3_TEMPERATURE_SO	Temperature sensor 3 near SO detector structure
SO	AOTF_TEMPERATURE_SO	Temperature inside SO AOTF box
LNO	FPA_1_FULL_SCALE_TEMPERATURE	LNO focal plane array full scale

	_LNO	temperature
LNO	FPA_2_ZOOMED_TEMPERATURE_LNO	LNO focal plane array zoomed temperature
LNO	SENSOR_1_TEMPERATURE_LNO	Temperature sensor 1 near LNO AOTF housing
LNO	SENSOR_2_TEMPERATURE_LNO	Temperature sensor 2 near LNO grating structure
LNO	SENSOR_3_TEMPERATURE_LNO	Temperature sensor 3 near LNO detector structure
LNO	AOTF_TEMPERATURE_LNO	Temperature inside LNO AOTF box
UVIS	TEMPERATURE_1	Temp 1 (Proximity Board)
UVIS	TEMPERATURE_2	Temp 2 (CCD)
UVIS	TEMPERATURE_3	Temp 3 (Detector Board)

Table 45: A list of temperature sensors embedded in NOMAD. NOMAD ANC temperature sensors will be monitored and read out continuously by spacecraft. SINBAD temperatures are recorded by the central processor when switched on. SO/LNO/UVIS temperatures are read out only while that channel is operating.

6.2 Conversion of Housekeeping Raw Data to Physical Units

The following tables contain calibration coefficients for conversion of raw housekeeping values to physical units.

code	parameter name	transfer function	size (bits)	description	Raw Value Range	Calculated Value Range	Calculated Units
NMHK1103	DC_DC_MODULE_TEMPERATURE	real_val (°C) = 0.1362*code - 273.2	16	temperature of DC/DC module	1638 to 2739	-50.10 to 99.85	deg C
NMHK1104	POWER_BOARD_TEMPERATURE	real_val (°C) = 0.1362*code - 273.2	16	temperature of POW board	1638 to 2739	-50.10 to 99.85	deg C
NMHK1105	LNO_DETECTOR_TEMPERATURE	real_val (°C) = -0.0721*code + 99.702	16	temperature of LNO cold section	0 to 3747	99.70 to -170.46	deg C
NMHK1106	LNO_TEMPERATURE	real_val (°C) = -4.7346538E-09*code*code*code + 3.1940866E-05*code*code - 0.093183624*code + 121.48852	16	temperature of LNO	362 to 4095	91.72 to -49.61	deg C
NMHK1107	UVIS_TEMPERATURE	real_val (°C) = -4.7346538E-09*code*code*code + 3.1940866E-05*code*code - 0.093183624*code + 121.48852	16	temperature of UVIS	362 to 4095	91.72 to -49.61	deg C
NMHK1108	SO_TEMPERATURE	real_val (°C) = -4.7346538E-09*code*code*code + 3.1940866E-05*code*code - 0.093183624*code +	16	temperature of SO	362 to 4095	91.72 to -49.61	deg C

		121.48852					
NMHK1109	ADC_1_REFERENCE_VOLTAGE_0_V	real_val (V) = code*(5/4095)	16	reference voltage 0 V for ADC1	0 to 10	0 to 0.013	V
NMHK1110	ADC_1_REFERENCE_VOLTAGE_3_3_V	real_val (V) = code*(5/4095)	16	reference voltage 3.38 V for ADC1	2702 to 2826	3.3 to 3.45	V
NMHK1111	SO_VOLTAGE	real_val (V) = 0.0105*code - 0.116	16	voltage for SO	11 to 3059	0 to 32	V
NMHK1112	LNO_VOLTAGE	real_val (V) = 0.0107*code - 0.1282	16	voltage for LNO	12 to 3003	0 to 32	V
NMHK1113	UVIS_VOLTAGE	real_val (V) = 0.0106*code - 0.117	16	voltage for UVIS	11 to 3030	0 to 32	V
NMHK1114	SO_CURRENT	real_val (A) = 0.0003*code - 0.0413	16	current of SO	139 to 3000	0 to 0.859	A
NMHK1115	LNO_CURRENT	real_val (A) = 0.0003*code - 0.0511	16	current of LNO	173 to 3013	0 to 0.85	A
NMHK1116	UVIS_CURRENT	real_val (A) = 4E-05*code - 0.0111	16	current of UVIS	310 to 4095	0 to 0.153	A
NMHK1117	HEATER_CURRENT	real_val (A) = 0.0001*code - 0.0147	16	current op operational heaters	106 to 4095	0 to 0.4	A
NMHK1118	ADC_2_REFERENCE_VOLTAGE_3_3_V	real_val (V) = code*(5/4095)	16	reference voltage 3.38 V for ADC2	2702 to 2826	3.3 to 3.45	V

Table 46: SINBAD housekeeping conversion formulae

code	**parameter name**	**transfer function (a)**	**size (bits)**	**description**	**Raw Value Range**	**Calculated Value Range**	**Calculated Units**
NMHK2310	POSITIVE_12_V_MEASURED_ON_SO_CCC	real_val (V) =code*(3/8192)*(47+12)/12	16	+12 V measured on CCC board of SO	-8192 to 8191	-14.75 to 14.75	V
NMHK2311	NEGATIVE_12_V_MEASURED_ON_SO_CCC	real_val (V) =code*(3/8192)*(47+12)/12	16	-12 V measured on CCC board of SO	-8192 to 8191	-14.75 to 14.75	V
NMHK2312	POSITIVE_8_5_V_MEASURED_ON_SO_HSK	real_val (V) = code*(3/8192)*(33.2+10)/10	16	+8.5 V measured on HSK board of SO	-8192 to 8191	-12.96 to 12.96	V
NMHK2313	NEGATIVE_8_5_V_MEASURED_ON_SO_HSK	real_val (V) = code*(3/8192)*(33.2+10)/10	16	-8.5 V measured on HSK board of SO	-8192 to 8191	-12.96 to 12.96	V
NMHK2314	POSITIVE_3_3_V_MEASURED_ON_SO_CCC	real_val (V) = code*(3/8192)*(2.5+10)/10	16	+3.3 V measured on CCC board of SO	-8192 to 8191	-3.75 to 3.75	V
NMHK2315	POITIVE_2_5_V_MEASURED_ON_SO_CCC	real_val (V) = code*(3/8192)	16	+2.5 V measured on CCC board of SO	-8192 to 8191	-3 to 3	V
NMHK2316	POSITIVE_5_V_ME	real_val (V) =	16	+5 V measured on	-8192 to 8191	-6 to 6	V

	ASURED_ON_SO_HSK	code*(3/8192)*(10+10)/10		HSK board of SO			
NMHK2317	NEGATIVE_5_V_MEASURED_ON_SO_HSK	real_val (V) = code*(3/8192)*(10+10)/10	16	-5 V measured on HSK board of SO	-8192 to 8191	-6 to 6	V
NMHK2318	FPA_1_FULL_SCALE_TEMPERATURE_SO	x=code*(3/8192)*(10/29.1) real_val (°K) =-460,66*x*x*x*x + 1053,2*x*x*x - 813,45*x*x - 227,36*x + 539,7	16	SO focal plane array full scale temperture	0 to 8191	74.46 to 539.7	deg K
NMHK2319	FPA_2_ZOOMED_TEMPERATURE_SO	real_val (V) = code*(3/8192)	16	SO focal plane array zoomed temperature	-8192 to 8191	-3 to 3	V
NMHK2320	SENSOR_1_TEMPERATURE_SO	real_val (°C) = (code*(3*1000/8192)+3/11)/51	16	temperature sensor 1 near SO AOTF housing	-8192 to 8191	-58.83 to 58.82	deg C
NMHK2321	SENSOR_2_TEMPERATURE_SO	real_val (°C) = (code*(3*1000/8192)+3/11)/51	16	temperature sensor 2 near SO grating structure	-8192 to 8191	-58.83 to 58.82	deg C
NMHK2322	SENSOR_3_TEMPERATURE_SO	real_val (°C) = (code*(3*1000/8192)+3/11)/51	16	temperature sensor 3 near SO detector structure	-8192 to 8191	-58.83 to 58.82	deg C
NMHK2323	AOTF_TEMPERATURE_SO	real_val (°C) = (code*(3*1000/8192)+3/11)/51	16	temperature inside SO AOTF box	-8192 to 8191	-58.83 to 58.82	deg C
NMHK2324	RF_AMPLITUDE_SO	real_val (V) = code*(3/8192)	16	RF amplitude of SO AOTF driver	-8192 to 8191	-3 to 3	V
NMHK2325	GROUND_MEASURED_ON_SO_HSK	real_val (V) = code*(3/8192)	16	ground potential measured on SO HSK board	-8192 to 8191	-3 to 3	V
NMHK2326	MOTOR_POWER_DAC_CODE_SO	real_val = code	16	SO cooler motor power DAC control	-8192 to 8191	0 to 8191	ADU

Table 47: SO housekeeping conversion formulae

code	parameter name	transfer function (a)	size (bits)	description	Raw Value Range	Calculated Value Range	Calculated Units
NMHK2610	POSITIVE_12_V_MEASURED_ON_LNO_CCC	real_val (V) =code*(3/8192)*(47+12)/12	16	+12 V measured on CCC board of LNO	-8192 to 8191	-14.75 to 14.75	V
NMHK2611	NEGATIVE_12_V_MEASURED_ON_LNO_CCC	real_val (V) =code*(3/8192)*(47+12)/12	16	-12 V measured on CCC board of LNO	-8192 to 8191	-14.75 to 14.75	V
NMHK2612	POSITIVE_8_5_V_MEASURED_ON_LNO_HSK	real_val (V) = code*(3/8192)*(33.2+10)/10	16	+8.5 V measured on HSK board of LNO	-8192 to 8191	-12.96 to 12.96	V
NMHK2613	NEGATIVE_8_5_V_MEASURED_ON_	real_val (V) = code*(3/8192)*(33.2+10)/10	16	-8.5 V measured on HSK board of	-8192 to 8191	-12.96 to 12.96	V

	LNO_HSK			LNO			
NMHK2614	POSITIVE_3_3_V_MEASURED_ON_LNO_CCC	real_val (V) = code*(3/8192)*(2.5+10)/10	16	+3.3 V measured on CCC board of LNO	-8192 to 8191	-3.75 to 3.75	V
NMHK2615	POSITIVE_2_5_V_MEASURED_ON_LNO_CCC	real_val (V) = code*(3/8192)	16	+2.5 V measured on CCC board of LNO	-8192 to 8191	-3 to 3	V
NMHK2616	POSITIVE_5_V_MEASURED_ON_LNO_HSK	real_val (V) = code*(3/8192)*(10+10)/10	16	+5 V measured on HSK board of LNO	-8192 to 8191	-6 to 6	V
NMHK2617	NEGATIVE_5_V_MEASURED_ON_LNO_HSK	real_val (V) = code*(3/8192)*(10+10)/10	16	-5 V measured on HSK board of LNO	-8192 to 8191	-6 to 6	V
NMHK2618	FPA_1_FULL_SCALE_TEMPERATURE_LNO	x=code*(3/8192)*(10/29.1) real_val (°K) =-460,66*x*x*x*x + 1053,2*x*x*x - 813,45*x*x - 227,36*x + 539,7	16	LNO focal plane array full scale temperture	0 to 8191	74.46 to 539.7	deg K
NMHK2619	FPA_2_ZOOMED_TEMPERATURE_LNO	real_val (V) = code*(3/8192)	16	LNO focal plane array zoomed temperature	-8192 to 8191	-3 to 3	V
NMHK2620	SENSOR_1_TEMPERATURE_LNO	real_val (°C) = (code*(3*1000/8192)+3/11)/51	16	temperature sensor 1 near LNO AOTF housing	-8192 to 8191	-58.83 to 58.82	deg C
NMHK2621	SENSOR_2_TEMPERATURE_LNO	real_val (°C) = (code*(3*1000/8192)+3/11)/51	16	temperature sensor 2 near LNO grating structure	-8192 to 8191	-58.83 to 58.82	deg C
NMHK2622	SENSOR_3_TEMPERATURE_LNO	real_val (°C) = (code*(3*1000/8192)+3/11)/51	16	temperature sensor 3 near LNO detector structure	-8192 to 8191	-58.83 to 58.82	deg C
NMHK2623	AOTF_TEMPERATURE_LNO	real_val (°C) = (code*(3*1000/8192)+3/11)/51	16	temperature inside LNO AOTF box	-8192 to 8191	-58.83 to 58.82	deg C
NMHK2624	RF_AMPLITUDE_LNO	real_val (V) = code*(3/8192)	16	RF amplitude of LNO AOTF driver	-8192 to 8191	-3 to 3	V
NMHK2625	GROUND_MEASURED_ON_LNO_HSK	real_val (V) = code*(3/8192)	16	ground potential measured on LNO HSK board	-8192 to 8191	-3 to 3	V
NMHK2626	MOTOR_POWER_DAC_CODE_LNO	real_val = code	16	LNO cooler motor power DAC control	0 to 8191	0 to 8191	ADU

Table 48: LNO housekeeping conversion formulae

code TM(29)	code TM(28)	parameter name	transfer function	size (bits)	description	Raw Value Range	Calculated Value Range	Calculated Units
NMHK2910	NMTM2810	POSITIVE_10_V_RAIL_VOLTAGE	real_val (V) = code * (3980/4096) / 20000 * (100+20)	16	+10V rail voltage	1500 to 1833	9 to 11	V
NMHK2911	NMTM2811	NEGATIVE_10_V_RAI	real_val (V) = -code*	16	-10V rail	1800 to	minus 9 to	V

		L_VOLTAGE	(3980/4096) / 20000 * 100		voltage	2200	minus 11	
NMHK2912	NMTM2812	POSITIVE_5_V_RAIL_VOLTAGE	real_val (V) = code* (3980/4096) / 20000 * (20+30.1)	16	+5V rail voltage	1600 to 2400	4 to 6	V
NMHK2913	NMTM2813	NEGATIVE_5_V_RAIL_VOLTAGE	real_val (V) = -code * (3980/4096) / 20000 * 50	16	-5V rail voltage	1600 to 2400	minus 4 to minus 6	V
NMHK2914	NMTM2814	POSITIVE_12_V_RAIL_CURRENT	real_val (mA) = code* (3980/4096) * 0.2	16	+12V rail current	0 to 500	0 to 100	mA
NMHK2915	NMTM2815	NEGATIVE_12_V_RAIL_CURRENT	real_val (mA) = code* (3980/4096) * 0.2	16	-12V rail current	0 to 500	0 to 100	mA
NMHK2916	NMTM2816	POSITIVE_5_V_RAIL_CURRENT	real_val (mA) = code* (3980/4096) * 0.2	16	+5V rail current	0 to 250	0 to 50	mA
NMHK2917	NMTM2817	NEGATIVE_5_V_RAIL_CURRENT	real_val (mA) = code* (3980/4096) * 0.002	16	-5V rail current	0 to 5000	0 to 10	mA
NMHK2918	NMTM2818	CCD_IMAGE_CLOCK_HIGH	real_val (V) = code* (3980/4096) / 20000 * (20 +80)	16	CCD image clock HI	1600 to 3000	8 to 15	V
NMHK2919	NMTM2819	CCD_IMAGE_CLOCK_LOW	real_val (V) = code* (3980/4096) /1000	16	CCD image clock LO	0 to 3000	0 to 3	V
NMHK2920	NMTM2820	CCD_READOUT_REGISTER_HIGH	real_val (V) = code* (3980/4096) / 20000 * (20 +80)	16	CCD readout register HI	1600 to 3000	8 to 15	V
NMHK2921	NMTM2821	CCD_READOUT_REGISTER_LOW	real_val (V) = code* (3980/4096) /1000	16	CCD readout register LO	0 to 3000	0 to 3	V
NMHK2922	NMTM2822	SUBSTRATE_VOLTAGE_VSS	real_val (V) = code* (3980/4096)/ 2490 * (6.8+2.49)	16	Substrate Voltage (VSS)	2087 to 2870	8 to 11	V
NMHK2923	NMTM2823	OUTPUT_GATE_VOLTAGE_VOG	real_val (V) = code* (3980/4096) /1000	16	Output gate voltage (VOG)	1000 to 5000	1 to 5	V
NMHK2924	NMTM2824	OUTPUT_DRAIN_VOLTAGE_VOD	real_val (V) = code * (3980/4096) / 20000 * (249+20)	16	Output drain voltage (VOD)	2007 to 2379	27 to 32	V
NMHK2925	NMTM2825	RESET_TRANSISTOR_DRAIN_VOLTAGE_VRD	real_val (V) = code* (3980/4096) / 20000 * (20+150)	16	Reset transistor drain voltage (VRD)	1764 to 2236	15 to 19	V
NMHK2926	NMTM2826	DIODE_DRAIN_VOLTAGE_VDD	real_val (V) = code* (3980/4096) / 20000 * (20+226)	16	Diode drain voltage (VDD)	1788 to 2033	22 to 25	V
NMHK2927	NMTM2827	TEMPERATURE_1	real_val (°C) = code* (3980/4096) /2.49 - 273.27	16	Temp 1 (Proximity Board)	530 to 930	minus 60 to + 100	deg C
NMHK2928	NMTM2828	TEMPERATURE_2	real_val (°C) = code* (3980/4096) /2.49 - 273.27	16	Temp 2 (CCD)	530 to 930	minus 60 to + 100	deg C
NMHK2929	NMTM2829	TEMPERATURE_3	real_val (°C) = code* (3980/4096) /2.49 - 273.27	16	Temp 3 (Detector Board)	530 to 930	minus 60 to + 100	deg C

NMHK2930	NMTM2830	MOTOR_CURRENT_A	real_val (mA) = code* (3980/4096)* 0.2	16	Motor current	0 to 600	0 to 120	mA

Table 49: UVIS housekeeping conversion formulae

6.2.1 TC20 Parameters

The timestamped TC20 sent to NOMAD will be stored in a PDS4 compatible product by the SOC and archived in the PSA. Discussion is ongoing with the SOC on how this data should be stored.